

TECHNICAL UNIVERSITY OF LIBEREC

Faculty of Mechatronics, Informatics and Interdisciplinary
Studies



Molecular biology tools for diagnostics of ongoing remediation

Ph.D. THESIS

Mgr. Iva Dolinová

Thesis topic:	Remediation technologies using genetics methods
Thesis topic in Czech:	Sanační technologie s využitím molekulárně-genetických analýz
Name and surname:	Iva Dolinová
Study program:	P3901 / Applied sciences in engineering
Study subject:	3901V055 Applied sciences in engineering
Workplace:	Institute of New Technologies and Applied Informatics, Faculty of Mechatronics, Informatics and Interdisciplinary Studies, Technical University of Liberec
Supervisor:	RNDr. Alena Ševců, PhD.
External Consultant:	doc. Ing. Ondřej Uhlík, Ph.D.
Consultant:	Mgr. Ing. Lukáš Dvořák, Ph.D.
Thesis assignment:	15. 3. 2012

Declaration

I hereby certify that I have been informed that Act 121/2000, the Copyright Act of the Czech Republic, namely Section 60, School-work, applies to my PhD thesis in full scope. I acknowledge that the Technical University of Liberec (TUL) does not infringe my copyrights by using my PhD thesis for TUL's internal purposes.

I am aware of my obligation to inform TUL on having used or licensed to use my PhD thesis, in which event TUL may require compensation of costs incurred in creating the work at up to their actual amount.

I have written my PhD thesis myself using literature listed therein after consulting with my supervisor and my tutor.

I hereby also declare that the hard copy of my PhD thesis is identical with its electronic form as saved at the IS STAG portal.

Date:

Signature:

Acknowledgment

I would especially like to thank my supervisor, RNDr. Alena Ševců, Ph.D., for her personal approach, help and valuable advice during my study. I would also like to thank doc. Ing. Ondřej Uhlík, PhD. for consultations that helped my experiments and for consultation regarding thesis structure. I also thank Ing. Mgr. Lukáš Dvořák Ph.D. for professional consultations. My great thanks go to Ing. Magda Nechanická and Bc. Denisa Vlková for helping me with the laboratory experiments. Likewise, thanks go to Ing. Monika Stavělová for personal and professional help. I also would like to thank to Mgr. Kevin F. Roche BSc. CSc. for language corrections. Last but not least, I would like to thank Ing. Jan Neměček PhD. for fruitful collaboration on research of CEs polluted site and writing an article.

Special thanks belong to my husband Jan, children Matěj, Kačka and Anička and loved ones for tolerance, understanding and all-round support during my postgraduate studies.

Research funding

My research was supported by Technology Agency of the Czech Republic, Czech Science Foundation, European Commission, and MŠMT of the Czech Republic through the following projects:

- Integrative technology for assessment and enhancement of complete removal of chloroethenes from groundwater (TA02020534) [2012-2015]
- Microbial meta-omic in relation to the functioning of ecosystems: the role of populations and their metabolic pathways in degradation of chloroethenes (GA14-32432 S) [2014-2016]
- Microbial colonization of the fiber surface for analytical and diagnostic practice and technical applications (TA04021210) [2014-2017]
- Integrated Approach to Management of Groundwater quality In functional urban Areas (2014 - 2020 INTERREG VB Central Europe, No. CE32) [2016-2019]
- SGS project no. 21176/115 of the Technical University of Liberec (Ministry of Education, Youth and Sports of the Czech Republic)

Abstract

This thesis focuses on bioremediation, molecular genetic methods and the preparation of nanofibre carriers for actual microbial community sampling. The research was focused exclusively on chlorinated ethenes with severe negative effects on both the environment and human health.

The combination of chemical and biological methods, along with application of Fenton's reagent and enhanced reductive dechlorination, are the most common remediation strategies for removal of chlorinated ethenes. In this thesis study, the influence of such techniques on indigenous bacteria was assessed using a wide spectrum of molecular genetic markers, including the 16S rRNA gene, specific chlorinated ethene degraders and reductive dehalogenase genes, together with sulphate-reducing and denitrifying bacteria. Bioremediation was monitored through the level of individual enzymes or bacterial strains.

Molecular genetics and hydrochemical tools were also used to evaluate natural attenuation of chlorinated ethenes in a Quaternary alluvial aquifer located close to a historical source of large-scale tetrachloroethylene contamination. Next generation sequencing of the middle and/or lower zones served as a tool for detailed characterisation. The relative abundance of specific degraders was identified using real-time PCR. The combined results confirm the hypothesis that there is significant potential for reductive dechlorination by natural attenuation.

At present, sampling and processing of groundwater for DNA analysis is complicated and influenced by transport and filtration in the laboratory. Regular soil sampling is not always possible due to the financial costs and reproducibility. The aim of this research was to develop a system of nanofibre carriers that could be used repeatedly for long-term monitoring of contaminated localities. The newly developed nanofibre carrier displayed non-preferential growth, is small thus easily transportable, and the material meets the requirement for DNA isolation. Long-term testing *in situ* proved that the nanofibre carriers are more than suitable for molecular genetic analysis. Individual composition and the arrangement of the nanofibre carriers were patented.

Keywords: bioremediation; contaminated sites; chlorinated ethenes, molecular genetic methods, nanofibre carriers.

Abstrakt

Předkládaná dizertační práce řešila dva hlavní cíle. Prvním byl monitoring a hodnocení bioremediačních procesů *in situ* pomocí molekulárně genetických metod. Druhým cílem byla příprava nanovlákných nosičů biomasy, které by měly sloužit k odběru a izolaci DNA ze vzorků získaných na reálné lokalitě. Výzkum byl cílený na problematiku chlorovaných ethenů patřících mezi nejčastější kontaminanty s prokázaným negativním vlivem na životní prostředí i lidské zdraví.

Kombinace chemické a biologické sanace patří k častým strategiím odstranění chlorovaných ethenů. V disertační práci byl zkoumán vliv těchto technik na přítomná bakteriální společenstva pomocí molekulárně genetických metod. Použité markery zahrnovaly 16S rRNA gen specifických degradérů i geny pro reduktivní dehalogenázy. Dále byly testovány markery charakterizující denitrifikační a síru redukující bakterie. Monitoring hladin jednotlivých testovaných markerů dovozoval hodnotit průběh a efektivitu probíhajících sanačních procesů.

Metody molekulární genetiky spolu s hydrogeochemickými analýzami byly také použité při hodnocení biologických dějů v kvartérním aluviálním podloží nacházejícím se v blízkosti historického zdroje rozsáhlé kontaminace tetrachlorethylenem. Relativní hladiny specifických degradérů byly měřené metodou polymerázové řetězové reakce v reálném čase (real-time PCR). Detailní charakterizace zkoumané lokality, respektive autochtonní mikroflóry, byla prováděná metodou sekvenace nové generace. Výsledky obou metod potvrdily hypotézu zonace aktivní reduktivní dechlorace v souladu s hydrogeochemickými parametry.

Druhým cílem dizertační práce bylo vyvinout nanovláknenné nosiče, které by bylo možné opakovaně použít při dlouhodobém sledování kontaminované lokality, protože odběr vzorků podzemních vod, jejich transport a zpracování je komplikovaný. Podobně pravidelný odběr vzorků půdy není možný nejen z důvodu finančních, ale i sporné reprodukovatelnosti. Vyvinuté nanovláknenné nosiče jsou kompaktní, dostatečně malé, snadno přenositelné, a především vhodné pro izolaci DNA. Dlouhodobé testy *in situ* potvrdily funkčnost pro využití nanovláknenných nosičů pro molekulárně genetické analýzy autochtonní mikroflóry. Jednotlivé varianty nanovláknenných nosičů byly patentovány.

Klíčová slova: bioremediace, kontaminované lokality, chlorované etheny, molekulární genetika, nosiče nanovlákn.

Thesis structure

This thesis is divided into three main parts: a Literature overview (Introduction, Bioremediation, Biodegradation of chlorinated ethenes, Molecular biology tools and Nanofibre carriers for biomass sampling at contaminated site), Experimental part (Evaluation of CEs bioremediation using molecular biology tools, real time PCR and NGS analysis of natural microbial communities and Development of nanofibre carriers for microbial sample collection) and Conclusions.

The **Literature overview** is divided into four subchapters. It is partly based on a published review (Dolinová et al., 2017, 2016b). The first summarizes the latest findings in bioremediation and focuses on the area of chlorinated hydrocarbons. This subchapter deals primarily with biological cleaning methods, other methods being mentioned marginally. The second focuses on the biological processes taking place at contaminated sites and possibilities for their detection by molecular biology methods. The third subchapter summarizes the molecular genetic tools used in this thesis. The last subchapter is devoted to problems related to actual sampling and the development of nanofibre carriers.

The **Experimental part** represents the main part of the thesis. It contains both a methodical description of the experiments and results with comments. This key part is based primarily on published articles and is divided into three chapters:

The **first chapter** focusses on the development and application of real-time PCR analysis performed on samples taken from polluted sites. It is mostly based on a published study (Dolinová et al., 2016a) and shows progress in bioremediation supported with chemical remediation procedures and describes the specific benefits of molecular genetic analysis. Different remediation strategies from other polluted sites (project No. TA02020534 report) were taken into account such that the conclusions obtained are as universal as possible.

The **second chapter** focusses on the development and application of next generation sequencing analysis for the evaluation of microbial communities involved in the remediation process. The results are based on a published study from a CE-polluted locality (Němeček et al., 2017) focusing on diagnostics that involve vertical stratification of an aquifer, meaning that physico-chemical parameters are linked to microbial

community analysis. The specific case studies described (Němeček et al., 2017) were correlated with the different types of remedial intervention techniques used.

The **third chapter** focusses on how to obtain representative samples for molecular genetic analysis. The sampling of soil and contaminated groundwater at an actual site and the subsequent processing of the material obtained has many limitations. The development of the new sampling method reported facilitates not only sampling and transport but also DNA isolation. In this thesis research, a range of nanofibre carriers were developed and patented, which significantly reduce the limitations of common sampling methods (project No. TA04021210 report, Nechanická et al., 2017 and Utility model No. 31266).

The last part, **Conclusions**, summarizes the most important findings of my thesis.

Table of contents

Declaration	i
Acknowledgment.....	ii
Research funding	ii
Abstract.....	iii
Abstrakt	iv
Thesis structure.....	v
Table of contents	vii
List of figures.....	xi
List of tables	xiv
Abbreviation.....	xv
Thesis Aims.....	xvii

LITERATURE OVERVIEW

1 Introduction	1
2 Bioremediation.....	2
3 Biodegradation of chlorinated ethenes (CEs)	7
3.1 Anaerobic metabolic degradation – reductive dechlorination.....	8
3.1.1 Bacteria involved in anaerobic degradation	10
3.1.2 Enzymes and functional genes in organohalide respiration	12
3.2 Aerobic metabolic degradation	17
3.2.1 Bacteria capable of aerobic metabolic degradation.....	17
3.2.2 Enzymes and functional genes in aerobic metabolic degradation.....	19
3.3 Aerobic cometabolic degradation	23
3.3.1 Bacteria capable of aerobic cometabolic degradation.....	23
3.3.2 Main enzymes involved in cometabolic degradation	23

4	Molecular biology tools	25
4.1	Introduction	25
4.2	Real-time PCR analysis.....	26
4.3	Next-generation sequencing.....	28
4.3.1	Amplicon analysis of 16S rRNA genes.....	30
5	Nanofibre carriers for biomass sampling at contaminated sites.....	33
5.1	Problems related to sampling procedure	33
5.2	Nanofibre carriers.....	34
5.3	Nanofibre preparation	35

EXPERIMENTAL SECTION

I. Evaluation of CE bioremediation using molecular biology tools

1	Background	37
2	Materials and methods.....	38
2.1	Study site.....	38
2.2	Application and reference wells.....	38
2.3	Physical and chemical analysis	41
2.4	Molecular genetic analysis.....	41
3	Results and discussion.....	43
3.1	Application of hydrogen peroxide for the Fenton-like reaction.....	43
3.1.1	ORP measurement.....	43
3.1.2	Influence on CEs	44
3.1.3	Changes in the organohalide-respiring bacterial populations	45
3.2	Application of sodium lactate	48
3.2.1	ORP measurement.....	48
3.2.2	Influence on CEs	49
3.2.3	Changes in COD and redox sensitive parameters	49
3.2.4	Impact on bacterial populations	50
3.3	Enhanced reductive dehalogenation process (ERD).....	51
4	Summary	54

II. NGS analysis of natural microbial communities

1	Background	55
2	Material and methods	55
2.1	Study site	56
2.2	Soil borings and collection of soil samples	57
2.3	Installation of monitoring wells and collection of groundwater samples	57
2.4	Measurement of physical and chemical parameters	58
2.5	DNA extraction	59
2.5.1	Soil samples	59
2.5.2	Water samples	59
2.6	Real-time PCR analyses (qPCR)	59
2.7	PCR amplification and next generation sequencing	60
3	Results and discussion	61
3.1	Physico-chemical and inorganic groundwater parameters	61
3.2	Concentration of CEs in groundwater	62
3.3	Bacteria and functional genes at different groundwater zones	63
3.4	Concentration of CEs in soil	64
3.5	Bacteria and functional genes in soil	64
3.6	Next generation sequencing (NGS)	66
4	Summary	72

III. Development of nanofibre carriers for sampling microbial communities

1	Background	74
2	Materials and methods	75
2.1	Study sites	75
2.2	Electrospinning and designing of nanofibre carriers	77
2.2.1	Multi-cluster linear arrangement	79
2.2.2	Linear arrangement	80
2.2.3	Tassle arrangement	80
2.2.4	Cylindrical arrangement	81
2.2.5	Planar arrangement	81

2.2.6	Circular arrangement.....	82
2.3	Sample preservation during transport	82
2.4	Selection of the best nanofibre carrier.....	83
2.4.1	Test of nanofibre carrier material.....	83
2.4.2	Effect of matrix	84
2.4.3	Effect of selected arrangements and nanofibre density	85
2.5	DNA isolation	85
2.6	Molecular genetic analysis.....	85
3	Results and discussion.....	86
3.1	Development of the nanofibre carrier	86
3.1.1	Multi-cluster linear arrangement.....	88
3.1.2	Linear arrangement	88
3.1.3	Tassle arrangement.....	89
3.1.4	Cylindrical arrangement.....	90
3.1.5	Planar arrangement.....	90
3.1.6	Circular arrangement.....	91
3.2	Effect of transport method on DNA yield.....	92
3.3	Effect of carrier arrangement and nanofibre surface density	94
3.3.1	Nanofibre carrier without coaxial protective fibre	95
3.3.2	Nanofibre carrier with coaxial protective fibre	96
3.3.3	Monitoring of groundwater	96
3.3.4	Nanofibre stability.....	97
3.4	Effect of nanofibre carrier arrangement on bacterial diversity	98
3.4.1	Influence of arrangement	98
3.4.2	Influence of nanofibre density	99
3.5	Comparison of microbial diversity in different matrices	102
4	Summary	103
	THESIS CONCLUSION.....	104-107
	List of References.....	I-XIV

List of figures

LITERATURE OVERVIEW

Fig. 1: <i>In situ</i> bioremediation strategies based on site parameters.....	3
Fig. 2: Specification of soil environment.....	4
Fig. 3: Conceptual model of a chlorinated ethene.....	5
Fig. 4: Enzymes involved in the biodegradation of CEs and the products of degradation.	8
Fig. 5: Microbial pathway for reductive dehalogenation of PCE.....	9
Fig. 6: a) Principle of real time PCR; b) effect of SYBR™ Green colour.....	27
Fig. 7: Principle of Real time PCR detection.....	27
Fig. 8: Changes in the relative abundance of markers in a CE-polluted well.	28
Fig. 9: Principle of NGS sequencing on the Ion Torrent device.	30
Fig. 10: NGS approaches – amplicon and whole genom sequencing.	30
Fig. 11: 16S rRNA structure.	31
Fig. 12: Heat map showing the abundance of individual microbial taxa.	32
Fig. 13: OTU column diagram showing individual microbial taxa	32
Fig. 14: Venn diagram showing the numbers of unique and shared OTUs for each sample combination.....	33
Fig. 15: Scheme of a needleless electrospinning set up.	36
Fig. 16: Electrospinning from a free liquid surface on a rotating electrode.....	36

EXPERIMENTAL SECTION

I. Evaluation of CE bioremediation using molecular biology tools

Fig. 1: A) Location of sampling and reference wells; and, B) geological cross-section of the site and direction of water flow.	40
Fig. 2: Oxidation-reduction potential depth profile in wells RW5-11 and RW5-12 before dosing of hydrogen peroxide.	44
Fig. 3: Changes in the relative abundance of organohalide-respiring bacteria markers and 16S rRNA gene following application of hydrogen peroxide in well RW5-11.	45
Fig. 4: Changes in the relative abundance of organohalide-respiring bacteria markers and 16S rRNA gene following application of hydrogen peroxide in well RW5-12.	46

Fig. 5: Change in the relative abundance of markers in well RW5-49 following infiltration of sodium lactate.	50
Fig. 6: Scheme summarizing applicability of enhanced reductive dehalogenation method.	52
Fig. 7: Remediation strategy by ERD.	53

II. NGS analysis of actual microbial communities

Fig. 1: Map of the study site with direction of groundwater flow.....	56
Fig. 2: Durov graph showing basic groundwater chemistry for the three wells samples.....	62
Fig. 3: Changes in total concentration of chlorinated ethenes in soil (left) and chlorine number (right) at depth.....	64
Fig. 4: Changes in total bacterial (prokaryotic) biomass, bacterial genera and functional genes in soil (in relative units) at depth.	65
Fig. 5: Venn diagram of bacterial communities present at different depths in the aquifer	67
Fig. 6: Abundance of microbial taxa (phylum level) present in 1.5, 2.5 and 3.1 m bgl.....	68
Fig. 7: Abundance of microbial taxa (family level) present in 1.5, 2.5 and 3.1 m bgl.....	69
Fig. 8: Phylum level community analysis.	70
Fig. 9: Family level community analysis.	71

III. Development of nanofibre carriers for microbial sample collection

Fig. 1: Location of the CE contaminated sites studied within this study.	75
Fig. 2: Black high-density polyethylene tubes with nanofibre carriers inside.	78
Fig. 3: Technical drawing of multi-cluster linear arrangement.....	79
Fig. 4: Technical drawing of the linear arrangement of support thread.	80
Fig. 5: Technical drawing of tassle arrangement.	80
Fig. 6: Technical drawing of the cylindrical arrangement.	81
Fig. 7: Technical drawing of the planar arrangement.	81
Fig. 8: Technical drawing of the circular arrangement.	82
Fig. 9: Scheme of nanofibre carriers experiment at Spolchemie site.....	83
Fig. 10: SEM micrographs of modified threads with CPF with and without a nanofibre layer..	87
Fig. 11: Nanofibre carriers: Multi-cluster linear arrangement.	88
Fig. 12: Nanofibre carriers: Linear arrangement.....	89
Fig. 13: Nanofibre carriers: Tassle arrangement.....	89

Fig. 14: Nanofibre carriers: Cylindrical arrangement.	90
Fig. 15: Nanofibre carriers: Planar arrangement.	91
Fig. 16: Nanofibre carriers: Circular arrangement.	91
Fig. 17: Comparison of DNA yield between two sampling rounds in 2013.	93
Fig. 18: SEM image of nanofibre thread (10 dtex) with and without CPF.	94
Fig. 19: Evolution of total bacterial biomass on different arrangements.	95
Fig. 20: Evolution of total bacterial biomass on different arrangements.	96
Fig. 21: Evolution of total bacterial biomass in groundwater in the monitoring wells	97
Fig. 22: SEM image of nanofibre thread at 10 dtex after one year's exposure.	97
Fig. 23: Comparison of bacterial diversity between different arrangements	98
Fig. 24: Comparison of bacterial diversity between planar arrangements and water..	100
Fig. 25: Family level community analysis.	101
Fig. 26: Comparison of bacterial diversity between three different matrices.	102

List of tables

LITERATURE OVERVIEW

Table 1: Summary of bacteria capable of degrading PCE, TCE, cDCE, and VC via anaerobic organohalide respiration.....	11
Table 2: Primers used for detection of functional reductive dehalogenase genes.....	14
Table 3: Summary of bacteria capable of degrading PCE, TCE, cDCE and VC via aerobic metabolic or co-metabolic pathways.....	18
Table 4: Primers used for detection of functional genes in aerobic bacteria degrading chloroethenes metabolically or cometabolically.....	22
Table 5: Properties of different nanofibre carriers	34

EXPERIMENTAL SECTION

I. Evaluation of CE bioremediation using molecular biology tools

Table 1: Characteristics of the sampling wells.....	39
Table 2: Specific primers used for quantitative PCR.....	42

II. NGS analysis of actual microbial communities

Table 1: Relative abundance of total bacterial biomass, <i>nirS</i> , <i>apsA</i> , <i>Dehalococcoides</i> sp., <i>Dehalobacter</i> sp., <i>Desulfurospirillum</i> sp. and the <i>vcrA</i> and <i>bvcA</i> genes in groundwater.....	63
Table 2: Correlation matrix with values for soil parameters.....	66

III. Development of nanofibre carriers for microbial sample collection

Table 1: Characterization of the test wells in the experiment evaluating transport techniques. .	75
Table 2: Chemical analysis of test wells in the experiment evaluating transport techniques.	76
Table 3: Chemical analysis of wells in an experiment with nanofibre carrier arrangement.	77
Table 4: Composition of prepared nanofibre carriers.	77
Table 5: Summary of arrangements used in experiment with threads without CPF.....	78
Table 6: Summary of arrangements used in experiment with threads with CPF.....	78
Table 7: Contaminated locality with test wells.....	83
Table 8: Schedule of long-term testing of nanofibre carriers without CPF.....	84
Table 9: Schedule of long-term testing of nanofibre carriers with CPF.....	84
Table 10: Sampling campagne for different matrix comparison.....	85
Table 11: Advantages and disadvantages of nanofibre carriers tested <i>in situ</i>	92

Abbreviation

16S rRNA	16S ribosomal RNA
AkMO	Encode genes for VC degradation, alkene monooxygenase
apsA	Encode adenylyl-sulphate reductase alfa-subunit
bgl	Below ground level
BTEX	Benzene, Toluene, Ethylbenzene, Xylene
bvcA	Encode vinyl chloride reductase
CCD	Charge-coupled device
cDCE	cis-1,2-dichloroethylene
CEs	Chlorinated ethenes
CHC	Chlorinated hydrocarbons
COD	Chemical oxygen demand
CPF	Coaxial protective fibre
Cq	Cycle quantification (crossing point, cycle threshold in real time PCR)
CxI	Institute for Nanomaterials, Advanced Technologies and Innovation
DCE	1,2-dichloroethane
DHC	<i>Dehalococcoides</i> sp.
DNA	Deoxyribonucleic acid
DNAPL	Dense Nonaqueous Phase Liquid
Dre	<i>Dehalobacter</i> spp.
Dsb	<i>Desulfitobacterium</i> spp.
DsrA	Encode dissimilatory sulfite reductase subunit A gene
dtex	Decitex
EaCoMT	Encode genes for VC degradation, epoxyalkane: coenzyme M transferase
EPA	U.S. Environmental Protection Agency
ERD	Enhanced reductive dehalogenation process
etnE	Encode encodes an EaCoMT
etnEABCD	Encode a putative four-component alkene monooxygenase.
HCH	Hexachlorocyclohexane

HDPE	High density polyethylene
linA	Encode γ -hexachlorocyclohexane dehydrochlorinase.
MMO	Methane monooxygenase enzyme
MNA	Monitored natural attenuation
NGS	Next generation sequencing
nirK	Encode nitrite reductase gene
nirS	Encode nitrite reductase gene
nZVI	Nanoscale zerovalent iron
ORP	Oxidation Reduction Potential
OTU	Operational taxonomic unit
PCE	Perchloroethylene / Tetrachloroethylene
pceA	Encode tetrachloroethene reductive dehalogenase
PCR	Polymerase chain reaction
pMMO	Membrane bound particulate methane monooxygenase enzyme
qPCR	Real-time PCR
RDases	Reductive dehalogenase enzymes
rdhA	Encode chloroethene reductive dehalogenase
rdhB	Encode reductive dehalogenase anchoring protein
RNA	Ribonucleic acid
SDIMO	Soluble di-iron monooxygenase alpha subunit
sMMO	Soluble methane monooxygenase enzyme
TCE	Trichloroethylene
tceA	Encode trichloroethene reductive dehalogenase
TOC	Total organic carbon
U16SRT	Universal microbial recovery via gene 16S rRNA
VC	Vinyl chloride
vcrA	Encode vinyl chloride reductase
VOCs	Volatile organic compounds

Thesis Aims

The overarching aim of this thesis was to study *in situ* bioremediation of CE polluted areas by means of advanced molecular genetic methods. The first task was to establish reliable and reproducible methods for microbial DNA analysis (qPCR and NGS) as all molecular genetic results were obtained by analysis of DNA isolated from complicated environmental samples.

The next aim was to monitor expression of specific enzymes and bacteria associated with biodegradation and to evaluate ongoing processes in different polluted environments. These findings served as a basis to describe principles and to draw general conclusions about the influence of remediation processes on natural microbial communities important in biodegradation.

The final objective was to develop nanofibre carriers of bacterial biomass in order to obtain quality DNA from polluted sites. The nanofibre carrier material was designed to persist in harsh environments and to enable non-preferential growth of biofilm, reflecting the structure of present microbial communities.

LITERATURE OVERVIEW

1 Introduction

Chloroethenes Tetrachloroethene (Perchloroethylene, PCE) and trichloroethene (Trichloroethylene, TCE) are commonly occurring contaminants, due to both their extensive usage and careless handling and storage (Paul and Smolders, 2014, Moran et al., 2007). Great quantities of PCE and TCE have been manufactured and are widely used in a wide range of fields, including industrial, farming, military and some household products. They have been used as solvents, mainly for metal degreasing, paint strippers, cleaning and drying of electronic components, dry cleaning, textile finishing, dyeing, as extraction solvent for fats, oils, and waxes, and for splattering liquid oxygen in the aerospace industry (Wittlingerova et al., 2013). While use of chloroethenes brings many advantages, they are known for their toxic effects, propensity for bioaccumulation and difficulty in biodegradation. PCE and TCE are hydrophobic and thus are insoluble in water. Owing to their low tendency to sorb they can easily spread in aquifers and their high density and viscosity enable them to be transported to considerable depths. Moreover, the relatively high volatility of chloroethenes allows them to be released into the atmosphere.

The original source of PCE and TCE in contaminated aquifers was from artificial synthesis, whereas cis-1,2-dichloroethene (cis-1,2-dichloroethylene, cDCE) and vinyl chloride (VC) mainly originate from *in situ* microbial degradation, though industrial production of PVC plastics could also be direct source of VC (Hartmans et al., 1985). Evidence of natural chloroethene degradation in aquifers is commonly observed. Moreover, chloroethenes remain persistent contaminants at many sites and byproducts cDCE and VC that accumulate after degradation of PCE and/or TCE are more toxic than the parent compounds (Mattes et al., 2010). Besides anthropogenic origin, small amounts of chloroethenes are also produced naturally by abiotic reactions in soils, e.g. production of VC during humic acid, Fe(III) and chloride reactions and by biosynthesis of PCE and TCE by marine algae. Natural production of chloroethenes can support microorganisms to develop detoxification pathways for chloroethenes, which can be used for bioremediation.

Environmental microbial genetics has become very useful in recent years for the detection of bacterial species capable of biodegradation and for the monitoring of specific enzymes involved in TCE degradation. Moreover, characterization of whole bacterial consortia

by next generation sequencing (NGS) is increasingly being employed for diagnostics of ongoing bioremediation (Maphosa et al., 2012).

Many physical and chemical remediation treatments have been used for decontamination of polluted sites. Physical treatments include pump-and-treat, venting, air sparging and *in situ* and *ex situ* thermal desorption, while common chemical processes include oxidation, using agents such as hydrogen peroxide, ozone, persulphate or permanganate, or reduction, often using zero valent iron (Němeček et al., 2017; Tobiszewski and Namieśnik, 2012; Waclawek et al., 2015).

Most of these treatments have disadvantages, however, such as high-cost, incomplete degradation and time taken. Elimination of chloroethenes by microorganisms is an advantageous remediation approach as at most sites it is very effective and environmentally friendly and can enhance chemical or physical treatments (Bradley, 2003; Majone et al., 2015; Miura et al., 2015). Despite its positive environmental aspects, bioremediation does have some disadvantages, with side effects such as production of harmful metabolites and pathogens, pH changes, loading of groundwater with organic material with subsequential long-term changes of groundwater chemistry or aquifer clogging (Mattes et al., 2010; Nijenhuis and Kuntze, 2016). This can be minimalized or avoided if the *in situ* biological and abiotic conditions are adequately known in advance and the bioremediation process is optimised accordingly (Tarnawski et al., 2016).

2 Bioremediation

Three different approaches have been applied to degrade contaminants by bacteria (Fig. 1). The first is ‘monitored natural attenuation’ (MNA), which employs natural abiotic and biotic (the existing microbial community at a contaminated site) degradation processes. This treatment includes monitoring of chloroethene removal, increase in concentration of metabolites and presence of bacteria or specific enzymes capable of the degradation. The MNA process includes monitoring of the plume over time to verify that natural attenuation is occurring at rates to attain site-specific remediation objectives within the predicted time frame. Analytical techniques for assessment of MNA potential are limited to organic and inorganic chemistry and inorganic chemistry/geochemistry (VOCs, dissolved oxygen, nitrate, Fe(II), sulphate, methane,

ethene, ORP, pH, temperature and salinity) and do not consider microbial parameters. While MNA is low-cost, natural processes are typically too slow.

At sites where MNA is insufficient to meet treatment goals, a second treatment approach, known as ‘enhanced natural attenuation’ or ‘biostimulation’, may be considered. This includes principles of MNA but includes the addition of carbon sources or other electron donors that support, and thus accelerate, natural degradation (Dolinová et al., 2016a; Lacinová, 2013). In order to achieve successful biostimulation, the requisite microbial populations must already be present in the aquifer. Molecular biological tools are frequently used nowadays to evaluate the microbial status of polluted sites. Detection of specific microorganisms and genes are both used prior to the remedial approach chosen. Molecular analysis is then used during the remedial process to quantify changes in specific genes and microorganism. to evaluate the influence of biostimulation and to verify bioaugmentation of an aquifer, if applied.

The third approach, known as ‘bioaugmentation’, may be used if the target aquifer does not harbour the requisite microbial populations at a useful density. Bioaugmentation involves the addition of pre-cultured bacteria with known degradation activity. In all cases, the addition of electron donors is usually necessary for the process to be successful (Ellis et al., 2000; Steffan et al., 1999). Bioaugmentation has one strong disadvantage, however, in that pre-cultured bacteria are usually unable to proliferate (or even survive) in the harsh conditions of a contaminated locality. Wells with ongoing microbial biodegradation could serve as a good source of groundwater for bioaugmentation of those wells where biodegradation is slow.

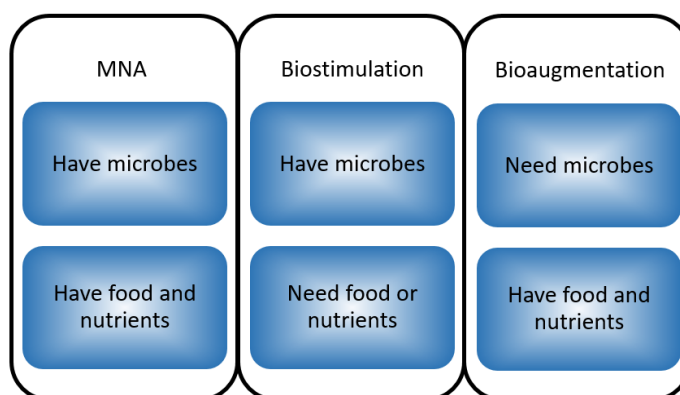


Fig. 1: *In situ* bioremediation strategies based on site parameters (Dolinová et al., unpublished data).

Anaerobic organohalide respiration (reductive dechlorination), aerobic metabolic and cometabolic oxidative dechlorination are the three main clean-up processes that can be applied for bioremediation of CE contaminated sites. Characterization and distribution of the contaminated environment to different redox zones according to basic biological-physicochemical parameters is shown in Fig. 2.

Specification of soil environment in accordance with redox potential, microbial metabolism and electro-acceptors occurrence							
Strongly reductive		Reductive		Anoxic		Oxic	Redox conditions
Anaerobic		Facultative anaerobic				Aerobic	Microbial metabolism
-300	-200	-100	0	+100	+200	+300	+400 →
CO ₂	SO ₄ ²⁻	Fe ³⁺	Mn ⁴⁺	NO ₃ ⁻	O ₂		
↓	↓	↓	↓	↓	↓	↓	Typical redox reaction for particular area E _h
CH _n	H ₂ S + S ²⁻	Fe ²⁺	Mn ²⁺	NO ₂ ⁻	H ₂ O	N ₂	
Methanogenic bacteria	Sulphatereductive bacteria	Fe ³⁺ reductive bacteria	Mn ⁴⁺ reductive bacteria	Denitrification bacteria	Aerobic Bacteria		Examples of active microflora
<i>Methanotrix</i> <i>Methanococcus</i> <i>Methanobacter</i>	<i>Sulfurospirillum</i> <i>Desulfitobacter</i> <i>Desulfovibrio</i>	<i>Gebacter</i> <i>Desulfuromonas</i>		<i>Thiobacillus denitrificans</i>	<i>Pseudomonas</i> <i>Polaromonas</i>		
	<i>Dehalococcoides</i> <i>Dehalobacter</i>						

Fig. 2: Specification of soil environment (Stavělová, unpublished data).

Reductive dechlorination requires an anaerobic environment, presence or addition of the genus *Dehalococcoides* and enough electron donors for complete chloroethene biodegradation. Chloroethenes can migrate into the aerobic zone (Fig. 3), where they can be further degraded by oxidizing bacteria. This can happen by either cometabolic or metabolic means. Bacteria with aerobic cometabolic degradation activity have been used successfully for bioremediation (Semprini, 1997) but have limitations, such as enzyme inhibition by growth or cometabolic substrates or competition for degrading enzyme active sites, exhaustion of reductant and toxicity of epoxide or aldehyde oxidation products, causing enzyme inactivation and cell death.

Recently, Schmidt et al., 2014 studied the metabolic aerobic biodegradation of TCE by an enriched mixed bacterial culture and concluded that aerobic biodegradation of TCE could prove beneficial as a bioremediation method. Aerobic metabolic degradation has certain advantages over aerobic cometabolic degradation as there is no need for auxiliary substrates, and thus no competition between auxiliary substrates and chloroethenes for the degrading enzyme, and no oxygen utilization by the auxiliary substrates, thus no competition for oxygen, no toxicity of oxidation products and higher degradation rates.

However, the use of aerobic metabolic degradation during *in situ* chloroethene bioremediation is difficult because of the limited number of bacterial strains capable of metabolic degradation of chloroethenes. Moreover, PCE is not degradable through this process.

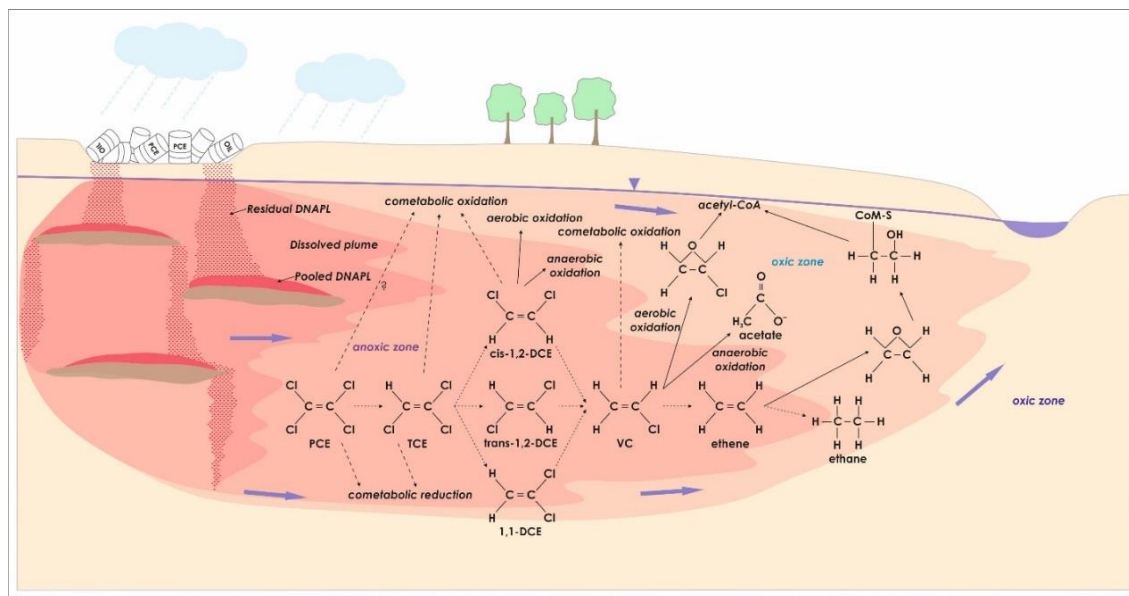


Fig. 3: Conceptual model of a chlorinated ethene – contaminated aquifer and relevant biological degradation pathways. Dotted arrows indicate reductive reactions, solid arrows indicate oxidative reactions, dashed arrows indicate cometabolic reactions. DNAPL (Dense Nonaqueous Phase Liquid) - a pollutant in the form of a separate phase from the water, Dolinová et al., 2016a modified after Mattes et al., 2010).

An alternative to anaerobic or aerobic biodegradation only is sequential anaerobic and aerobic biodegradation. This method has recently been reviewed from the perspective of remediation (Frasconi et al., 2015). Anaerobic reduction of cDCE and VC is slow and incomplete in some cases, with absence or shortage of suitable bacteria (i.e. *Dehalococcoides* group) or adverse environmental conditions restricting complete chloroethene degradation. However, complete dechlorination of PCE can be advantageously accomplished by sequential reductive and oxidative degradation when aerobic degradation is involved. The rate of reductive dechlorination of chloroethenes decreases with decreasing number of chlorine substituents, and *vice versa*, the rate of oxidative dechlorination increases with decreasing number of chlorine substituents. The only means of complete PCE degradation, however, is through anaerobic dechlorination. As cDCE and VC is often accumulated during reductive dechlorination,

sequential anaerobic-aerobic biodegradation that includes complete and fast cDCE and VC degradation via aerobic degradation can be applied at some chloroethene-contaminated sites. Moreover, if reductive dechlorination happens under methanogenic conditions and methane is produced, this can serve as a growth substrate for aerobic cometabolic degradation and speed up the degradation.

Sequential anaerobic and aerobic biodegradation of chloroethenes has been observed in both batch reactors and in the natural environment. Frascari et al., 2013 used aerobic-anaerobic-aerobic degradation of chloroethenes in batch reactors, where TCE and VC were first degraded during the aerobic phase by cometabolism, PCE degraded to TCE and cDCE during the second anaerobic phase and TCE and cDCE degraded by cometabolism in the last aerobic phase. If reductive dechlorination was the first step that produced VC, which was then degraded by the aerobic cometabolic process, it could conceivably run without the addition of growth substrate supplement. To conclude, a combination of anaerobic-aerobic conditions appears to be the most powerful technology for biodegradation of chloroethenes.

In addition to biological methods, a number of chemical techniques are also available for *in situ* remediation, with chemical oxidation, using Fenton's reagent (a mixture of hydrogen peroxide [H₂O₂] and an iron catalyst [Fe²⁺]) or a Fenton-like reaction (where there is a sufficient concentration of iron in the environment) for example, being one of the most frequently applied methods for chlorinated ethenes (CEs). Chemical oxidation can significantly restrict the activity of organohalide-respiring bacteria, however, and cause changes in microbial community structure. Chemical oxidation can also oxidise organic matter in preference to CEs, resulting in a lack of carbon for autochthonous microorganisms (Chapelle et al., 2005). While changes in microbial populations are a side-effect of chemical oxidation, application of a substrate (electron donor) such as lactate directly improves conditions for biological organohalide respiration. This can be employed either alone or during the remediation of residual contamination, often present following the application of other techniques such as the Fenton reaction. Although biological methods exhibit slower reaction kinetics, they have the advantage of being less expensive than chemical methods and being more environmentally friendly. Despite this, many of the processes involved in biological methods are still not fully understood (Kang, 2014; Farai Maphosa et al., 2010).

Previous studies involving Fenton-like reactions or application of sodium lactate ($\text{NaC}_3\text{H}_5\text{O}_3$) have either focused purely on chemical parameters or on total organohalide-respiring microbial colonisation (Chapelle et al., 2005; Mattes et al., 2010; Sutton et al., 2011). Though a number of studies have also conducted molecular genetics analysis, these have usually been undertaken at a laboratory scale only or following bioaugmentation with organohalide-respiring bacteria (Behrens et al., 2008; Damgaard et al., 2013; Kranzioch et al., 2013; Scheutz et al., 2008).

3 Biodegradation of chlorinated ethenes (CEs)

In the case of CEs, the main biodegradation metabolic pathways are known; hence, biodegradation can be monitored in detail (Fig. 4) and it is possible to monitor anaerobic and aerobic pathways. In addition to specific biodegradation enzymes, it is possible to monitor other groups of bacteria necessary for ongoing active bioremediation.

PCE and TCE can be degraded by microorganisms with less CEs, cDCE, trans-1,2- and 1,1-dichloroethene (trans-1,2-dichloroethylene, tDCE and 1,1-dichloroethylene, 1,1DCE) and VC to ethene. The dominant DCE isomer generated during microbial reductive dechlorination of PCE and TCE is cDCE. Various groups of bacteria with different dechlorination activity coexist at CE-contaminated aquifers, their actual activity depending on environmental conditions, which could be aerobic or anaerobic. Bacterial degradation of CEs occurs via anaerobic organohalide respiration (CEs used as electron acceptors), anaerobic and aerobic metabolic degradation (CEs used as electron donors) or aerobic cometabolic degradation (degradation of CEs occurs fortuitously during microbial metabolism using other growth substrates, without carbon or energy benefit for the bacteria). Although bacterial anaerobic oxidation of VC under Fe(III)-reducing conditions has been detected (Bradley and Chapelle, 1998), no bacteria capable of anaerobic oxidation of VC have been observed to date.

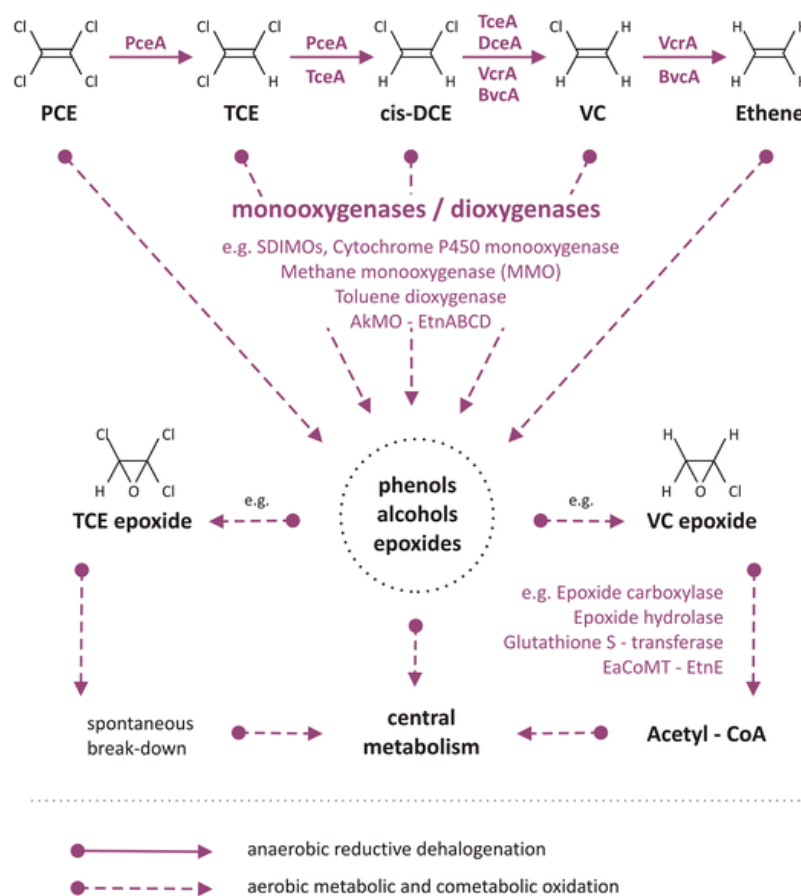


Fig. 4: Enzymes involved in the biodegradation of chloroethenes and the products of degradation (Dolinová et al., 2017).

3.1 Anaerobic metabolic degradation – reductive dechlorination

Organohalide respiration is a major degradation route of CEs in anaerobic environments (Chambon et al., 2013; Furukawa, 2006; Futagami et al., 2008; Häggblom et al., 2006; Hug et al., 2013; Jugder et al., 2015; Maphosa et al., 2010; Smidt and de Vos, 2004; Uchino et al., 2015). During anaerobic organohalide respiration, CEs are used as electron acceptors and energy generated from exergonic dehalogenation reactions is used for microorganism growth. Hydrogen is usually the final electron donor (Löffler et al., 2000) and many different hydrogen-releasing substrates (e.g. acetate, benzoate, butyrate, ethanol, glucose, lactate, propionate and vegetable oils) can be utilized as the primary electron donor during organohalide respiration of CEs (Fig. 5).

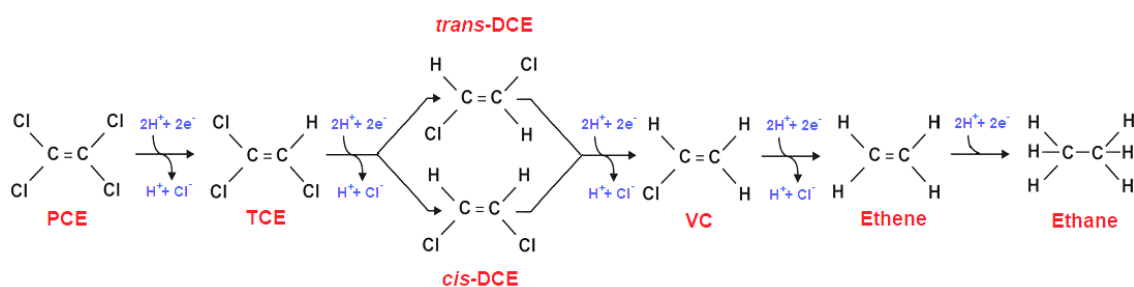


Fig. 5: Microbial pathway for reductive dehalogenation of PCE (adapted from Leeson et al., 2004).

The inclination of chloroethenes for reductive dechlorination decreases with decreasing number of chlorine substituents and *vice versa*. Hence, low-chlorinated cDCE and VC are often accumulated at sites where PCE and TCE are degraded via microbial organohalide respiration. This accumulation is a result of either partial dechlorination or decreased dechlorination rate of lower CEs. Both cDCE and VC are toxic, thus degradation of cDCE and VC to non-toxic ethene is an important step in the biodegradation of CEs.

Rates of organohalide respiration are influenced by interactions with biogeochemical processes and competition for hydrogen by diverse microbial populations (Azizian et al., 2010). Thus, the addition of an electron donor may not only stimulate the activity of dehalogenating microorganisms but also the activity of competing microbial populations, such as methanogens, acetogens, sulphate, nitrate, iron and manganese reducers. However, the relationship between reductive dechlorination and redox processes, such as sulphate and iron reduction, has not been fully clarified yet, though several studies have shown that sulphate and iron reduction competes for hydrogen and, therefore, slows dechlorination (Aulenta et al., 2008; Azizian et al., 2010; Paul et al., 2016). Sulphate reduction slows dechlorination of cDCE and VC, but it is possible that the accumulation of sulphide also causes problems for dechlorination. On the contrary, addition of sulphate increases dechlorination efficiency in microcosm studies (Harkness et al., 2012). These conflicting results may be caused by generation of slightly alkaline conditions during sulphate reduction and the prevention of a pH decrease that is otherwise unfavourable for dechlorinating bacteria.

3.1.1 Bacteria involved in anaerobic degradation

There are only a few bacterial taxa known to be capable of complete degradation of PCE to ethene (Table 1 and references therein). All members of the *Dehalococcoides* (phylum *Chloroflexi*) group able to complete reductive degradation from PCE to ethene were recently defined as one species, *Dehalococcoides mccartyi*. *Dehalococcoides mccartyi* strains 195 and BTF08 in particular are able to degrade PCE up to ethene.

Most groups of bacteria are only able to partially degrade PCE and TCE to cDCE or VC. On the other hand, *Propionibacterium* sp. strain HK-1 and *Propionibacterium acnes* strain HK-3 isolated from sediments are able to anaerobically degrade PCE and cDCE to ethene. For the first time, this study suggests that bacteria other than members of *Dehalococcoides* can degrade PCE without producing toxic by-products. More species showing such a capability are probably awaiting discovery.

Members of *Dehalococcoides* are indigenous at many chloroethene-contaminated sites and their presence correlates with ethene formation, while their absence could correlate with an accumulation of cDCE. Thus, presence of *Dehalococcoides* may well indicate a potential for biodegradation at contaminated sites. However, the mere presence of *Dehalococcoides* does not always indicate their activity during *in situ* remediation as presence of bacteria can be due to presence of inactive or dead bacteria originating from other sites in the aquifer. Members of *Dehalococcoides* are limited to anaerobic conditions and are inhibited by oxygen. Various strains of *Dehalococcoides* have been described as capable of partial chloroethene degradation, e.g. strains BAV1, CBDB1, FL2, GT, KB-1, MB and VS (Table 1 and references therein).

Typically, more than one *Dehalococcoides* population is involved in complete chloroethene dechlorination. Some isolated *Dehalococcoides* strains are incapable of complete metabolic dechlorination but can dechlorinate certain CEs cometabolically (Duhamel et al., 2004; He et al., 2005, 2003; Holmes et al., 2006; Lee et al., 2008, 2006; Maymó-Gatell et al., 1999). Furthermore, *Dehalococcoides* possess higher dechlorination and growth rates when grown in mixed cultures, most likely as other strains provide substances that members of *Dehalococcoides* are unable to synthesize. Hence, mixed cultures containing the *Dehalococcoides* group, fermentative bacteria, methanogens, iron or sulphate reducers are often used for laboratory experiments as well as *in situ*

applications. Examples of such dechlorinating cultures are ANAS, EV, KB-1, PM, TM, and SDC-9.

Several *Dehalococcoides* genomes have already been sequenced and described (Uchino et al., 2015). Although members of pure cultures or bacterial communities can be determined by analysis of the 16S rRNA gene, this is unsuitable for resolution of different members of the genus *Dehalococcoides* as differences in their 16S rRNA gene sequences are very small. Phylogenetic test results obtained by 16S rRNA analysis do not correlate with results obtained using phylogenetic analysis of functional reductive dehalogenase enzymes (RDases) as this analysis is distorted by the horizontal transfer of RDase genes. Thus, despite variance in dechlorination efficiency, *Dehalococcoides* genomes share high homologies and, therefore, discrimination of *Dehalococcoides* by DNA sequencing of a small part of the genome is almost impossible.

Table 1: Summary of bacteria capable of degrading PCE, TCE, cDCE, and VC via anaerobic organohalide respiration. PC – pure culture, MC – mixed cultures, CFE – cell-free extract (from Dolinová et al., 2017).

Species	Degraded chloroethenes	Material studied	References
<i>Acetobacterium woodii</i>	PCE	CFE	Egli et al., 1988; Terzenbach and Blaut, 1994
<i>Clostridium</i> sp. strain DC-1	cDCE, VC	PC, MC	Bhowmik et al., 2012; Hata et al., 2004
<i>Clostridium</i> sp. strain KYT-1	cDCE, VC	PC	Kim et al., 2006
<i>Clostridium bifermentans</i> strain DPH-1	PCE, TCE, cDCE	CFE	Chang et al., 2001; Okeke et al., 2001
<i>Clostridium formicoaceticum</i>	PCE	CFE	Terzenbach and Blaut, 1994
<i>Dehalobacter restrictus</i> strain PER-K23	PCE, TCE	PC	Holliger et al., 1998
<i>Dehalobacter restrictus</i> strain TEA	PCE, TCE	PC	Wild et al., 1996
<i>Dehalococcoides</i> sp. strain CBDB1	PCE, TCE	PC	Marco-Urrea et al., 2011
<i>Dehalococcoides</i> sp. strain FL2	TCE, cDCE	PC	He et al., 2005
<i>Dehalococcoides</i> sp. strain GT	TCE, cDCE, VC	PC	Sung et al., 2006b
<i>Dehalococcoides</i> sp. strain UCH007	TCE, cDCE, VC	PC	Uchino et al., 2015
<i>Dehalococcoides</i> like bacterium VS	cDCE, VC	MC	Cupples et al., 2003
<i>Dehalococcoides</i> sp. strain BAV1	cDCE, VC	PC	He et al., 2003
<i>Dehalococcoides mccartyi</i> * strain 11a	TCE, cDCE, VC	PC	Lee et al., 2013
<i>Dehalococcoides mccartyi</i> strain 11a5	TCE, cDCE	PC	Lee et al., 2013
<i>Dehalococcoides mccartyi</i> strain 195	PCE, TCE, cDCE, VC	PC	Maymó-Gatell et al., 1999
<i>Dehalococcoides mccartyi</i> strains ANAS1	TCE, cDCE	PC	Lee et al., 2011
<i>Dehalococcoides mccartyi</i> strain ANAS2	TCE, cDCE, VC	PC	Lee et al., 2011
<i>Dehalococcoides mccartyi</i> strain BTF08	PCE, TCE, cDCE, VC	PC	Poritz et al., 2013
<i>Dehalococcoides mccartyi</i> strain DCMB5	PCE, TCE, cDCE	PC	Poritz et al., 2013
<i>Dehalococcoides mccartyi</i> strain MB	PCE, TCE	PC	Cheng and He, 2009
<i>Dehalospirillum multivorans</i> gen. nov., sp. nov	PCE, TCE	PC	Scholz-Muramatsu et al., 1995
<i>Desulfitobacterium</i> sp. strain KBC1	PCE	PC	Tsukagoshi et al., 2006

<i>Desulfitobacterium</i> sp. strain PCE1	PCE	PC	Gerritse et al., 1996
<i>Desulfitobacterium</i> sp. strain Y-51	PCE, TCE	PC, CFE	Lee et al., 2001; Suyama et al., 2001
<i>Desulfitobacterium</i> sp. strain PCE-S	PCE, TCE	CFE	Miller et al., 1997
<i>Desulfitobacterium frappieri</i> strain TCE1	PCE, TCE	PC	Gerritse et al., 1999
<i>Desulfitobacterium</i> cf. <i>hafniense</i> strain DCB-2	PCE	PC, CFE	Suyama et al., 2001
<i>Desulfitobacterium hafniense</i> strain JH1	PCE, TCE	PC	Fletcher et al., 2008
<i>Desulfitobacterium metallireducens</i>	PCE, TCE	PC	Finneran et al., 2002
<i>Desulfomonile tiedjei</i> strain DCB-1	PCE	PC	DeWeerd et al., 1990
<i>Desulfuromonas chloroethenica</i> strain TT4B	PCE, TCE	PC	Krumholz, 1997
<i>Desulfuromonas michiganensis</i> strains BB1 and BRS1	PCE, TCE	PC	Sung et al., 2003
family <i>Enterobacteraceae</i> strain MS-1	PCE, TCE	PC	Sharma and McCarty, 1996
<i>Enterobacter agglomerans</i> biogroup 5	PCE, TCE	PC	Sharma and McCarty, 1996
<i>Geobacter lovleyi</i> strains KB-1 and SZ	PCE, TCE	PC	Wagner et al., 2012
<i>Geobacter lovleyi</i> strain SZ	PCE, TCE	PC	Sung et al., 2006a
<i>Methanobacterium thermoautotrophicum</i> MARBURG	PCE	PC	Egli et al., 1987
<i>Methanolobus tindarius</i>	PCE	CFE	Terzenbach and Blaut, 1994
<i>Methanosarcina</i> sp.	PCE	PC	Fathepure and Boyd, 1988
<i>Methanosarcina mazei</i> strain S6	PCE	PC	Fathepure and Boyd, 1988
<i>Methanosarcina thermophila</i>	TCE, cDCE, VC	CFE	Jablonski and Ferry, 1992
<i>Propionibacterium</i> sp. strain HK-1	PCE, TCE, cDCE, VC	PC, CFE	Chang et al., 2011
<i>Propionibacterium acnes</i> strain HK-3	PCE, TCE, cDCE, VC	PC, CFE	Chang et al., 2011
<i>Shewanella sediminis</i>	PCE	CFE	Lohner and Spormann, 2013
<i>Sporomusa ovata</i>	PCE	PC, CFE	Terzenbach and Blaut, 1994
<i>Sulfurospirillum</i> spp.	PCE, TCE	MC	Maillard et al., 2011
<i>Sulfurospirillum halorespirans</i> strain PCE-M2T=DSM 13726T=ATCC BAA-583T	PCE, TCE	PC	Luijten et al., 2003

*Formerly *Dehalococcoides ethenogenes*

3.1.2 Enzymes and functional genes in organohalide respiration

RDases are key enzymes of organohalide respiration that directly catalyze cleavage of the carbon-chlorine bond. A range of RDases may be present in each bacterial strain (Fung et al., 2007; Liang et al., 2012; McMurdie et al., 2009; Poritz et al., 2013). PCE reductive dehalogenase (PCE-RDase) dechlorinates PCE via TCE to cDCE. TCE-RDase dechlorinates TCE via cDCE to VC and ethene. VC-RDase *vcrA* dechlorinates cDCE to VC and ethene, while VC-RDase *BvcA* dechlorinates VC to ethene. However, these RDases may have a greater range of catalyzing reactions than hitherto known. Recently, it has been suggested that *BvcA* catalyzes dechlorination of all dichloroethene isomers.

Genes encoding biochemically characterized RDases (or non-identical homologous genes for RDases; *rdh*) usually include the RDase subunit gene *rdhA* for the catalytically active

enzyme (RDase with an identical function, otherwise *RdhA*) and *rdhB*, a gene encoding a putative membrane-anchoring protein. The catalytic subunit of most RDases contains a cobalamin cofactor and iron–sulfur clusters. Recently, Payne et al., 2015 proposed a new paradigm stating that RDases reduce organohalide by the formation of a halogen–cobalt complex. Although the majority of RDases are bound to the cell membrane, cytoplasmic RDases have been detected in *Desulfitobacterium*, *Dehalobacter* and *Sulfurospirillum multivorans*.

A variety of genes encoding RDases are expressed in the presence of different chlorinated organics and under different environmental conditions, though the relationship between enzyme activity and gene expression has not been fully elucidated. The genomes of dechlorinating bacteria may include one, two or more than two different *rdhA* genes. It is known that approximately 650 putative *rdhA* genes exist, with over 100 of them from *Dehalococcoides*. Islam et al., 2014 studied transcriptomic and proteomic data for *Dehalococcoides mccartyi* strains 195 and a mixed culture KB-1 using a range of experiments and confirmed the presence of most putative proteins and genes in *Dehalococcoides mccartyi* strain 195 and *Dehalococcoides mccartyi* from KB-1 culture. Interestingly, genes encoding the active subunit of RDase (*rdhA*) were transcribed even in the absence of CEs. The known *Desulfitobacterium* genomes show only 2–7 RDase genes; *Desulfitobacterium hafniense* strain DCB-2 containing seven putative *rdhA* genes compared to 10–39 in the *Dehalobacter* genomes, with *Dehalobacter restrictus* containing ca. 25 RDase genes. The *Dehalococcoides mccartyi* genome contains 10–36 different *rdhA* genes, while *Dehalococcoides mccartyi* strain 195 contains 17 *rdhA* genes. Genes encoding RDases are often present as more copies in the genome. Just a few of the RDases have been purified and characterized, and only some of the RDase genes have been defined for function.

Monitoring of genes directly associated with dechlorination activity could overcome some of the limitations of methods based on 16S rRNA. Targeting the presence and expression of RDase genes could represent a useful diagnostic tool for dechlorination activity. Specific primers of the functionally characterized RDase genes, such as *pceA*, *tceA*, *vcrA* and *bvcA*, or amplification of highly conserved regions of functional genes, could be used for determination of growth and activity of CEs degraders (Damgaard et al., 2013). Primers published for detection of functional *rdhA* genes are listed in Table 2.

Table 2: Primers used for detection of functional reductive dehalogenase genes. F = forward primer, R = reverse primer, FAM = 6-carboxyfluorescein, TAMRA = 6-carboxymethylrhodamine (from Dolinová et al., 2017).

Target gene	Target microorganism	Primer/Probe	Primer sequence (5'-3')	Amplicon (bp)	Method used	References
pceA	<i>Dehalospirillum multivorans</i>	Primer F Primer R	GCTGCTGGATGGACCTTAGA CATAGCGATACCTGCAACGA	339	PCR	Neumann et al., 1998
	<i>Desulfotobacterium hafniense</i> strain Y51	Primer F Primer R	GGCGGGGATCCAATGGGAGAAATCAACGGCGGGT CGACTGTTTTATAGACTCAG	334	PCR	Suyama et al., 2002
	<i>Dehalobacter restrictus</i> ; <i>Desulfotobacterium hafniense</i> strain TCE1	Primer F Primer R	ATGCAATTATTATTAAGGAGGAAG CTAAGCAGAAATAGTATCCGAACT	592	PCR	Maillard et al., 2003
	<i>Dehalobacter restrictus</i> strain PER-K23; <i>Desulfotobacterium</i> sp. strains TCE1, PCE-S, Y51	Primer F Primer R	TTGGATGAGGCCTTGAACGC GCGCTGCATAATAGCCAAGC	618	Inverse PCR	Regeard et al., 2004
	<i>Dehalobacter restrictus</i> strain PER-K23; <i>Desulfotobacterium</i> sp. strains TCE1, PCE-S, Y51	Primer F Primer R	CGTTGGACCTATTCCACCTG CAAGAACGAAGGCAATCACA	199		
	<i>Sulfurospirillum multivorans</i> strain K	Primer F Primer R	TCGTTGCAGGTATCGCTATG TTCAACAGCAAAGGCAACTG	194		
	<i>Desulfotobacterium hafniense</i> strain Y51	Primer F Primer R	CGGACATCGTGGCTCCGAT CTTGTCGGAGCAAGTTC	935	PCR	Fletcher et al., 2008
	<i>Dehalobacter</i> spp.; <i>Dehalococcoides mccartyi</i> ; <i>Dehalococcoides mccartyi</i> strain BAV1; <i>Desulfotobacterium</i> spp.; <i>Desulfomonile</i> spp.; <i>Desulfuromonas</i> spp.	Primer F Primer R	ACCGAAACCAGTTACGAACG GACTATTGTTGCCGGCACTT	100	qPCR	Behrens et al., 2008; Kranzioch et al., 2015; Popat et al., 2012
	<i>Desulfotobacterium hafniense</i> strain Y51; <i>Shimwellia blattae</i>	Primer F Primer R	CTGGCTATGGAGGGGAAATT AGTATCGGAAATGGGTGCAA	114	qPCR	Mac Nelly et al., 2014
		Primer F Primer R	ATTGCCCATTTATCCGTTCAA ACCGACTCGAACTTCCATTG	137		
		Primer F Primer R	GTCCAAGTTAAAGCCCAAAGT TCTTTTCAATGTTCCCGACG	107		
		Primer F Primer R	CGGAACAGATGTCCCAGAAT GCGCCTTGTTGGGAATAGTAG	105		
		Primer F Primer R	GGTAAAATACGCTCCAAACTTC TCCGCTTCAGATGTCATTTT	131		
		Primer F Primer R	GATTCGGGCTTTGGGTTATGC CGCAGACGCTTGATGATTTC	138		

tceA	<i>Dehalobacter</i> spp.; <i>Dehalococcoides mccartyi</i> ; <i>Dehalococcoides mccartyi</i> strains 11a5, 195, BAV1; <i>Desulfotobacterium</i> spp.; <i>Desulfuromonas</i> spp.; <i>Geobacter</i> spp.; <i>Sulfurospirillum</i> spp.; microorganisms from ANAS culture	Primer F Primer R	ACGCCAAAGTGGCGAAAAAGC TAATCTATTCCATCCTTTCTC	1693	Inverse PCR, qPCR	Holmes et al., 2006; Johnson et al., 2005; Lee et al., 2013; Magnuson et al., 2000; Silva et al., 2006; Sung, 2005
	<i>Dehalococcoides mccartyi</i> strain 195	Primer F Primer R	GCTTTGGCGGTGATGATAAG GTTATAGCCAAGGCCTGCAA	194	Inverse PCR	Regeard et al., 2004
	<i>Dehalococcoides mccartyi</i> ; <i>Dehalococcoides mccartyi</i> strains 195, BAV1, FL2, GT; microorganisms from ANAS and KB-1 culture	Primer F Primer R Probe	ATCCAGATTATGACCCTGGTGAA GCGGCATATATTAGGGCATCTT FAM-TGGGCTATGGCGACCCGAGG-TAMRA		qPCR	Bælum et al., 2013; Holmes et al., 2006; Johnson et al., 2005; Lee et al., 2008; Ritalahti et al., 2006; Sung, 2005
	<i>Dehalococcoides mccartyi</i> strain 195	Primer F Primer R	TAATATATGCCGCCACGAATGG AATCGTATACCAAGGCCGAGG	295	qPCR	Fung et al., 2007
	<i>Dehalobacter</i> spp.; <i>Dehalococcoides mccartyi</i> ; <i>Dehalococcoides mccartyi</i> strains 195, BAV1, FL2; <i>Desulfotobacterium</i> spp.; <i>Desulfomonile</i> spp.; <i>Desulfuromonas</i> spp.	Primer F Primer R	GCCACGAATGGCTCACATA TAATCGTATACCAAGGCCCG	306	qPCR	Behrens et al., 2008; Kranzioch et al., 2015; Popat et al., 2012
vcrA	<i>Dehalobacter</i> spp.; <i>Dehalococcoides mccartyi</i> ; <i>Dehalococcoides mccartyi</i> strain VS; <i>Desulfotobacterium</i> spp.; <i>Desulfuromonas</i> spp.; <i>Geobacter</i> spp.; <i>Sulfurospirillum</i> spp.	Primer F Primer R	TGCTGGTGGCGTTGGTGCTCT TGCCCGTCAAAAAGTGGTAAAG	441	qPCR	Müller et al., 2004; Silva et al., 2006; Sung, 2005
	<i>Dehalococcoides mccartyi</i> ; <i>Dehalococcoides mccartyi</i> strains 195, BAV1, FL2, GT	Primer F Primer R Probe	CGGGCGGATGCACTATTTT GAATAGTCCGTGCCCTTCCTC FAM-CGCAGTAACTCAACCATTCTGGTAGTGG-TAMRA		qPCR	Ritalahti et al., 2006; Sung, 2005
	<i>Dehalococcoides mccartyi</i> strains 195, BAV1; microorganisms from ANAS culture	Primer F Primer R	CTATGAAGGCCCTCCAGATGC GTAACAGCCCCAATATGCAAGTA	1,482	qPCR	Holmes et al., 2006
	<i>Dehalococcoides mccartyi</i> ; <i>Dehalococcoides mccartyi</i> strains 195, BAV1; microorganisms from ANAS and KB-1 culture	Primer F Primer R Probe	CTCGGCTACCGAACGGATT GGGCAGGAGGATTGACACAT FAM-CGCACTGGTTATGGCAACCACTC-TAMRA		qPCR	Bælum et al., 2013; Holmes et al., 2006 Lee et al., 2008
	<i>Dehalobacter</i> spp.; <i>Dehalococcoides mccartyi</i> ; <i>Dehalococcoides mccartyi</i> strains BAV1, VS; <i>Desulfotobacterium</i> spp.; <i>Desulfomonile</i> spp.; <i>Desulfuromonas</i> spp.	Primer F Primer R	CCCTCCAGATGCTCCCTTTA ATCCCTCTCCCGTGTAACC	139	qPCR	Behrens et al., 2008; Kranzioch et al., 2015; Popat et al., 2012
	<i>Dehalococcoides mccartyi</i> strain 11a	Primer F Primer R Probe	GTATGGTCCGCCACATGATTC TCTTCTGGAGTACCCTCCCAITF FAM-CGCCACCTGATGGGAGCGTACC-TAMRA		qPCR	Lee et al., 2013
	<i>Dehalococcoides mccartyi</i> ; microorganisms from KB-1 culture	Primer F Primer R	GAAAGCTCAGCCGATGACTC TGTTGAGGTAGGGTGAAGG	204	qPCR	Scheutz et al., 2008; Waller et al., 2005

bvcA	<i>Dehalobacter</i> spp.; <i>Dehalococcoides mccartyi</i> ; <i>Dehalococcoides mccartyi</i> strains 195, BAV1; <i>Desulfotobacterium</i> spp.; <i>Desulfuromonas</i> spp.; <i>Geobacter</i> spp.; <i>Sulfurospirillum</i> spp.; microorganisms from ANAS culture	Primer F	TGCCTCAAGTACAGGTGGT	839	PCR, qPCR	Holmes et al., 2006; Krajmalnik- Brown et al., 2004; Silva et al., 2006; Sung, 2005
		Primer R	ATTGTGGAGGACCTACCT			
	<i>Dehalococcoides mccartyi</i> ; <i>Dehalococcoides mccartyi</i> strains 195, BAV1, FL2, GT	Primer F	AAAAGCACTTGGCTATCAAGGAC		qPCR	Ritalahti et al., 2006; Sung, 2005
		Primer R	CCAAAAGCACCACCAGGTC			
	Probe	FAM-TGGTGGCGACGTGGCTATGTGG-TAMRA GGTGCCGCGACTTCAGTT				
	<i>Dehalococcoides mccartyi</i> ; <i>Dehalococcoides</i> <i>mccartyi</i> strains 195, BAV1; microorganisms from ANAS and KB-1 culture	Primer F	TCGGCACTAGCAGCAGAAATT		qPCR	Bælum et al., 2013; Holmes et al., 2006; Lee et al., 2008
	Primer R	FAM-TGCCGAATTTTCACGACTTGGATGAAG- TAMRA				
	Probe					
	<i>Dehalobacter</i> spp.; <i>Dehalococcoides mccartyi</i> ; <i>Dehalococcoides mccartyi</i> strain BAV1; <i>Desulfotobacterium</i> spp.; <i>Desulfomonile</i> spp.; <i>Desulfuromonas</i> spp.	Primer F	TGGGGACCTGTACCTGAAAA	247	qPCR	Behrens et al., 2008; Kranzloch et al., 2015; Popat et al., 2012
	Primer R	CAAGACGCATTGTGGACATC				

3.2 Aerobic metabolic degradation

In aerobic environments, CEs can be metabolically oxidized. During metabolic oxidative dechlorination, CEs are used as a growth substrate (electron donor) under aerobic conditions, bacteria utilizing CEs as a carbon and energy source. Oxidative degradation of CEs is more efficient with decreasing number of chlorine substituents. Aerobic metabolic degradation has been observed for TCE, cDCE and VC (Bradley, 2003). Aerobic metabolic degradation of VC is widespread, while aerobic TCE and cDCE oxidation occurs rarely. Notably, metabolic oxidative dechlorination may occur at very low oxygen concentrations. Microcosm studies indicate that aerobic oxidation of VC occurs often and that VC anaerobic oxidation in presumed anaerobic environments may in fact be aerobic oxidation occurring at low oxygen concentrations.

3.2.1 Bacteria capable of aerobic metabolic degradation

Several bacteria have been identified as capable of aerobic metabolic degradation of CEs. So far, no bacteria have been isolated for PCE and TCE degradation; however, evidence for growth on TCE has been provided (Schmidt et al., 2014). *Polaromonas* sp. strain JS666 is able to degrade cDCE through metabolic oxidative processes (Table 3 and references therein). Other examples of bacteria that are capable of aerobic metabolic degradation of VC are listed in Table 1. Three potential VC assimilating bacteria, *Rhodoferax*, *Tissierella* and *Brevundimonas*, have also recently been detected (Paes et al., 2015).

Table 3: Summary of bacteria capable of degrading PCE, TCE, cDCE and VC via aerobic metabolic or co-metabolic pathways. PC – pure culture, MC – mixed culture, CFE – cell-free extract (from Dolinová et al., 2017).

Species	Degradation aerobic pathway		Degraded chloroethenes	Material used	References
	Metabolic	Cometabolic			
<i>Alcaligenes eutrophus</i> strain JMP		+	TCE	PC	Harker and Kim, 1990
<i>Bacillus</i> sp. strain 2479	+	+	TCE	PC	Dey and Roy, 2009; Kim et al., 2010
<i>Bordetella</i> sp. strain KP22		+	TCE	PC	Hanada et al., 1998
<i>Brevundimonas</i> sp.	+		VC	MC	Paes et al., 2015
<i>Burkholderia cepacia</i> strain KP24		+	TCE	PC	Hanada et al., 1998
<i>Burkholderia cepacia</i> strain G4		+	TCE	PC	Nelson et al., 1987, 1986
<i>Burkholderia</i> sp. E1		+	TCE	PC	Futamata et al., 2001a
<i>Comamonas testosteroni</i> strain R5, E6, R2, R5		+	TCE	PC	Futamata et al., 2001a, 2001b
<i>Methylobacter</i> sp. strain BB5.1		+	TCE	PC	Smith et al., 1997
<i>Methylococcus capsulatus</i>		+	TCE	PC, CFE	Stirling and Dalton, 1979
<i>Methylocystis</i> sp. strain M		+	TCE, cDCE	PC	Uchiyama et al., 1989
<i>Methylomonas methanica</i> strains KSWIII, KSPIII and KSPII		+	TCE	PC	Hanada et al., 1998; Shigematsu et al., 1999
<i>Methylomonas methanica</i> strain 68-1		+	TCE	PC	Koh et al., 1993
<i>Methylosinus sporium</i> strain 27		+	TCE	PC	Tsien and Hanson, 1992
<i>Methylosinus trichosporium</i> strain OB3b		+	TCE	PC	Oldenhuis et al., 1989; Tsien et al., 1989
<i>Mycobacterium</i> sp. strains JS60, JS61, JS616, JS617	+		VC	PC	Coleman et al., 2002a
<i>Mycobacterium</i> sp. strain TRW-2	+		cDCE, VC	PC	Fatpure et al., 2005
<i>Mycobacterium aurum</i> strain L1	+		VC	PC	Hartmans et al., 1985
<i>Mycobacterium vaccae</i> strain JOB5		+	TCE, cDCE, VC	PC	Wackett et al., 1989
<i>Nitrosomonas europaea</i>		+	TCE	PC	Arciero et al., 1989
<i>Nocardioides</i> sp. strain JS614	+		VC	PC	Coleman et al., 2002b
<i>Nocardioides</i> sp. strain CF8		+	TCE	PC	Hamamura et al., 1997
<i>Ochrobactrum</i> sp. strain TD	+		VC	PC	Danko et al., 2004
<i>Polaromonas</i> sp. strain JS666	+		cDCE	PC	Coleman et al., 2002a
<i>Pseudomonas</i> sp. strains CF600, PsF WAS2		+	TCE	PC	Futamata et al., 2001a
<i>Pseudomonas</i> sp. strain JR1		+	TCE, cDCE, VC	PC	Dabrock et al., 1992
<i>Pseudomonas</i> sp. strain ENVPC5		+	TCE	PC	McClay et al., 1995
<i>Pseudomonas aeruginosa</i> strain DL1	+	+	VC	PC	Verce et al., 2001
<i>Pseudomonas aeruginosa</i> strain MF1	+		VC	PC	Verce et al., 2000
<i>Pseudomonas butanavora</i>		+	CDCE	PC	Doughty et al., 2005
<i>Pseudomonas butanavora</i> strains Rev WT, F321Y, L279F, G113N		+	TCE, cDCE	PC	Halsey et al., 2007
<i>Pseudomonas fluorescens</i>		+	TCE	PC	Y. Li et al., 2014
<i>Pseudomonas jessenii</i>		+	TCE	PC	Futamata et al., 2001a
<i>Pseudomonas mendocina</i> strain KR-1		+	TCE	PC	Winter et al., 1992
<i>Pseudomonas plecoglossicida</i>		+	TCE, cDCE	PC	J. Li et al., 2014
<i>Pseudomonas putida</i>		+	TCE	PC	Heald and Jenkins, 1994
<i>Pseudomonas putida</i> strain P-2, P-5, P-6, P8, P35X, BP and ATCC 17484		+	TCE	PC	Futamata et al., 2001a
<i>Pseudomonas putida</i> strain AJ	+		VC	PC	Danko et al., 2004

<i>Pseudomonas putida</i> strains B5 and PpF1	+	TCE	PC	Nelson et al., 1988
<i>Pseudomonas putida</i> strain F1	+	TCE, cDCE	PC	Wackett and Gibson, 1988
<i>Pseudomonas rhodesiae</i>	+	TCE	PC	Futamata et al., 2001a
<i>Pseudomonas stutzeri</i> strain OX1	+	PCE	PC	Ryoo et al., 2000
<i>Ralstonia</i> sp. strain P-10	+	TCE	PC	Futamata et al., 2001a
<i>Ralstonia</i> sp. strain TRW-1	+	cDCE, VC	PC	Elango et al., 2006
<i>Ralstonia eutropha</i>	+	TCE	PC	Hanada et al., 1998
<i>Ralstonia eutropha</i> strain KT-1	+	TCE	PC	Futamata et al., 2001a
<i>Rhodococcus</i> sp. strain L4	+	TCE	PC	Suttinun et al., 2009
<i>Rhodococcus</i> sp. strain PB1	+	cDCE, VC	PC	Frasconi et al., 2008
<i>Rhodococcus corallinus</i> strain B-276	+	TCE	PC	Saeki et al., 1999
<i>Rhodococcus erythropolis</i> strain BD1	+	TCE, cDCE	PC	Dabrock et al., 1992
<i>Rhodococcus gordoniae</i> strain P3	+	TCE	PC	Suttinun et al., 2004
<i>Rhodoferax</i> sp.	+	VC	MC	Paes et al., 2015
<i>Stenotrophomonas maltophilia</i> strain PM102	+	TCE	PC	Mukherjee and Roy, 2012
<i>Tissierella</i> sp.	+	VC	MC	Paes et al., 2015
<i>Variovorax</i> sp. strains c24, YN08, HAB-24, HAB-30	+	TCE	PC	Futamata et al., 2005
<i>Variovorax</i> sp. strain WFF52	+	TCE	PC	Futamata et al., 2001a
<i>Xhobacter</i> sp. strain Py2	+	TCE, cDCE, VC	PC	Ensign et al., 1992; Reij et al., 1995

3.2.2 Enzymes and functional genes in aerobic metabolic degradation

The main enzymes involved in aerobic metabolic degradation of CEs are the oxygenases. Monooxygenases and dioxygenases catalyze the reduction of oxygen with incorporation of one or two oxygen atoms, respectively, into the substrate being oxidized. During aerobic metabolic degradation of CEs, bacteria mainly use epoxidation catalyzed by monooxygenases and dioxygenases, resulting in the formation of CEs epoxides. Monooxygenases are induced by growth substrates and/or non-growth substrates degraded by cometabolism. There are many differences within the monooxygenases, including different substrate ranges, cellular locations (soluble or particulate), prosthetic groups and protein structures. Similarly, there are many different monooxygenase types in bacteria, with the soluble di-iron monooxygenase (SDIMO) family the most common. SDIMOs are multicomponent enzymes encoded by operons of at least four genes (Leahy et al., 2003) and six SDIMO groups have been distinguished by gene sequences (Coleman et al., 2006).

Epoxides are formed during aerobic degradation of CEs. Epoxides are not stable in aqueous systems as they react very quickly and may cause cell damage through formation of epoxide-macromolecule adducts. Thus, organisms produce epoxide-transforming enzymes for epoxide detoxification, such as EaCoMT (Coleman and Spain, 2003), epoxide carboxylases, epoxide hydrolases and glutathione S-transferases (GSTs).

Polaromonas sp. strain JS666 has been thoroughly investigated for its cDCE biodegradation capability. Using the carbon isotope fractionation method, it has been shown that this strain can degrade cDCE by monooxygenase-catalyzed epoxidation. The initial step of cDCE degradation in *Polaromonas* sp. strain JS666 catalyzes cytochrome P450 monooxygenase (Nishino et al., 2013; Shin, 2010). The degradation pathway for cDCE is probably through formation of dichloroacetaldehyde as its accumulation has been observed during cDCE degradation and activities of dichloroacetaldehyde dehydrogenase were detected in *Polaromonas* sp. strain JS666 cell extracts (Nishino et al., 2013). This degradation pathway reduces the formation of cDCE epoxide. Nishino et al. (2013) suggested that cDCE degradation via dichloroacetaldehyde, with the involvement of cytochrome P450 monooxygenase, could be the main pathway by which this is achieved. On the other hand, it has been hypothesized that cDCE degradation in *Polaromonas* sp. strain JS666 through epoxidation may be a minor degradation pathway and that the first step during degradation is carbon-chloride cleavage catalysed by glutathione S-transferase.

The degradation pathway of VC has also only partly been described (Mattes et al., 2005). Several bacterial strains appear to use the same enzymes during VC and ethene degradation (Coleman and Spain, 2003; Hartmans and De Bont, 1992; Mattes et al., 2005). An important enzyme in VC metabolic degradation is alkene monooxygenase (AkMO), which catalyzes epoxidation of VC to chlorooxirane (VC epoxide), followed by epoxyalkane coenzyme M transferase (EaCoMT), which mediates conjugation of coenzyme M to the epoxide and converts to 2-hydroxyethyl coenzyme M. The remaining steps in the VC degradation pathways are poorly understood.

Genes for VC degradation (such as those encoding AkMO and EaCoMT) are encoded on large plasmids. AkMO and EaCoMT are encoded by a single operon, *etnEABCD*, while the functional genes encoding EaCoMT and the AkMO alpha subunit are *etnE* and *etnC*, respectively (Mattes et al., 2010). Coleman and Spain (2003) suggested that AkMO of *Mycobacterium* sp. strain JS60 is a four-component enzyme encoded by *etnABCD* genes. The functional gene *etnC* encodes the alpha subunit of AkMO. Products of the *etn* locus include the *etnA* gene, which encodes the beta subunit of AkMO, *etnB*, which encodes the AkMO coupling-effector protein, and *etnD*, which encodes AkMO reductase.

However, our knowledge of pathway details for CEs biodegradation and the enzymes involved remains incomplete. Detection of the functional genes *etnC* and *etnE* (Coleman et al., 2006; Jin and Mattes, 2010; Paes et al., 2015) is a useful tool for determination of active VC assimilating bacteria. Previously published primers for the detection of functional *etnC* and *etnE* genes are listed in Table 4. Note that application of the *etnC* and *etnE* genes for detection of active VC assimilating bacteria can be hindered as these gene sequences are the same, or very similar, to genes in ethene assimilating bacteria (Coleman, 2015). Primers used for detection of functional genes in aerobic bacteria degrading CEs metabolically or co-metabolically are listed in Table 4.

Table 4: Primers used for detection of functional genes in aerobic bacteria degrading chloroethenes metabolically or cometabolically. F = forward primer, R = reverse primer (from Dolinová et al., 2017).

Target gene	Target microorganism	Primer/Probe	Primer sequence (5'-3')	Amplicon (bp)	Method used	Reference		
etnC	VC-assimilating bacteria	Primer F	CAGGAGTCSCTKGACCGTCA	360	PCR	Coleman et al., 2006		
		Primer R	CARACCGCCGTAKGACTTTGT					
		Primer F	ACCTGGTCGGTGTKSTYTC	106	qPCR		Jin and Mattes, 2010	
		Primer R	TCATGTAMGAGCCGACGAAGTC					
		Primer F	ACACTCGTCGGCGTTGTTTC	106	qPCR			Jin and Mattes, 2011
		Primer R	TCATGTACGAGCCGACGAAGTC					
etnE	VC-assimilating bacteria	Primer F	AACTACCCSAAYCCSCGCTGGTACGAC	891	PCR	Coleman and Spain, 2003		
		Primer R	GTCGGCAGTTTCGGTGATCGTGC TCTTGAC					
		Primer F	CAGAA YGGCTGYGACATYATCCA	151	qPCR		Jin and Mattes, 2010	
		Primer R	CSGGYGTGCCGAGTAGTTWCC					
		Primer F	CAGAATGGCTGTGACATTATCCA	151	qPCR			Jin and Mattes, 2011
		Primer R	CTGGTGTGCCGAGTAGTTTCC					
SDIMO	diverse bacteria	Primer F	CAGTCNGAYGARKCSCGN CAYAT	1100	PCR	Coleman et al., 2006		
		Primer R	CGDATRTCRTCDATNGTCCA	720				
		Primer F	CARATGYTNGAYGARGTNCGNCA	810				
		Primer R	CCANCCNGGRTAYTTRTTYTCRAACCA	420				
		Primer F	GGNGACTGGGACTTCTGG	525			PCR	Holmes et al., 1995 Costello and Lidstrom, 1999 Bourne et al., 2001
		Primer R	GAASGCNGAGAAGAASGC					
pmoA	methanotrophic bacteria	Primer F	GGNGACTGGGACTTCTGG	470	PCR	Holmes et al., 1995 Costello and Lidstrom, 1999 Bourne et al., 2001		
		Primer R	CCGGMGCAACGTCYTTACC					
		Primer F	GGNGACTGGGACTTCTGG	500				
		Primer R	ACGTCCTTACCGAAGGT					
		Primer F	GGNGACTGGGACTTCTGG	500				
		Primer R	CCGGMGCAACGTCYTTACC					
mmoX	methanotrophic bacteria	Primer F	ATCGCBAARGAATAYGCSCG	719	PCR	Hutchens et al., 2004		
		Primer R	ACCCANGGCTCGACYTTGAA					

3.3 Aerobic cometabolic degradation

CEs are degraded by many methanogenic, acetogenic, sulphate and iron oxidizing bacteria, with no carbon or energy benefit, during cometabolic degradation. Aerobic cometabolic degradation has been observed for PCE, TCE, cDCE and VC. Bacteria capable of degrading CEs via aerobic cometabolic degradation use other growth substrates (auxiliary substrates); the CEs being degraded by enzymes originally produced for the degradation of bacterial growth substrates. Hence, the cometabolic degradative process requires growth substrates, such as 2,4-diphenoxyacetic acid, ammonium, cumene, ethane, ethene, isoprene, phenol, propene, methane or toluene, to provide an energy source and induce production of the cometabolic enzymes. Cometabolic processes run relatively slowly compared to metabolism of growth substrates.

3.3.1 Bacteria capable of aerobic cometabolic degradation

Many bacteria have been identified as capable of aerobic cometabolic degradation of CEs, though only *Pseudomonas stutzeri* OX1 can cometabolically degrade PCE (Table 1 and references therein). Bacteria capable of aerobic cometabolic degradation of TCE, cDCE and VC are listed in Table 3.

3.3.2 Main enzymes involved in cometabolic degradation

It is assumed that during aerobic cometabolic degradation of CEs, bacteria primarily use epoxidation of the carbon-carbon double bond catalysed by monooxygenases and dioxygenases, forming CE epoxides as monooxygenases or dioxygenases incorporate one or two atoms of molecular oxygen into the CEs. CE epoxides react with macromolecules in cells, or are spontaneously hydrolysed into carbon monoxide, chloride, formic acid, dichloroacetic acid and other products. Subsequently, these water-soluble products undergo bacterial mineralization and are converted to carbon dioxide, chloride and water.

While a number of enzymes with broad substrate ranges are used during CE cometabolism, there are many differences between them. The most common enzymes are methane monooxygenase (soluble monooxygenase and membrane-bound or particulate monooxygenase), toluene mono- and dioxygenase (toluene-2-monooxygenase, toluene-4-monooxygenase, xylene monooxygenase and toluene dioxygenase), alkene monooxygenase and ammonia monooxygenase. A variety of monooxygenases or

dioxygenases have now been detected. Examples include isopropyl benzene/toluene dioxygenase (expressed by *Rhodococcus erythropolis* strain BD2 and *Rhodococcus* sp. strain L4), alkene monooxygenase (expressed by *Rhodococcus corallines*), ammonia monooxygenase (expressed by *Nitrosomonas europaea*), butane monooxygenase (expressed by *Pseudomonas butanovora*, *Mycobacterium vaccae* and *Nocardioides* sp. strain CF8), soluble methane monooxygenase (sMMO) (expressed by *Methylosinus trichosporium* strain OB3b and *Methylococcus capsulatus*), toluene dioxygenase (expressed by *Pseudomonas putida* strain F1), and toluene 2-monooxygenase (expressed by *Burkholderia cepacia* strain G4).

The non-specific enzyme methane monooxygenase (MMO) is important for catalyzing cometabolism of chlorinated solvents in methanotrophs. MMO exists in two forms, soluble MMO (sMMO) and membrane-bound or particulate MMO (pMMO). sMMO catalyzes CEs more rapidly than pMMO during cometabolic degradation. sMMO also has the highest specific activity to TCE from *Methylosinus trichosporium* strain OB3b. While epoxides are generated during TCE degradation by sMMO of *Methylosinus trichosporium* strain OB3b, TCE degradation of *Pseudomonas putida* strain F1 by toluene dioxygenase appears not to generate any.

During CE oxidation by sMMO, corresponding reactive epoxides are formed with harmful degradation products. The instability of epoxides in aqueous solutions complicates their analysis; hence, little is known of their degradation kinetics. Both abiotic and biotic conversion of epoxides has been detected during CE cometabolism in *Methylosinus trichosporium* OB3b expressing sMMO (van Hylckama et al., 1996). Van Hylckama et al. (1996) also showed that almost all epoxides leave the cell and that only cis-1,2-DCE epoxide is transformed by sMMO.

Active sites of enzymes involved in catalyzing cometabolic reactions may react with a range of substrates; hence, competition for active sites may occur resulting in a decrease in enzyme affinity for each substrate. Competitive inhibition between growth and cometabolic substrates can be found in many bacteria. While the presence of a growth substrate stimulates reductant recovery, the growth substrate can cause competitive inhibition. Moreover, noncompetitive inhibition may also occur, whereby the enzyme has different binding sites for growth and cometabolic substrates, causing a decrease in reaction rate without a decrease in substrate affinity.

During aerobic cometabolic degradation, CEs and their oxidation products may cause toxic conditions, leading to decreased enzyme activity for CE degradation and bacterial damage and inactivation (Yeager et al., 2001). These toxic products can also have a harmful effect on essential cellular components. However, microorganisms can recover, despite the constant presence of a damaging contaminant. For example, TCE-damaged cells of *Nitrosomonas europaea* were still active and their reparation enzymatic apparatus helped them recover, though this capacity depended on the site and type of injury. Direct alkylation or other impacts on active sites may cause serious damage, therefore, but not necessarily cell death, as long as metabolic and recovery processes remain functional.

4 Molecular biology tools

4.1 Introduction

Molecular biology tools were first used for the testing of human health in the late twentieth century and have been increasingly used since in many scientific fields. Molecular biological techniques can be used to study encoded information wherever DNA (deoxyribonucleic acid) or RNA (ribonucleic acid) are present. Regarding microbiology, molecular biology was first used for characterization and manipulation of bacterial strains, with pure bacterial strains tested and described in amazing detail. The newly gained knowledge of bacterial genomes and metabolism led to the establishment of specific markers typical for specific bacterial groups. Environmental microbial genetics in relation to bioremediation has become very popular in recent years. Detection of bacterial strains capable of biodegradation and specific degradation pathway enzymes, together with the characterization of whole bacterial consortia by next generation sequencing, are the methods most used today.

The polymerase chain reaction (PCR), developed in 1983 by Kary Mullis, is now a commonly used and key method, allowing a huge expansion in molecular biology applications. The method is applied not only for detection of specific markers but also serves as the first amplification step for numerous other techniques and as the basis for modification (e.g. DNA cloning for sequencing, gene mutagenesis, functional analysis of genes, diagnosis of hereditary diseases, analysis of genetic fingerprints for DNA profiling, detection of pathogens). In 1993, Mullis, along with Michael Smith, was awarded the Nobel Prize in Chemistry for his work on PCR.

Real-time PCR (qPCR), the most frequent modification to the basic method, is employed for quantification of genes. During the amplification reaction, a fluorescent signal is detected by a CCD camera, enabling the detection of specific genera (e.g. *Dehalococcoides* for CE biodegradation), enzymes (e.g. *linA* for hexachlorocyclohexane (HCH) biodegradation) or bacterial groups (e.g. the *dsrA* gene for sulphate-reducing bacteria during environmental analysis).

Next-generation sequencing (NGS), the next most widely used technique in microbial genetics, allows for the characterization of both unique bacterial species and whole bacterial consortia. Additionally, the technique has great potential for describing the functionality of both single bacterial strains and whole bacterial consortia present at a contaminated locality.

4.2 Real-time PCR analysis

qPCR techniques are routinely used for the characterization of contaminated localities. qPCR is a major development of PCR technology that enables reliable detection and measurement of products generated during each cycle of the PCR process. Combining PCR amplification and detection into a single step (Fig. 6a), this approach eliminates the need to detect products using gel electrophoresis and, more importantly, it enables the method to be truly quantitative. qPCR reactions use the same components as standard end-point PCR reactions, with the addition of a fluorescent label (fluorescent probe or fluorescent dye) that creates a signal during the PCR reaction. Fluorescent dyes label PCR products during thermal cycling and the accumulation of fluorescent signals is measured during the exponential phase of the reaction. As an example, SYBR™ Green dye binds to double-stranded DNA and emits fluorescence only when bound (Fig. 6b).

By using highly efficient PCR primers and optimal amplification conditions, each target molecule is copied once in each cycle (Fig. 7) and data are captured throughout thermal cycling.

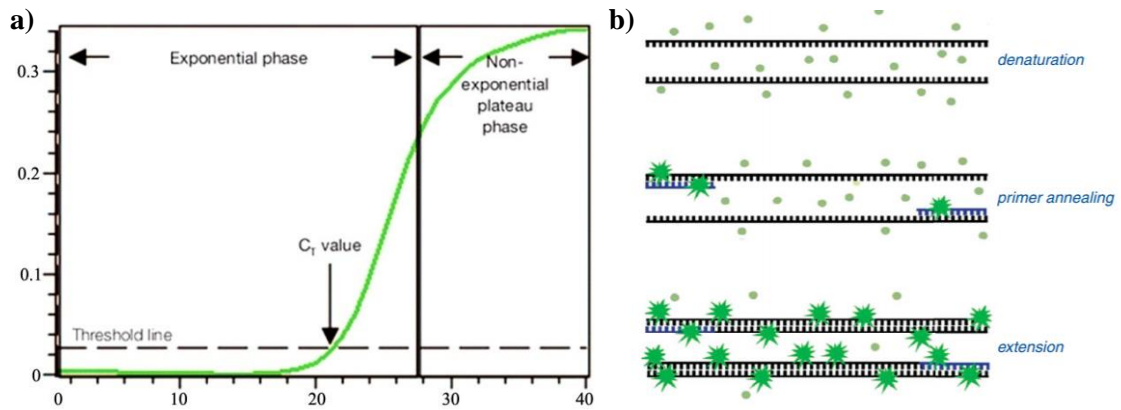


Fig. 6: a) Principle of real time PCR; b) effect of SYBR™ Green colour during PCR amplification (Fraga et al., 2014).

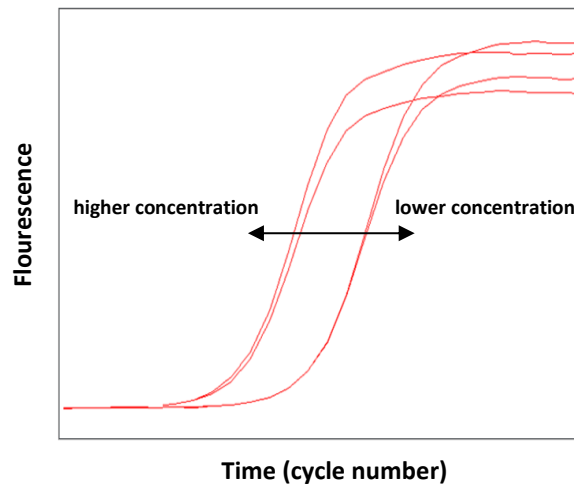


Fig. 7: Principle of Real time PCR detection. (Dolinová et al., unpublished data).

Positive and negative DNA are added during each reaction to ensure that the specific product is amplified. The use of a positive control acts as an amplification control when all DNA tests prove negative. If the negative control (reaction mixture without DNA) shows an amplification signal, it indicates that the reaction mixture is contaminated. All raw fluorescent results are later analyzed using software installed on the instrument. The relative quantity calculation based on Pfaffl (2001) is demonstrated in Equations 1-3. The relative quantities of specific strains and functional genes is calculated by comparing C_q values as a power, with primer amplification efficiency (EF) as a base and the difference between the measured and normalized crossing point and first sampling reference crossing point as an exponent.

Relative quantity calculation:

$$C_q \text{ standardization} = C_q \text{ value} + \log_{10}(\text{sample amount} - g, L) / \log_{10}(EF) \quad (\text{Eq. 1})$$

$$\text{Relative quantification} = EF^{-(C_{q_{\text{sample}}} - C_{q_{\text{ref}}})} \quad (\text{Eq. 2})$$

$$\text{Dilution standartization} = \text{relative quantification} / \text{dillution} \quad (\text{Eq. 3})$$

An example of the output from a qPCR analysis is shown in Fig. 8. The Figure shows the relative quantity of specific markers after carbo-iron application. Depending on the approach used, each molecular biological marker should be considered separately rather than comparing absolute numbers, thereby allowing observation of trends in relative abundance.

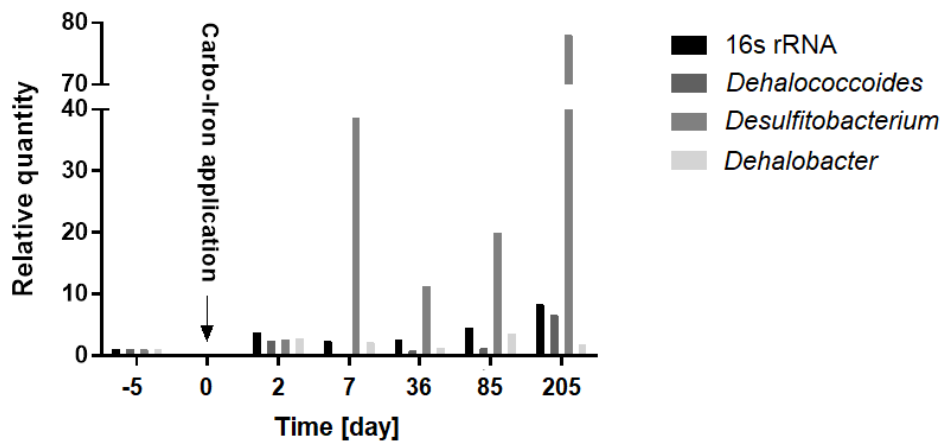


Fig. 8: Changes in the relative abundance of markers in a CE-polluted well following carbo-iron application. Note fragmentation of the y-axis (Dolinová, unpublished data).

4.3 Next-generation sequencing

NGS analysis is a relatively new molecular genetics approach that can be applied in a wide range of analyses. NGS, also known as high-throughput sequencing, includes a range of sequencing technologies such as Illumina sequencing (iSeq, MiniSeq, MiSeq, NextSeq, HiSeq, HiSeq X and NovaSeq) or Thermo Fisher Scientific platforms (Ion Torrent, Ion S5 and SOLiD). Emerging technologies, such as nanopore sequencing pioneered by Oxford Nanopore Technologies (SmidgION, MinION, GridION and PromethION) or the Pacific Biosciences platform (PacBio RSII and the Sequel system), can be considered as the next step in NGS. These recent technologies allow more rapid and cheaper sequencing of DNA and RNA than capillary Sanger sequencing.

Regarding environmental samples, NGS can be used to analyse bacterial communities in detail. NGS is the only method that enables analysis of a complex bacterial community without the necessity of cloning DNA fragments into vectors and subsequent culturing in the cell. This allows bacterial communities from different contaminated sites or different matrix samples to be analysed and compared. One restriction of NGS analysis is the input concentration of isolated DNA, which will ultimately affect the quality of the data obtained. At concentrations below $2 \text{ ng}\cdot\text{mL}^{-1}$, results are less representative, especially for less frequent microbial taxa.

NGS method also allow sequencing of whole bacterial genomes in mixed samples (metagenome) and complex genomes of single bacterial strains. Hence, this method can determine the degradation potential of a given bacterial community or a particular bacterial strain.

Last but not least, mRNA sequencing enables monitoring of the profiles of actively transcribed genes for enzymes that perform specific activities or actively propagating bacteria. This allows differences in the expression of enzymes to be tracked at different depths in contaminated groundwater or soil, or observation of differences under aerobic and anaerobic conditions.

One NGS sequencing methods used extensively in this thesis is the detection of pH changes using the Ion Torrent device (Thermo Fisher Scientific, USA). Signal detection uses the amplification principle, whereby a hydrogen proton is released during each base polymeration. The hydrogen protons released lead to differences in pH, which can then be detected. This system does not need light signals for detection; hence, high quality and unmodified enzymes can be used. The principle of the sequencing reaction is shown in Fig. 9.

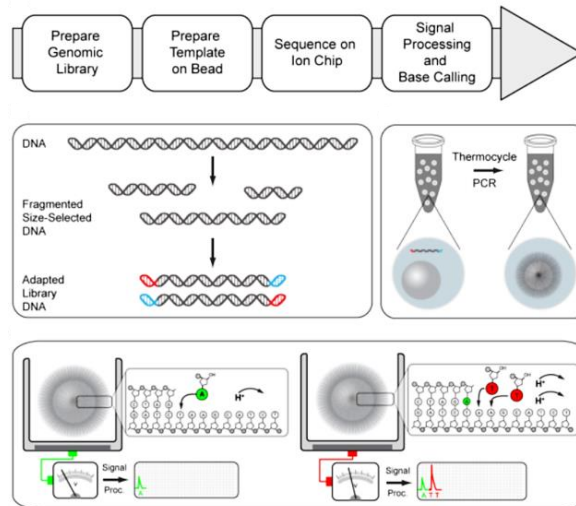


Fig. 9: Principle of NGS sequencing on the Ion Torrent device (Genomics, http://www.genomics.cn/en/navigation/show_navigation?nid=2640, verified 2.6.2018.).

4.3.1 Amplicon analysis of 16S rRNA genes

A further NGS approach is amplicon sequencing, which allows sequencing of part of a genome, allowing one to focus on either functional genes or the 16S rRNA gene during phylogenetic bacterial analysis. Amplicon sequencing requires primers designed to target the genes of interest, allowing for the analysis of particular genes (Fig. 10).

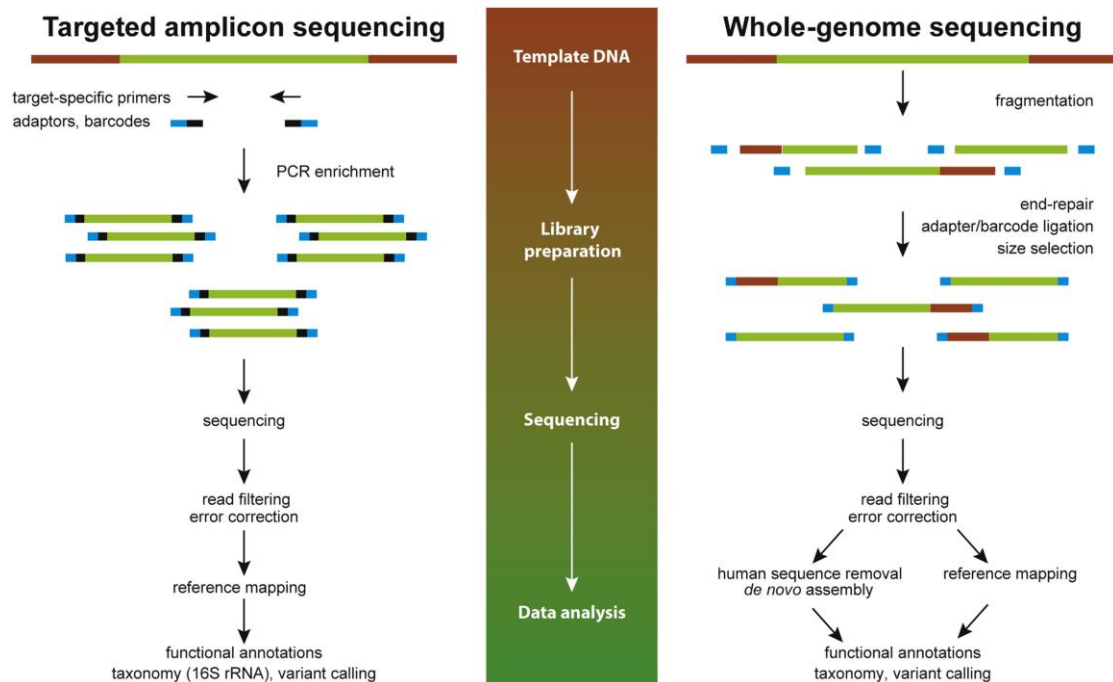


Fig. 10: NGS approaches – amplicon and whole genom sequencing (Lefterova et al., 2015).

The 16S rRNA gene is a component of the 30S small subunit of a prokaryotic ribosome and is used for reconstructing phylogenies due to the slow rate of evolution in this region (Fig. 11).

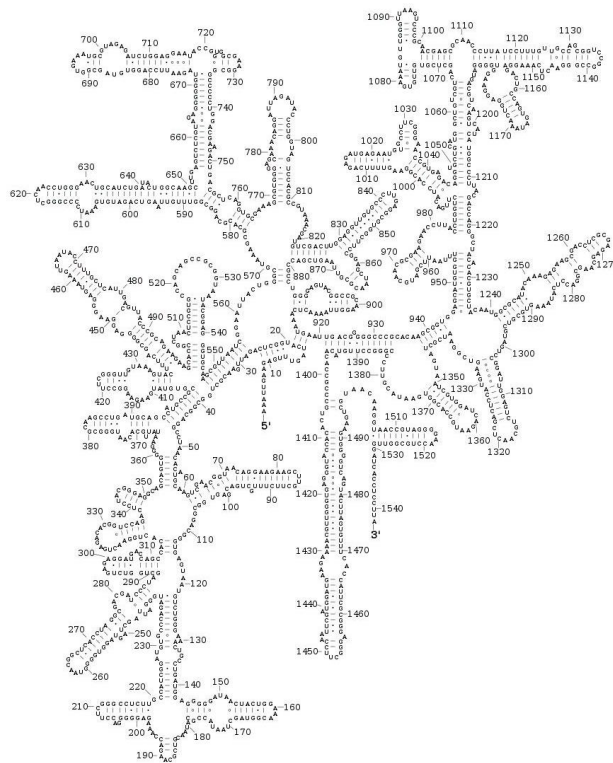


Fig. 11: 16S rRNA structure (http://rna.ucsc.edu/rnacenter/xrna/xrna_gallery.html, verified 2.6.2018.).

The 16S rRNA gene consists of exactly 1542 nucleotides containing areas that are very well preserved in all microorganisms, as well as areas that are variable and characteristic for each bacterial species. Sequencing of the 16S rRNA gene is used to create phylogenetic trees depicting possible kinships between the microorganisms studied.

NGS data can be displayed using three graphical outputs, heat maps, OTU graphs and Venn diagrams, examples of which are provided in Figs. 12, 13 and 14. Heat-maps (Fig. 12) display individual sample relationships based on bacterial diversity. OTU graphs (Fig. 13), on the other hand, show bacterial diversity and differences within individual samples, while Venn diagrams show numerically shared and unique OTUs (Fig. 14).

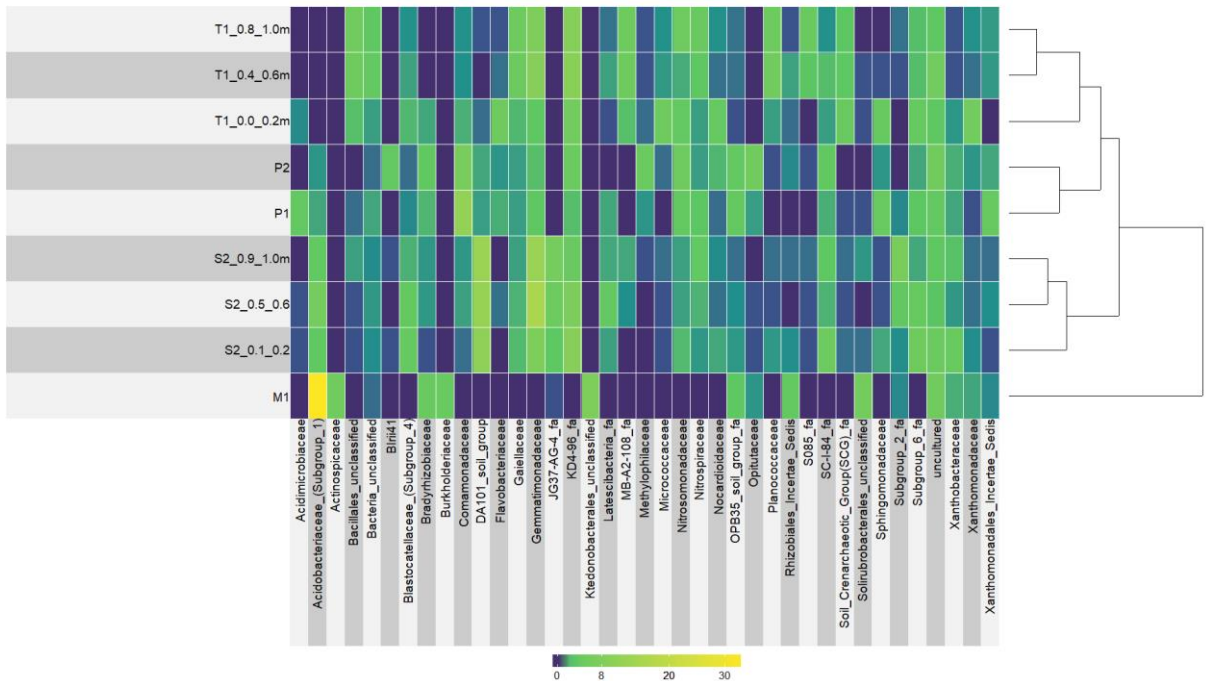


Fig. 12: Heat map showing the abundance of individual microbial taxa and the relationship between individual samples (Dolinová et al., unpublished data).

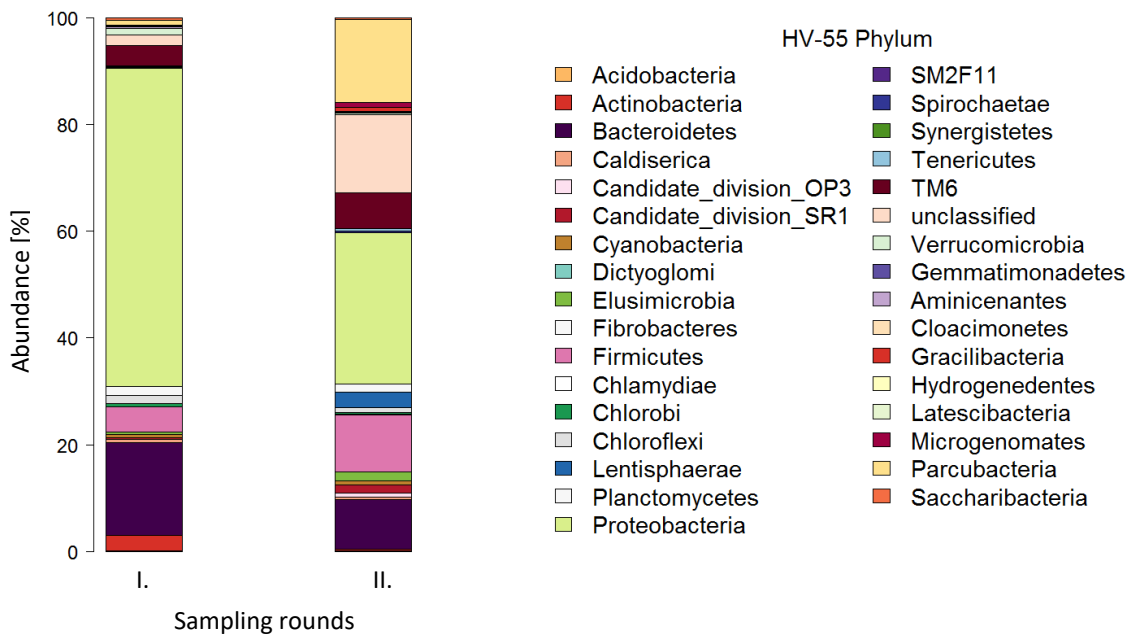


Fig. 13: OTU column diagram showing individual microbial taxa and their percentage representation (Dolinová et al., unpublished data).

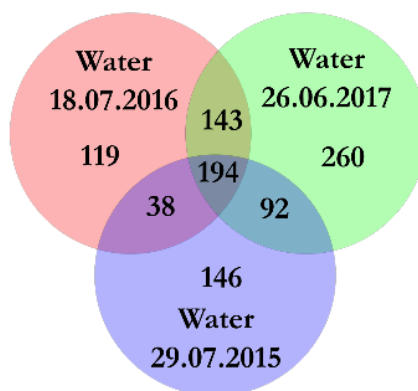


Fig. 14: Venn diagram showing the numbers of unique (exclusive) and shared OTUs for each sample combination (Dolinová et al., unpublished data).

5 Nanofibre carriers for biomass sampling at contaminated sites

5.1 Problems related to sampling procedure

Characterization, including proper sampling, of a microbial community is a crucial factor in understanding and controlling remediation processes or the assessment of the microbial quality of water. The sampling procedure should not impact on the situation *in situ* and should be technically and economically feasible.

Groundwater from a well should be pumped out slowly until pH, ORP, conductivity and temperature are stabilized. Then, sterile plastic or glass bottles are filled with the groundwater and immediately transferred to the laboratory in a cooled box. Freezing of the samples is unnecessary the samples are transported to the laboratory quickly. When soil analysed, at least 50 g has to be sampled and stored in a sterile tube. Again, rapid transport in cooled box is crucial.

All groundwater samples are filtered through sterile 0.22 μM membrane filters (e.g. Durapore®, Merck Millipore, Germany) immediately after delivery to the laboratory. Filters with bacterial biomass are then used for DNA isolation and subsequent molecular biology analyses, or the samples can be stored at 80 °C.

Until recently, soil and water samples were collected at contaminated sites in order to characterize the microbial consortia. Although soil samples typically provide good results, their sampling is limited by high heterogeneity and thus low reproducibility and time and financial requirements.

As a result, water samples are now most often used for molecular genetic analysis. A disadvantage of water samples is the frequently low biomass concentration. This requires filtration of higher sample volumes, which is time-consuming, especially when particulate matter is high.

5.2 Nanofibre carriers

The problems mentioned above can be avoided by sampling biomass in the form of a biofilm, which develops on suitable carriers. Such carriers must be made of materials suitable for microbial cell colonization, i.e. high biocompatibility; chemical, physical and biological stability and convenient morphology (Lederer and Křiklavová, 2014).

Carriers used for biomass sampling can be classified by material, e.g. organic or inorganic, or by origin, e.g. natural or artificial (Dzionic et al., 2016). The properties of the individual groups are listed in Table 5.

Table 5: Properties of different biomass carriers in accordance to their origin and construction material (Dzionic et al., 2016).

Origin / Material	Inorganic	Organic
Natural	high chemical, physical and biological resistance <u>Examples:</u> volcanic rocks, zeolites	biodegradable, biocompatible, hydrophilic and inexpensive <u>Examples:</u> biopolymers (alginate), charcoal
Synthetic	high chemical, physical and biological resistance <u>Examples:</u> ceramics, porous glass	variable characteristics (density, shape, porosity, hydrophobicity,) determined by preparation parameters <u>Examples:</u> synthetic polymers (PP, PE, PU)

Although some natural biomass carriers are suitable for bioremediation purposes, they do not meet all the above requirements for molecular genetic analysis. For these methods, it is important that the maximum amount of biomass is obtained from the carrier with the minimum amount of substances that would interfere with DNA extraction and subsequent analysis. The biodegradability of natural organic carriers would also make long-term monitoring impossible. Inorganic carriers (natural or synthetic) have a number of significant disadvantages, including morphology, which complicates biomass extraction, and the presence of a small number of functional groups, which prevents sufficient bonding of the biocatalyst (Dzionic et al., 2016).

Synthetic organic carriers have the greatest potential of all four carrier-groups to meet the above-mentioned requirements, due to their variable characteristics (determined during preparation), which could result in the development of an optimal carrier for microbial biomass monitoring using molecular genetic analysis.

Chládek et al. (2000) proposed a biomass carrier formed from a system of fibres oriented in a defined manner. The fibre surface provides the carrier with a large area suitable for colonization by microorganisms and for fixation of a large amount of biomass. The large surface area also enables the volume of the carrier to be reduced. A support thread made of stronger fibres is incorporated into the carrier to improve carrier resistance to stress. Due to the flexibility of the fibres, the outer shape of the carrier varies and each of these structures can be of any size. These properties, and the ease with which the carrier can be dismantled, makes textile biomass carriers an effective monitoring tool.

Nanofibres deposited on a suitable substrate (e.g. threads) seems to be the optimal material for construction of biomass carriers. Nanofibres have a high specific surface area, an interconnecting structure and surface roughness on the nano- and micro-scale. Any surface constructed from hydrophobic materials and displaying these properties will be preferentially colonized by microbial cells, especially in the initial phase of biofilm formation. The characteristics of nanofibres (surface density, porosity and pore size) are determined by their preparation parameters (Niu et al., 2011; Sharma and Sharma, 2013).

5.3 Nanofibre preparation

Several methods have been developed for nanofibre preparation, e.g. drawing, template synthesis, phase separation and electrospinning. Currently, only needleless electrospinning (invented by Jirsák et al. 2009) allows for large-scale nanofibre production.

The needleless electrospinning system (Fig. 15) consists of three main parts, a high-voltage source, a rotating cylinder immersed in a polymer solution and a metal collector (grounded). The cylinder is connected to the high-voltage source and its surface is covered by a thin layer of the polymer material. As the applied voltage is increased, cones (known as Taylor cones) form on the surface of the liquid. When the applied voltage is higher than the threshold voltage, the electrostatic force becomes stronger than the surface tension of the liquid and a charged jet of the solution is ejected from the tip of each Taylor cone (Bhardwaj and Kundu, 2010; Wang and Li, 2012).

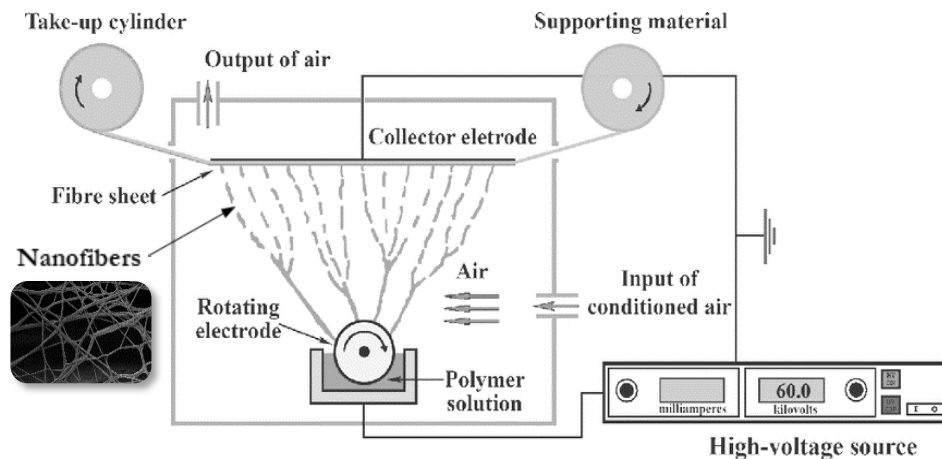


Fig. 15: Scheme of a needleless electrospinning set up. Adapted from Sasithorn et al. (2016).

The number and location of jets ejected from the free liquid surface (Fig. 16) naturally occur in their optimal positions (Petrik and Maly, 2009). Thinning and elongation of the jets occurs while they are drifting toward the collector. During these processes, the solvent evaporates.



Fig. 16: Electrospinning from a free liquid surface on a rotating electrode (Petrik and Maly, 2009).

The nanofibres generated are deposited on a supporting material (e.g. a textile or thread) situated in front of the collector electrode. The surface density of nanofibres on the supporting material is determined by the speed the supporting material is moved past the jets (Baji et al., 2010; Bhardwaj and Kundu, 2010).

EXPERIMENTAL SECTION

I. Evaluation of CE bioremediation using molecular biology tools

1 Background

The impact of different remediation procedures has been monitored during my studies at many localities varying in the level of contamination and in geochemical conditions. The influence of reducing (e.g. zero valent iron) and oxidizing (e.g. Fenton like reaction) agents on microbial taxa and biodegradation capability via molecular genetic markers were monitored. Detailed description of each individual experiment from all sites tested (i.e. Jablunkov, Náměšť nad Oslavou, Vysoké Mýto, Prague or Javořno in Poland) would be very demanding; hence, this chapter summarizes long-term *in situ* experiments at the Spolchemie site evaluated using molecular genetic analyses developed and adjusted during my Ph.D. study. At this site, the long-term effect of whey and hydrogen peroxide was monitored. The study was published in the journal *Chemosphere* (Dolinová et al., 2016a).

Microbial degradation of CEs takes place via anaerobic organohalide respiration, as explained above in the thesis background. In addition to bioremediation methods, a number of chemical techniques are also available for *in situ* remediation, with chemical oxidation using Fenton's reagent (a mixture of hydrogen peroxide [H_2O_2] and an iron catalyst [Fe^{2+}]) or a Fenton-like reaction (where there is a sufficient concentration of iron in the environment) being one of the most frequently applied methods for CEs. However, chemical oxidation can significantly restrict the activity of organohalide-respiring bacteria and cause changes in microbial population structure. Chemical oxidation can also oxidise organic matter in preference to CEs, resulting in a lack of carbon for autochthonous microorganisms (Chapelle et al., 2005). While changes to the microbial populations are a side effect of chemical oxidation, application of a substrate (electron donor), such as lactate, directly improves conditions for biological organohalide respiration.

Previous studies involving Fenton-like reactions or application of sodium lactate ($\text{NaC}_3\text{H}_5\text{O}_3$) have focused either purely on chemical parameters or on total organohalide-respiring microbial colonisation (Chapelle et al., 2005; Mattes et al., 2010; Sutton et al., 2011).

The aim of this study was to examine the influence of a Fenton-like reaction and biostimulation through sodium lactate application on dynamics of organohalide-respiring bacteria and their genes at actual site contaminated with CEs. To obtain more information for the accurate diagnosis of ongoing organohalide respiration, new approach combining analysis of molecular genetic markers, together with physical and chemical parameters, was used.

2 Materials and methods

2.1 Study site

The Spolchemie Company a.s. (Ústí nad Labem, Czech Republic) has been one of the leading synthetic resin and Freon manufacturers in Europe since the middle of the last century. Production of Freon, along with storage and distribution of raw materials (tetrachlormethane and tetrachlorethene), have led to extensive subsurface contamination with organic solvents, including CEs. The geological profile underlying the Spolchemie site consists of Mesozoic Cretaceous siltstones overlaid by a Quaternary terrace comprised mainly of fluvial sediments from the Rivers Bílina and Labe and the Klíšský stream. This subsurface Quaternary terrace has been contaminated.

The Spolchemie site is currently undergoing remediation treatment using a range of different approaches. In addition, newer methods such as application of nanoscale zero-valent iron and the Fenton reaction are also being tested at the site.

2.2 Application and reference wells

Samples were obtained from four wells at the Spolchemie site. Characteristics of sampling wells, including reagent and its dose applied, are displayed in Table 1. The well diameter was 180 mm.

Two wells located close to the source area of contamination (RW5-11 and RW5-12; Fig. 1A) were chosen to study the disposable effect of hydrogen peroxide application, used for the Fenton-like reaction, on organohalide-respiring bacteria. These wells are both situated along the outflow line from the former chlorinated hydrocarbons (CHC) production area and are predominantly contaminated with CEs and methanes, with methanes dominant at around 50 to 90%.

Table 1: Characteristics of the sampling wells. Also shown are the reagents and doses applied and the concentration of chlorinated hydrocarbons (CHC) prior to the experiment; bgl = below ground level.

Well	Depth [m bgl]	Ground water level [m bgl]	Drilling diameter [mm]	Volume of water [L]	Perforated casing [m bgl]	Reagent and dose	CHC prior dosing [$\text{mg}\cdot\text{L}^{-1}$]
RW5-11	15.0	3.3	220	280	4.0-14.0	3 wt. % H_2O_2 ; 100 L	1.93*
RW5-12	15.0	3.9	220	280	4.0-14.0	3 wt. % H_2O_2 ; 500 L	49.9*
RW5-49	15.5	3.3	220	220	4.0-14.5	sodium lactate ($12\text{ g}\cdot\text{L}^{-1}$); 20 m^3	0.15 [†]
RW5-24	11.5	3.4	300	290	2.0-10.1	none (reference well)	0.62 [†]

* 25 days prior to dosing

[†] 35 days prior to infiltration

No effect of *in situ* chemical oxidation originating from neighbouring wells was observed on the microbial consortium prior to this study. No reference well was used for comparison with those dosed with hydrogen peroxide, the conditions prior to application being taken as a reference point. Fig. 1B shows geological cross-section of the site showing the open casings of the wells and direction of underground water flow.

Well RW5-49 was used to study biostimulation through the application of sodium lactate and well RW5-24 was chosen as a control (no reagents applied) as it had not been influenced by any previous remedial action conducted at either the source area or the area of plume treatment (Fig. 1A).

Both wells RW5-49 and RW5-24 are situated along the marginal edge of the contamination plume zone (Fig. 1A) and are predominantly contaminated with PCE. Furthermore, well RW5-24 is situated on the inlet side and data from previous monitoring (2 years prior to this study) confirmed its long-term stability.

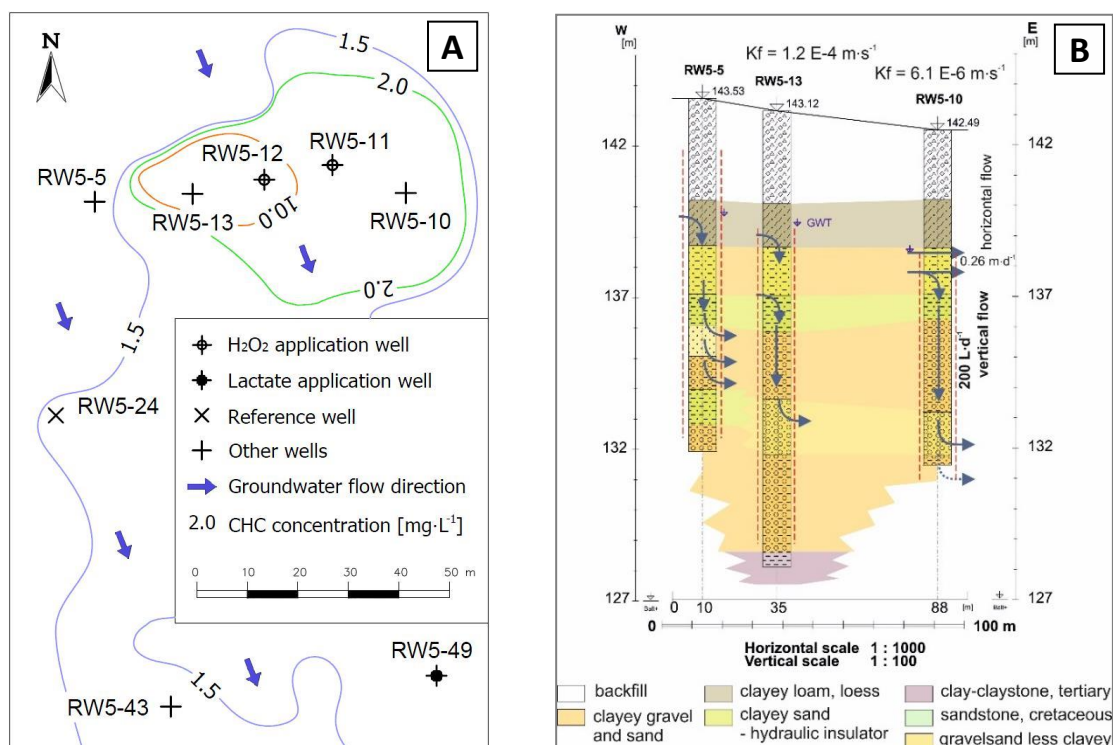


Fig. 1: A) Location of sampling and reference wells, including wells (RW5-5, RW5-10 and RW5-13) illustrating cross-section at the Spolchemie site (Ústí nad Labem, Czech Republic); and, B) geological cross-section of the site and direction of water flow (blue arrows).

As ferrous iron (Fe^{2+}) was present in the groundwater at a sufficient high concentration (reaching on average $51.7 \text{ mg}\cdot\text{L}^{-1}$) for a Fenton-like reaction at the contaminated wells (RW5-11 and RW5-12), no further iron was deemed necessary for the reaction to take place. Instead, reaction mixtures were prepared using hydrogen peroxide (3 wt.%, Eurosarm, Czech Republic), together with citric acid ($\text{C}_6\text{H}_8\text{O}_7$; $3 \text{ g}\cdot\text{L}^{-1}$; Eurosarm, Czech Republic) for ferrous ion stabilisation. A total of 100 L of hydrogen peroxide solution was injected in one dose into well RW5-11, and 500 L of hydrogen peroxide in well RW5-12. Low volumes of hydrogen peroxide (common amounts at this site range from 3 000 to 5 000 L per well applied in several doses) do not result in any release of waste gases; therefore, any venting installation was not needed.

A single 20 m^3 dose of sodium lactate (Galactic, Belgium), at a concentration of $12 \text{ g}\cdot\text{L}^{-1}$, was applied to well RW5-49 within 4 days. Application of sodium lactate was simple infiltration, it means without any overpressure applied during its dosing.

2.3 Physical and chemical analysis

Physical and chemical analysis were performed by Aquatest and laboratory of instrumental chemical analysis. All water samples were taken dynamically using a Gigant pump (Eijkelkamp, Netherlands). ORP was measured immediately after sampling using a WTW 3430 Multimeter (WTW, Germany) and recalculated against a standard H-electrode. The ORP depth profile was measured directly in the well using an Ekotechnika Ecoprobe 5 (Ekotechnika, Czech Republic).

Chlorinated hydrocarbons were determined according to EPA Method 8260 B. Concentration of ethene and ethane was analysed in accordance with the methodology described by Lewin et al. (1993). The degree of dechlorination (in %) was calculated according to the equation:

$$\text{Degree of dechlorination} = \frac{[TCE] + 2 \cdot [DCE] + 3 \cdot [VC] + 4 \cdot [\text{ethene}] + 4 \cdot [\text{ethane}]}{4 \cdot ([PCE] + [TCE] + [DCE] + [VC] + [\text{ethene}] + [\text{ethane}])} \cdot 100 \text{ [\%]},$$

where [contaminant] represents the concentration of the relevant contaminant in $\text{mmol} \cdot \text{L}^{-1}$.

Concentrations of nitrates, sulphates and ferrous iron were analysed according to Standard methods (APHA, 2012), while the chemical oxygen demand (COD) was measured using cuvette tests from Hach-Lange (Germany).

2.4 Molecular genetic analysis

All groundwater samples used for molecular genetic analysis were immediately cooled and stored in the dark at 4 °C until further use. Before analysis, samples (0.2–0.5 L) were concentrated by filtration through a 0.22 μm membrane filter (Merck Millipore, Germany). DNA was extracted from the filter using a FastDNA Spin Kit for Soil (MP Biomedicals, CA, USA) according to the manufacturer's protocol. The Bead Blaster 24 homogenisation unit (Benchmark Scientific, NJ, USA) was employed for cell lysis. Extracted DNA was quantified using a Qubit 2.0 fluorometer (Life Technologies, MA, USA).

Quantitative polymerase chain reactions (qPCR) were performed to assess the relative abundance of *Dehalobacter*, *Dehalococcoides* spp. and *Desulfitobacterium*, as well as the relative abundance of the VC reductase genes *vcrA* and *bvcA*. In addition, qPCR was also employed to monitor the presence of sulphate-reducing bacteria (by detecting levels

of genes for the adenosine-5'-phosphosulphate reductase *apsA* and dissimilatory sulphate reductase *dsrA* enzymes) and denitrifying bacteria (by detecting levels of genes for the nitrite reductase enzymes *nirK* and *nirS*). Relative abundance of 16S rRNA gene (total bacteria marker) was determined as a control marker. All primers used for qPCR are listed in Table 2.

Table 2: Specific primers used for quantitative PCR.

Name	Sequence (5'→3')	Product size (bp)	Target organism(s); gene(s)	Reference
U16SRT-F	ACTCCTACGGGAGGCAGCAGT	180	<i>Bacteria</i> ; 16S rRNA genes	Clifford et al., 2012
U16SRT-R	TATTACCGCGGCTGCTGGC			
vcrA880F	CCCTCCAGATGCTCCCTTA	139	<i>Dehalococcoides sp.</i> strain VS; <i>vcrA</i>	Behrens et al., 2008
vcrA1018R	ATCCCCTCTCCCGTGTAAAC			
bvcA277F	TGGGGACCTGTACCTGAAAA	247	<i>Dehalococcoides sp.</i> strain BAV-1; <i>bvcA</i>	Behrens et al., 2008
bvcA523R	CAAGACGCATTGTGGACATC			
Dre441F	GTTAGGGAAGAACGGCATCTGT	205	<i>Dehalobacter sp.</i> ; 16S rRNA genes	Smits et al., 2004
Dre645R	CCTCTCCTGTCTCAAGCCATA			
DHC793f	GGGAGTATCGACCCTCTCTG	191	<i>Dehalococcoides sp.</i> ; 16S rRNA genes	Yoshida et al., 2005
DHC946r	CGTTYCCCTTTCRGTTCACT			
Dsb406F	GTACGACGAAGGCCTTCGGGT	213	<i>Desulfotobacterium sp.</i> ; 16S rRNA genes	Smits et al., 2004
Dsb619R	CCCAGGGTTGAGCCCTAGGT			
RH1-dsr-F	GCCGTTACTGTGACCAGCC	164	<i>dsrA</i> (dissimilatory sulphate reductase)	Ben-Dov et al., 2007
RH3-dsr-R	GGTGGAGCCGTGCATGTT			
RH1-aps-F	CGCGAAGACCTKATCTTCGAC	191	<i>apsA</i> (adenosine-5'-phosphosulphate reductase)	Ben-Dov et al., 2007
RH2-aps-R	ATCATGATCTGCCAGCGCCGGA			
Cd3aF	G TSAACG TSAAGGARACSGG	425	<i>nirS</i> (Nitrite reductase)	Michotey et al., 2000; Throbäck et al., 2004
R3cd	GASTTCGGRTGSGTCTTGA			
nirK876F	ATYGCGGVCA YGGCGA	164	<i>nirK</i> (Nitrite reductase)	Henry et al., 2004
nirK1040R	GCCTCGATCAGRTRTGGTT			

Reaction mixtures for qPCR were prepared as follows: per 10 µL reaction volume, 5 µL LightCycler[®] 480 SYBR Green I Master (Roche, Switzerland), 0.4 µL of 20 µM forward and reverse primer mixture (Generi Biotech, Czech Rep., IDT, US) with the addition of 3.6 µL ultra-pure water (Biolone, Great Britain). Each DNA template was diluted five-times with ultra-pure water. 1 µL of this diluted DNA was then used for the qPCR reaction. Each sample was analysed in duplicate with ultra-pure water used as a template in a negative control.

All qPCR reactions were performed on a LightCycler[®] 480 instrument (Roche, Switzerland) with reaction conditions set as follows: 5 min at 95 °C initial denaturation, followed by 45 cycles of 10 s at 95 °C, 15 s at 60 °C and 20 s at 72 °C. Finally, a melting curve ranging from 60 to 98 °C was assessed with a temperature gradient of 0.6 °C per 10 s. Purity of the amplified fragment was determined through observation of a single melting peak. Crossing point (C_q) values were obtained using the Second Derivative Maximum method available in LightCycler[®] 480 Software. The amplification efficiency of each primer set was determined by measuring standard curves using serial dilution of template DNA from five different environmental samples. Relative quantification of each parameter was expressed as a fold change between two states (a given sampling time and a sampling time of zero) using the delta C_q method (described in Introduction part, section 4.2). The results of qPCR were evaluated as relative quantification, with the condition of the organohalide-respiring bacteria prior to the application taken as the starting point.

3 Results and discussion

3.1 Application of hydrogen peroxide for the Fenton-like reaction

3.1.1 ORP measurement

Prior to the addition of hydrogen peroxide, ORP showed a relatively constant decrease with depth in well RW5-11 (Fig. 2). In well RW5-12, however, ORP only showed a slow decrease (Δ ORP 20 mV over 7 m) down to a depth of 11 m below ground level (bgl), whereupon it decreased rapidly to -25 mV (Δ ORP 250 mV over 3 m) at a depth of 14 m bgl (Fig. 2). The ORP profiles indicate the different geological structure in each well (Fig. 1B), with higher ORP in RW5-12 being due to faster groundwater flow (80–150 L·d⁻¹) caused by the sandy gravel aquifer (down to 11 m bgl). Groundwater flow at the bottom of the well was much slower (10–20 L·d⁻¹) due to the presence of loamy sands. Additionally, loamy sands could contain higher content of organic matter, along with slow groundwater flow resulting in a significantly lower ORP and thus ongoing biological reduction.

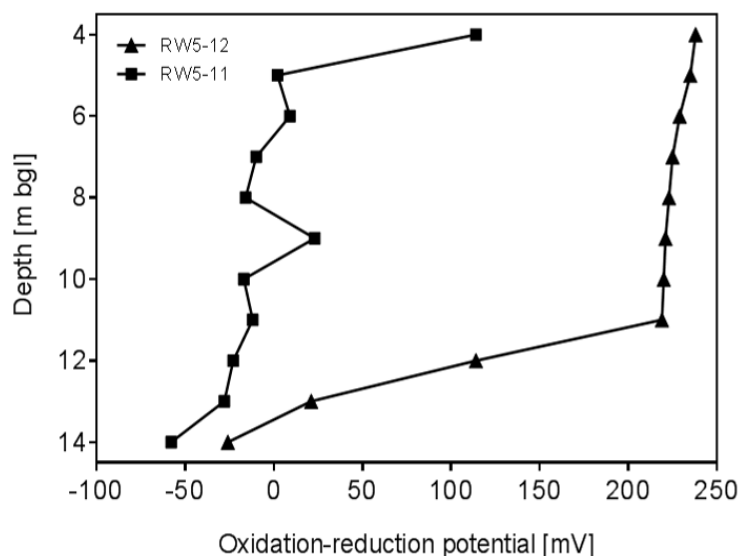


Fig. 2: Oxidation-reduction potential depth profile in wells RW5-11 and RW5-12 before dosing of hydrogen peroxide.

Application of hydrogen peroxide resulted in an increase in overall ORP from an initial level of approximately -30 mV at both depth strata in well RW5-11, and from 230 mV (8 m bgl) and 20 mV (13 m bgl) in well RW5-12 to more than 600 mV in both wells. Due to the small volume of hydrogen peroxide applied (Table 1), this increase in ORP only lasted five days, following which ORP returned to levels similar to those prior to application.

3.1.2 Influence on CEs

The small amount of hydrogen peroxide applied, i.e. 100 L in well RW5-11 and 500 L in well RW5-12 (amounts used at this site more commonly range from 3 000 to 5 000 L per well injected in several doses), did not result in a significant decrease in CEs concentration. Changes in the concentration of individual CEs were within the range of long-term fluctuations throughout the experiment.

Prior to the addition of hydrogen peroxide to well RW5-11, the degree of dechlorination was around 13%, indicating partly ongoing organohalide respiration. After application, degree of dechlorination did not change suggesting both the removal of CEs and simultaneous inflow of contamination from the Fenton-unaffected environment nearby. At the end of the experiment, the degree of dechlorination had increased to 22%, indicating a gradual recovery of the organohalide-respiring bacterial populations (see below) and ongoing organohalide respiration. As almost no degradation products

were detected in well RW5-12 (ca. 3%) and a low degree of dechlorination (< 1.4%) was reached, it can be assumed that no organohalide respiration of CEs took place. Such a low ratio could be explained by the high prevalence of chlorinated methanes in this well, and especially trichloromethane and tetrachloromethane. Moreover, Fenton-like reactions are known to be inefficient at removing chlorinated methanes (Teel and Watts, 2002).

3.1.3 Changes in the organohalide-respiring bacterial populations

In this study, the effect of small doses (disposable impact) of hydrogen peroxide on organohalide-respiring bacteria was evaluated in two contaminated wells and their recovery rate observed. In addition, the influence of depth was assessed by taking samples from 8 and 13 m in each well. The qPCR analysis prior to application confirmed the presence of organohalide-respiring bacteria (*Dehalococcoides* spp., *Dehalobacter*, *Desulfitobacterium*) in both wells, along with the VC reductase genes *vcrA* and *bvcA* (Fig. 3 & 4). All results are expressed as relative ratios, i.e. each marker in relation to its state prior to application (value #1).

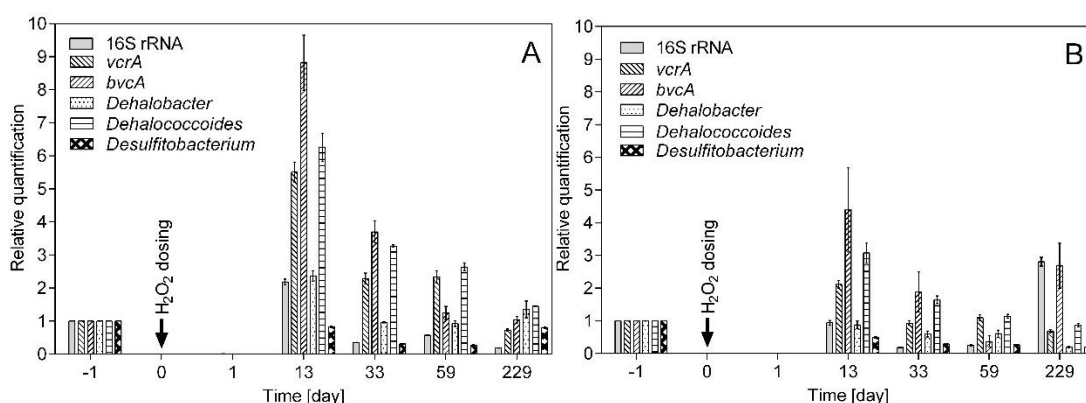


Fig. 3: Changes in the relative abundance of organohalide-respiring bacteria markers and 16S rRNA gene following application of hydrogen peroxide (100 L) in well RW5-11: A) depth 8 m, B) depth 13 m. No molecular genetic markers were detected one day after dosing.

One day after hydrogen peroxide application, all markers in both wells decreased rapidly to values below the detection limit (Fig. 3 & 4), independent of the volume of hydrogen peroxide applied.

Such a rapid decrease cannot be explained by a flushing-out effect alone. Clearly, hydrogen peroxide affected both the organohalide-respiring bacteria and the levels of individual reductive dehalogenase genes, thereby confirming the toxic nature of

hydrogen peroxide. Differences in local geological conditions and the ratio of chlorinated methanes to ethenes in each well resulted in differing changes in organohalide-respiring bacterial populations.

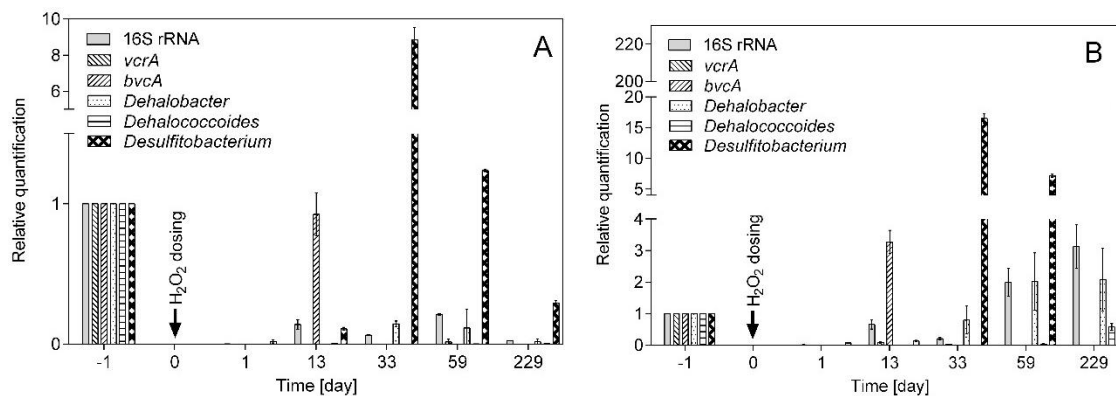


Fig. 4: Changes in the relative abundance of organohalide-respiring bacteria markers and 16S rRNA gene following application of hydrogen peroxide (500 L) in well RW5-12: A) depth 8 m, B) depth 13 m. Aside from the *Desulfitobacterium* (degrader of chloromethanes), no molecular genetic markers were identified one day after dosing. Note fragmentation of the y-axis.

Well RW5-11 exhibited significant recovery of organohalide-respiring bacteria after 13 days, with *Dehalococcoides* spp. dominant. Furthermore, this increase corresponded with an increase in the level of both VC reductase genes (*vcrA* and *bvcA*). A similar rise was observed at both depth strata (i.e. 8 and 13 m) in well RW5-11, corresponding with the reducing conditions found at both levels. As only 100 L of hydrogen peroxide was dosed into this well, both groundwater flow system and surrounding well environment was not significantly affected. The recovery can be explained, therefore, by faster flushing of hydrogen peroxide being followed by re-inoculation from the microbial populations in new groundwater from areas unaffected by the Fenton-like reaction. Moreover, the newly inflowing microbial populations were able to establish themselves rapidly as the original populations had been removed by the Fenton-like reaction, simultaneously providing high nutrient and substrate content for growth. Chappelle et al. (2005) and Sutton et al. (2011) both reported that application of Fenton reagents led to the mobilisation of fermentable organic carbon, which can be utilised by new microbial populations to support growth.

One month after application, the markers gradually decreased to levels comparable with those prior to application. Only *Dehalococcoides* spp. and both the *vcrA* and *bvcA* genes

were still approximately three-times higher after one month, corresponding with the higher chlorinated ethene degradation product ratios observed due to ongoing organohalide respiration. At the end of the experiment (i.e. after 230 days), all markers were close to their original values, with the exception of the *bvcA* gene, again suggesting ongoing activity of organohalide-respiring bacteria.

The influence of the Fenton-like reaction on organohalide-respiring microbial populations was very similar at both depth strata 8 and 13 m (Fig. 3). In terms of microbial recovery, all markers had increased two-fold at 8 m bgl, most likely due to more intensive groundwater flow in the well (approx. 80–150 L·d⁻¹ at 8 m bgl compared to 10–20 L·d⁻¹ in the underlying layer at 13 m bgl) and, therefore, faster re-inoculation by bacteria (Sutton et al., 2011).

As a higher volume of hydrogen peroxide was applied in well RW5-12, a wider surrounding environment was influenced. Zone of impact of hydrogen peroxide in aquifer was not, however, uniformly distributed over well depth. Whereas this zone was about 0.2 m in high-permeable layers (at 8 m bgl), at depth of 13 m bgl it ranged from 0.0 to 0.05 m due to the presence of low-permeable environment (Fig. 1B). Recovery of organohalide-respiring microbial populations in this well; therefore, differed to that in well RW5-11. Aside from *Desulfitobacterium*, no microbial recovery was observed and the levels of all markers remained at values only slightly above the detection limit observed at 8 m (Fig. 4). Faster groundwater flow at this depth, a more positive ORP (220 mV; Fig. 2) and decrease in pH caused by mixture of hydrogen peroxide together with citric acid (used for ferrous ion stabilisation) prevented recovery of anaerobic organohalide-respiring microbial populations. On the other hand, *Desulfitobacterium* appeared capable of growth also under such conditions, though only for a limited time as it needs reductive conditions (negative ORP) for stable and long-term growth (Kim et al., 2012). This would explain the decline in *Desulfitobacterium* relative abundance after 30 days (Miller et al., 1997).

No further microbial recovery was observed at 8 m until the end of experiment (230 days), suggesting that reductive conditions are critical for recovery of organohalide-respiring bacteria. As relative quantification was used (not providing information on total amount), the presence of all markers was detected prior to the application of hydrogen peroxide (Fig. 4A) even though positive ORP (Fig. 2) at this depth of 8 m. It can be explained

by occurrence of anoxic/anaerobic zones (Damgaard et al., 2013b), which disappeared after hydrogen peroxide application.

As at 8 m, organohalide-respiring bacteria disappeared completely at 13 m immediately after hydrogen peroxide application (Fig. 4B). In general, microbial recovery in well RW5-12 was affected by the different contaminants present, i.e. while CEs were the dominant contaminant in well RW5-11, trichloromethane and tetrachloromethane dominated in RW5-12. Organohalide respiration began again after 13-days, however, as indicated by the slow increase in marker levels and a two-fold increase in the levels of *bvcA* gene. Most likely due to the high concentration (~ 95%) of chlorinated methanes, *Desulfitobacterium* levels were up to 200-times higher at the end of the monitoring period compared to those prior to the experiment (Fig. 4B).

These results agree with those of Odom and Singleton (2013), who reported that this bacterial strain is capable of utilising chlorinated methanes for growth. Organohalide-respiring bacterial activity could be influenced by the high *Desulfitobacterium* levels, with relative abundances comparable with those prior to the experiment. This corresponds well with the chemical analysis results, which detected very low degradation product ratios throughout the experiment.

Chapelle et al. (2005) found comparable results, with a decrease in microbial colonisation in wells and microbial activity expressed as a rate of conversion of ^{14}C acetate to $^{14}\text{CO}_2$ two days after application of Fenton reagents. Hence, it would appear that the rate of microbial recovery depends on the groundwater flow, which influences the flushing out Fenton reagents as well as inflow of new microbial populations.

3.2 Application of sodium lactate

3.2.1 ORP measurement

The ORP in well RW5-49 decreased from 370 mV to 4 mV 30 days after application of sodium lactate (first measurement), with ORP remaining close to 0 mV until the end of the experiment after seven months, thereby indicating appropriate conditions for removal of CEs (van der Zaan et al., 2010). In contrast, reference well RW5-24, which received no dosing, showed fluctuations of ORP around 250 mV throughout the experiment.

3.2.2 Influence on CEs

Concentrations of all contaminants in well RW5-49 decreased as a result of enhanced microbial degradation activity (Fig. 5). The degree of dechlorination increased following sodium lactate addition from original value of 60.4 to 85.9% 30 days after infiltration, and 80.6% after 92 days.

In contrast, the degree of dechlorination in the reference well remained relatively stable over the same period, ranging from 18.3 to 26.0%. In addition to CEs, the concentrations of ethene and ethane, the end product of degradation, were also analysed. Ethene concentrations were approximately two-times higher than those before application of sodium lactate. Higher ethene concentrations, along with high ratios for degradation products (maximum 92%), after 30 days clearly indicate an increased rate of CEs degradation. The presence of ethene prior to application can be explained by ongoing dechlorination in well RW5-49. Ethene concentrations remained below the limits of detection throughout the experiment in the reference well (RW5-24), indicating undetectable or incomplete degradation of CEs (also due to the higher ORP ~ 250 mV). No effect of sodium lactate dosing was observed on concentrations of chlorinated methanes in well RW5-49.

3.2.3 Changes in COD and redox sensitive parameters

As 20 m³ of sodium lactate was infiltrated in well RW5-49, surrounding environment in diameter up to 10 m in high-permeable layers and about 0.1–0.3 m in the layers with low permeability was influenced. Due to the high-permeable layers, any significant increase in groundwater level and flow was not observed after sodium lactate infiltration. Only flow direction nearby to well was opposite during sodium lactate application. The amount of sodium lactate remaining in groundwater was determined by measuring the COD. COD increased by around 300% (from 82 to 250 mg·L⁻¹) following application of sodium lactate in well RW5-49. Over the next 92 days, COD gradually decreased to 15 mg·L⁻¹, whereupon they remained relatively stable until the end of experiment.

Nitrate in well RW5-49 decreased from about 1.5 mg·L⁻¹ to below the detection limit (0.20 mg·L⁻¹) over the first 92 days after application, though they had returned to their original values after 200 days due to inflow of groundwater, thereby confirming exhaustion of lactate for biological reduction (ORP about 35 mV). Sulphate concentrations in well RW5-49 decreased from 460 mg·L⁻¹ to 160 mg·L⁻¹ 30 days after

sodium lactate application, subsequently increasing to $290 \text{ mg}\cdot\text{L}^{-1}$ after 90 days and remaining relatively constant at this level throughout the rest of the experiment. While the concentrations of nitrate fluctuated slightly (from 79 to $108 \text{ mg}\cdot\text{L}^{-1}$) in reference well RW5-24, the concentrations of sulphate remained relatively stable (1090 – $1280 \text{ mg}\cdot\text{L}^{-1}$) throughout the experiment.

3.2.4 Impact on bacterial populations

Before sodium lactate application, *Dehalococcoides* spp., *Dehalobacter*, *Desulfitobacterium*, VC reductase genes *vcrA* and *bvcA* and sulphate-reducing (identified through the *apsA* and *dsrA* genes) and denitrifying (identified through the *nirK* and *nirS* genes) bacteria were all detected in well RW5-49. Apart from the *bvcA* gene, the same markers were also identified in reference well RW5-24.

The clear differences in microbial response observed in well RW5-49 following sodium lactate dosing confirm a positive influence over a shorter time interval (Fig. 5). The relative abundance of those markers responsible for organohalide-respiration remained three- to seven-times higher than those prior to application two months after sodium lactate dosing. An increase in *Dehalococcoides* spp. and *vcrA* and *bvcA* genes was observed, with *Desulfitobacterium* showing the highest increase over all markers tested. The dominance of *Desulfitobacterium* (at seven-times their original level) is likely to have been due to its broad substrate specificity, enabling more rapid growth than other organohalide-respiring bacteria (Lupa and Wiegel, 2015).

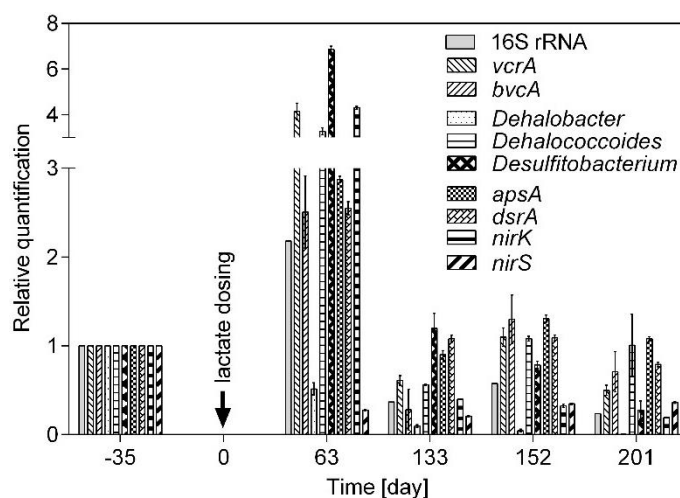


Fig. 5: Change in the relative abundance of markers in well RW5-49 following infiltration of sodium lactate. Note fragmentation of the y-axis.

The increase in *Dehalococcoides* spp., along with levels of the *vcrA* and *bvcA* genes, is in accordance with the results of chemical analysis, which showed a clear transformation of VC to ethene. On the other hand, sodium lactate application led to a decrease in the abundance of *Dehalobacter* (Fig. 5), primarily responsible for DCA degradation (Grostern and Edwards, 2006).

Approximately four months after sodium lactate application, levels of all markers had decreased, with final values similar to those before application. In well RW5-49, aside from the nitrite reductase gene *nirS* and *Dehalobacter*, all markers had returned to their original values within four months. Molecular genetic analysis and chemical analysis results both agreed, demonstrating a decrease in sulphates and nitrates together with a decrease in ORP. Increased relative abundance of denitrifying and sulphate-reducing bacteria corresponded with ongoing organohalide respiration, negative ORP being needed for both processes. This resulted in a clear decline in sulphate concentrations, accompanied by a simultaneous increase in the levels of *apsA* and *dsrA* genes responsible for sulphate reduction.

In the reference well (RW5-24), concentrations of CEs and marker relative abundance remained relatively stable throughout the experiment. 133 days after lactate application, however, marker levels had increased again, probably because of renewed contamination originating from inflow of untreated groundwater. Findings observed after sodium lactate application are in accordance with results by Damgaard et al. (2013b) and Scheutz et al. (2008) who also reported an increase in molecular genetic markers for ongoing organohalide respiration after molasses and sodium lactate dosing, respectively.

If the remediation effect of the Fenton-like reaction is to be increased, dosing with an organic substrate would be needed to support organohalide-respiring bacterial growth. Based on this, the combination of a Fenton-like reaction followed by dosing with sodium lactate (or other organic substrate) would appear to be efficient approach for enhancing stimulation of organohalide-respiring bacteria during *in situ* remediation of CEs.

3.3 Enhanced reductive dehalogenation process (ERD)

As explained in the introduction of the chapter, the results of only one experiment are presented. However, based on the all results of long-term testing, universally proven

technology has been developed to characterize sites according to available results and recommend bioremediation procedure (Fig. 6 and 7). The goal of the technology is to remediate groundwater collector contaminated by degreasers and chlorinated solvents in industrial areas in such a way that the final products of the process are non-toxic gaseous products (ethene and ethane) without cumulation of dichlorethene and vinyl chloride. The means to achieve the above-described goal is stimulation of autochthonous microflora participating in the ERD process.

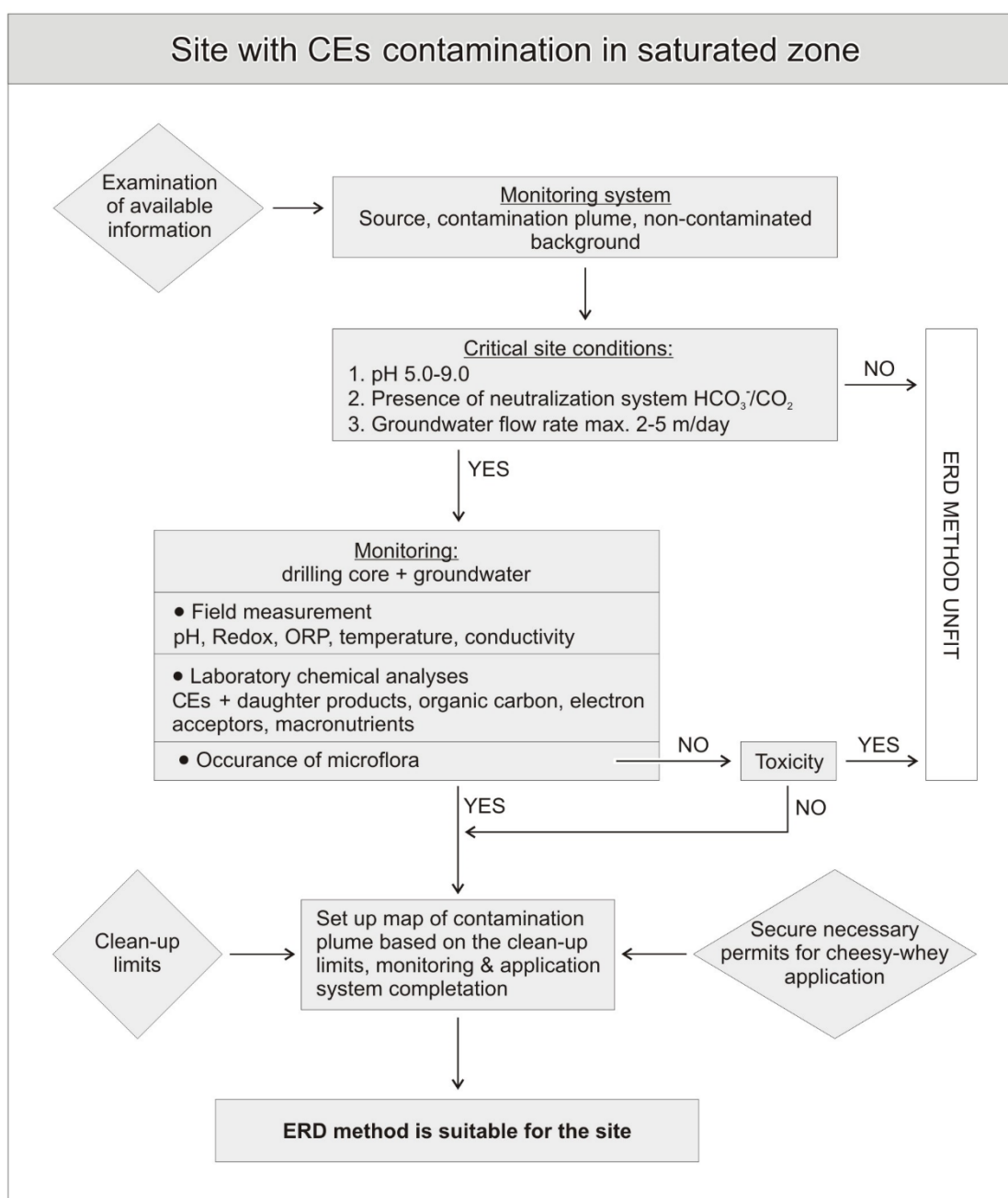


Fig. 6: Scheme summarizing applicability of enhanced reductive dehalogenation method.

This proven technology identifies critical points of the ERD process, describing in detail the appropriate practice for field measurement and collection of environmental samples in order to obtain relevant information for optimized management of *in situ* anaerobic reactors (zone with stimulated microflora, where contamination is being removed).

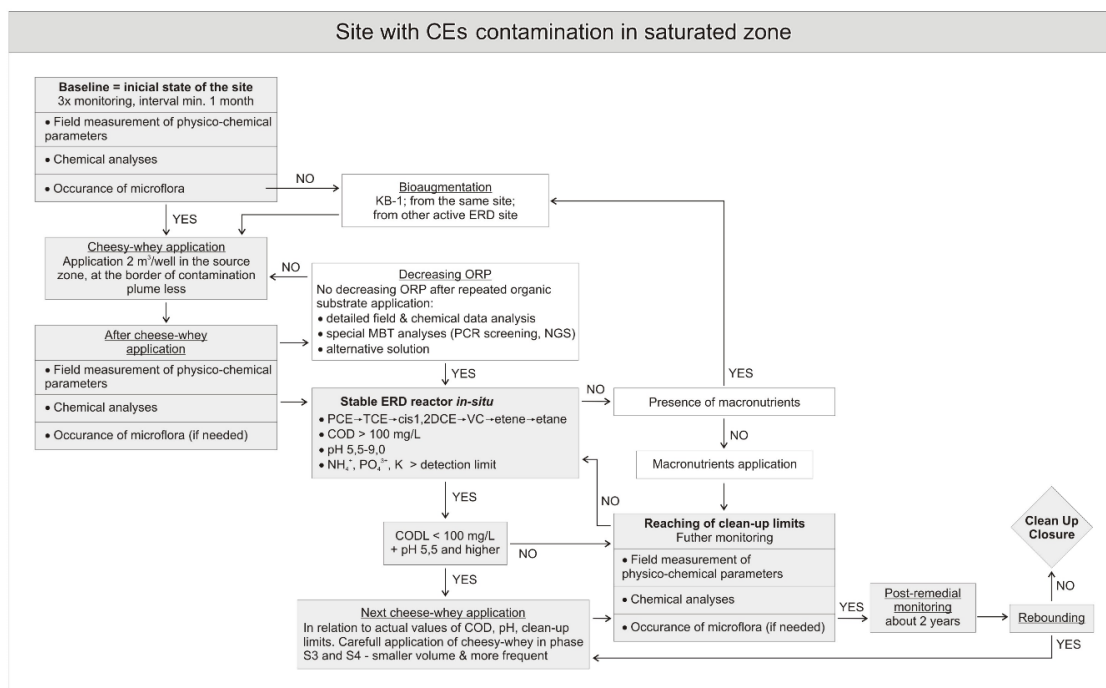


Fig. 7: Remediation strategy by ERD.

The technology includes similar procedures and a description of particular steps, including graphical interpretation in the form of decision-making diagrams. It also includes utilization of molecular biology methods and statistical analysis. Finally, the technology software provides useful answers to crucial questions such as “when and what volume of substrate do I need to apply?”, “does my anaerobic reactor work as expected?”, “is the composition of stimulated microflora optimal? If no, where should I look for the problem?” or “in which phase of the ERD process am I?”

4 Summary

Changes in anaerobic organohalide-respiring bacteria associated with *in situ* dehalogenation of CEs following a Fenton-like reaction and application of sodium lactate at a contaminated site was assessed. A combined approach based on molecular genetic assays along with detection of chemical parameters was used in this study.

While molecular genetic marker levels remained high two-months after sodium lactate application, most markers showed only a slight increase following the Fenton-like reaction. Although the Fenton-like reaction initially resulted in a decrease in all marker relative abundances, a subsequent increase was observed within 13 days. Most values returned to those prior to application within one month. Increase in molecular genetic markers associated with organohalide-respiring bacteria lasted longer when dosing with sodium lactate. Sodium lactate led to establishment of the reducing conditions necessary for growth of anaerobic organohalide-respiring bacteria. Ongoing organohalide respiration was proven by an increase in markers along with an increase in ethene concentration.

In situ application of hydrogen peroxide to induce a Fenton-like reaction caused an instantaneous decline in all markers below detection limit. Two weeks after application, the *bvcA* gene and *Desulfitobacterium* relative abundance increased to levels significantly higher than those prior to application. No significant decrease in the concentration of a range of CEs was observed due to the low hydrogen peroxide dose used. A clear increase in marker levels was also observed following *in situ* application of sodium lactate, which resulted in a seven-fold increase in *Desulfitobacterium* and a three-fold increase in *Dehalococcoides* spp. after 70 days. An increase in the *vcrA* gene corresponded with increase in *Dehalococcoides* spp. Analysis of selected markers clearly revealed a positive response of organohalide-respiring bacteria to biostimulation and unexpectedly fast recovery after the Fenton-like reaction.

II. NGS analysis of natural microbial communities

1 Background

New approaches of molecular genetics allow analysis of the contaminated site not only using specific markers (primers) by qPCR but also detailed insight into the composition of the autochthonous bacterial community through NGS (more details in Literature Overview). I have introduced and applied qPCR and NGS for numerous polluted sites (CEs, BTEX). Here, the main part of this chapter describes only one representative experiment, because description of all results is beyond the scope of this thesis.

Shallow groundwater systems are often oligotrophic; hence, *in situ* availability of electron donors has long been considered an important factor limiting the efficiency of microbial reductive dechlorination of CEs to ethene (e.g. Bouwer et al., 1994; Gibson and Sewell, 1992; McCarty, 1996).

Redox conditions and related biogeochemical processes can vary spatially within a single hydrogeological system (e.g. Damgaard et al., 2013a, 2013b; Kim et al., 2012). Hence, it is important to investigate redox condition zoning and related biogeochemical processes within the contaminated aquifer and to identify the primary factors affecting reductive dechlorination in order to assess the potential for natural attenuation of CEs. In this field experiment, two sample matrices were analysed: CE-contaminated groundwater from three depth profiles and a soils samples. Soils samples were processed only using qPCR method because very low DNA yields from deeper horizons (> 2 m) did not allow the use of NGS analysis. The principal objective of this study was to characterise biodegradation processes using physico-chemical analyses and molecular biology tools in an alluvial aquifer historically contaminated with CEs.

2 Material and methods

Natural degradation of CEs was evaluated based on a) analysis of CEs and their non-chlorinated metabolite content, b) biomolecular analysis of soil and groundwater samples and c) inorganic chemical analysis and measurement of physico-chemical parameters of groundwater. Soil samples and groundwater samples were collected at a range of depth intervals using soil bores and pre-installed monitoring wells.

2.1 Study site

This study was undertaken at the SAP Mimoň rendering plant (Fig. 1), which is located on the right bank floodplain of the River Ploučnice, a tributary of the River Elbe (50.632N, 14.721E; north Bohemia, Czech Republic). Geological conditions at the site comprise Quaternary alluvial sediments (maximum thickness 6 m), underlain by Middle Turonian sandstone. The Quaternary sediments consist of a thin layer of top soil underlain with sand and gravel, with grain size increasing with depth. The Middle Turonian sandstone holds a 60 m deep regional aquifer (Wittlingerova et al., 2016) that is hydraulically connected to the unconfined Quaternary alluvial aquifer via a less permeable layer of cemented sandstone of approx. 1 m. The Quaternary aquifer has a saturated thickness of approximately 2 – 5 m (0.7 to 2.8 m below ground level [bgl] at the study site) and a hydraulic conductivity level of between 20 to 50 m·day⁻¹, based on pumping tests.

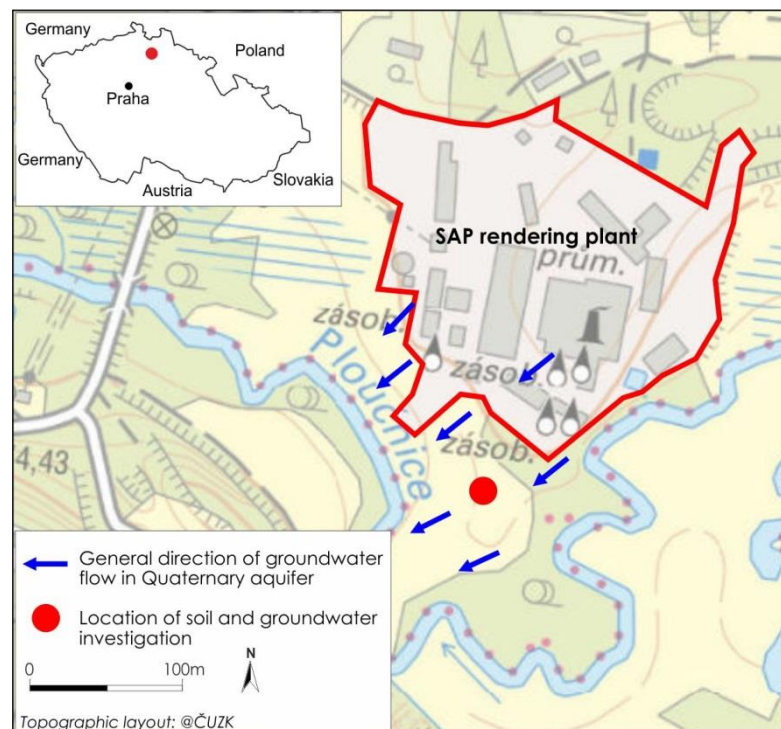


Fig. 1: Map of the study site with direction of groundwater flow.

Historical use of PCE as a fat extraction agent at the rendering plant, and especially discharge of wastewater containing PCE into the river floodplain, has resulted in extensive contamination of the plant's subsurface and the surrounding land down-gradient. CEs have also been found in the River Ploučnice itself following

discharge of contaminated groundwater, and in fish tissue and tree cores (Wittlingerova et al., 2016, 2013). Extensive remediation of both aquifers using pump and treat, venting, air sparging and *in situ* chemical oxidation with ozone significantly reduced the amount of PCE below the surface from 149–246 t in 1997 to 4.4–10.7 t in 2011 (Wittlingerova et al., 2016).

The site selected for this study is located in the peripheral part of the contaminant plume in the River Ploučnice floodplain, an area that has not yet been actively remediated.

2.2 Soil borings and collection of soil samples

A HVS137 drilling rig (JaNo s.r.o., Czech Republic) was used to drill four soil boreholes down to the base of the Quaternary alluvial sediments (3.25–3.50 m bgl) using direct push technology, whereupon HDPE 32 mm dual tube samplers (Ejkelkamp, The Netherlands) were inserted using hydraulic pressure and hammering. Soil core tubes were cut into 25-cm sections, which were quickly plugged with airtight caps, inserted into a cooling box containing liquid nitrogen and transported directly to the laboratory. Samples used for biomolecular analysis were stored in the dark at -85 °C until needed.

The chlorinated solvent degraders *Dehalobacter* sp., *Dehalococcoides mccartyi* and *Desulfitobacterium* spp. were detected using real-time polymerase chain reaction (qPCR) using the part of their 16S rRNA gene. The total bacterial biomass was estimated by qPCR using the same gene. The soil samples were also used for quantification of the reductive dehalogenase genes *vcrA* and *bvcA*, the nitrite reductase gene *nirK*, the sulphate reducing gene *apsA* and the sulphite reducing gene *dsrA*, again using qPCR. All qPCR results were analysed using relative quantification (see 2.6).

2.3 Installation of monitoring wells and collection of groundwater samples

Three monitoring wells with an HDPE Ø 32x25 mm casing (Ejkelkamp, The Netherlands) were installed close to the soil boreholes using the same drilling rig (Wells MW-1, MW-2, MW-3). Each well was screened at different depth intervals: well MW-1 from 1.0 to 1.5 m bgl (upper zone of the aquifer), well MW-2 from 2.0 to 2.5 m bgl (middle zone) and well MW-3 from 2.6 to 3.1 m bgl (lower zone). Groundwater samples were collected using a peristaltic pump (Ejkelkamp, The Netherlands) after the wells had been purged, with field parameters (pH, redox potential, dissolved oxygen concentration, electrical conductivity and temperature) measured and recorded during the sampling.

All samples were collected in duplicate following parameter value stabilisation. Samples for analysis of dissolved iron (Fe) and manganese (Mn) were filtered through a 0.4 µm filter in the field and acidified using hydrochloric acid (HCl), other samples were placed into dedicated sampling containers and transported in a cooling box directly to the laboratory. All water samples were immediately cooled and stored in the dark at 4 °C until needed.

CEs, ethene, ethane, methane, major anions (sulphate, nitrate, bicarbonates), ammonium (NH_4^+), dissolved Mn and Fe, and total organic carbon (TOC) were analysed using standard analysis protocols (see below), while qPCR was used to detect the presence of chlorinated solvent degraders (*Dehalobacter* sp., *Dehalococcoides* sp. and *Desulfitobacterium* spp.), the functional genes *vcrA*, *bvcA*, *nirS* and *apsA* (see below) and total bacterial biomass using the 16S rRNA gene. All qPCR results were analysed using relative quantification (see 2.6). Microbial community analysis was performed using next generation sequencing (NGS).

2.4 Measurement of physical and chemical parameters

Physical and chemical analysis of the samples was performed in the laboratory of instrumental chemical analysis at CxI. Ca, Mg, Na, K, Fe and Mn dissolved in groundwater were analysed according to ČSN EN ISO 11885 (2007). NH_4^+ was determined by the reaction with salicylate and hypochlorite ions in the presence of nitrosopentacyanoferrite, the blue colour produced being measured spectrophotometrically (ČSN EN ISO 7150-1, 1994). TOC was determined according to ČSN EN 1484 (1998).

Groundwater redox potential, oxygen concentration and pH were determined electrochemically in the field using a flow-through cell and a Multi 350i Multimeter (WTW, Germany). Chloride, nitrate and sulphate were analysed according to ČSN EN ISO 10304-1 (2007); bicarbonates and carbonates were analysed according to ČSN EN ISO 99631 (1994).

Volatile organic compounds, including CEs, ethene, ethane and methane were analysed by CP 3800/Saturn 2200 Gas chromatograph–mass spectrometer (GC-MS; Varian, USA). CEs were extracted from soil samples (approximately 50 g) with 50 ml of methanol.

Degree of PCE degradation was expressed in terms of the chlorine number (also referred to as the chlorine index) defined as weighted average number of Cl atoms per molecule of ethene (Bewley et al., 2015).

2.5 DNA extraction

2.5.1 Soil samples

Ten grams of frozen soil was collected from each 25-cm soil bore section for DNA extraction. DNA was extracted using the PowerMax® Soil DNA Isolation Kit (Mo Bio, CA, USA) according to the manufacturer's protocol. Extracted DNA was quantified using a Qubit 2.0 fluorometer (Life Technologies, CA, USA).

2.5.2 Water samples

Prior to analysis, water samples (0.35-0.5 L) were concentrated by filtration through a 0.22 µm membrane filter (Merck Millipore, Germany). DNA was extracted from the filter using the FastDNA Spin Kit for Soil (MP Biomedicals, CA, USA) following the manufacturer's protocol. A Bead Blaster 24 homogenisation unit (Benchmark Scientific, NJ, USA) was employed for cell lysis. Extracted DNA was quantified using a Qubit 2.0 fluorometer (Life Technologies, CA, USA).

2.6 Real-time PCR analyses (qPCR)

Real-time PCR was employed to assess the relative abundance of *Dehalobacter* sp., *Dehalococcoides mccartyi*, *Desulfitobacterium* spp. and the VC reductase genes *vcrA* and *bvcA*. In addition, qPCR was also employed to monitor the relative level of sulphate-reducing bacteria, by detecting levels of genes for the adenosine-5'-phosphosulphate reductase *apsA* and dissimilatory sulphate reductase *dsrA* genes, and denitrifying bacteria, by detecting relative levels of the nitrite reductase genes *nirK* and *nirS* (Braker et al., 1998). Relative abundance of the 16S rRNA gene (U16SRT total bacteria marker) was determined as a control marker. All primers used for qPCR are listed in the Table 2, section 2.4, chapter I.

Reaction mixtures were prepared as follows: per 10 µL reaction volume, 5 µL KAPA SYBR FAST qPCR Kit (Kapa Biosystems, Inc., MA, USA), 0.4 µL of 20 µM forward and reverse primer mixture (Generi Biotech, Czech Republic, IDT, US) with the addition of 3.6 µL ultra-pure water (Bioline, UK), 1 µL of DNA subsequently being used for

the qPCR reaction. Each sample was analysed in duplicate with ultra-pure water used as a template in a negative control.

All qPCR reactions were performed on a LightCycler® 480 (Roche, Switzerland) with reaction conditions set as follows: 3 min at 95 °C initial denaturation, followed by 40 cycles of 10 s at 95 °C, 20 s at 60 °C and 10 s at 72 °C. Finally, a melting curve was set for 5 s at 95 °C, 1 min at 65 °C and final ranging from 60 to 98 °C, with a temperature gradient of 40 °C per 10 s. Purity of the amplified fragment was determined through observation of a single melting peak. Crossing point values were obtained using the 'second derivative maximum' method included in the LightCycler® 480 Software. The method has different amplification efficiency for each primer. The individual amplification efficiency was determined by measuring the slope of curves constructed from a serial dilution of a template DNA from five environmental internal standards. Samples with qPCR inhibition detected were diluted (1, 10, 40, 160 times). Therefore, in the evaluation process each soil sample was normalized to dilution and total amount of DNA extracted.

For each depth, four DNA soil samples (duplicates from four parallel wells) were statistically evaluated (mean value μ and standard deviation σ). Any value was excluded from the evaluation if the value was lying outside the 3σ interval from the mean. A relative abundance of bacterial 16S rRNA gene and of functional genes was calculated as a power, with amplification efficiency as a base and difference between the respective measured and normalized crossing point and arbitrarily defined reference crossing point as an exponent. The soil data were plotted as a relative depth profile of individual specie (gene) relative abundance together with an appropriate standard deviation. Based on the approach used it is necessary to consider each molecular biological marker separately and see the trends in relative abundance with depth, rather than to compare the absolute numbers between each other.

2.7 PCR amplification and next generation sequencing

All samples for microbial community analysis were sequenced in duplicate, with two consecutive PCR reactions performed per sample to amplify DNA from the V4 region (normal and barcode fusion primers used). *In silico* analysis of primers was performed in order to cover as much diversity as possible while keeping the amplicon size below 400 bp. Amplification of the V4 region of the eubacterial 16S rRNA gene was performed

with primers 515F (5′–TGCCAGCMGCNGCGG–3′; Dowd et al., 2008) and barcode one 802R (5′–TACNVGGGTATCTAATCC–3′; Claesson et al., 2010). An in-house prepared mock community (collection of 12 bacterial genomes) was subsequently sequenced in order to verify data evaluation. PCR cycle conditions were as follows: first PCR 95 °C for 3 min; 10 cycles at 98 °C for 20 s, 50 °C for 15 s and 72 °C for 45 s, with a final extension at 72 °C for 1 min. Second PCR: 95 °C for 3 min; 35 cycles at 98 °C for 20 s, 50 °C for 15 s and 72 °C for 45 s, with a final extension at 72 °C for 1 min.

The concentration of purified PCR product was measured with a Qubit 2.0 fluorometer (Life Technologies, CA, USA). Barcode-tagged amplicons from different samples were then mixed in equimolar concentrations. Sequencing of bacterial amplicons was performed on the Ion Torrent platform (Life Technologies, CA, USA).

The raw Ion Torrent reads were processed with Mothur software (Schloss et al., 2009). Low quality reads were removed and sequences were assigned to each sample. Chimeric sequences were identified using UCHIME (Edgar et al., 2011) and subsequently removed. Sequences exceeding 400 bases were trimmed and sequences shorter than 180 bases were removed. Sequences were classified against Silva database version 123 with a bootstrap value set at 80%. Cut-off value of 97% was used for clustering of sequences into operational taxonomic units (OTUs). The number of sequences in each library was adjusted to 16 397 (based on the sample with least sequences) by random subsampling in Mothur. Cluster analysis was undertaken using the Vegan package in the R statistical package (Oksanen et al., 2012). Phyla/families with greater than 1.5% abundance were visualised as heat maps and the remaining visualised in graphs as others and unclassified.

3 Results and discussion

3.1 Physico-chemical and inorganic groundwater parameters

Field measurements of physico-chemical and inorganic parameters showed clear vertical zonation. Groundwater from the upper well (MW-1) was of a $\text{Ca}^{2+}\text{-NO}_3^-$ type (Pačes, 1983), had high redox potential (407 mV), high nitrate content ($96.50 \text{ mg}\cdot\text{L}^{-1}$), low content of manganese ($0.01 \text{ mg}\cdot\text{L}^{-1}$), iron ($0.27 \text{ mg}\cdot\text{L}^{-1}$) and sulphate ($33.40 \text{ mg}\cdot\text{L}^{-1}$) and no methane. In comparison, groundwater from the lower well (MW-3) was of a $\text{Ca}^{2+}\text{-HCO}_3^-$ type, with lower redox potential (183 mV) and nitrate content ($<2.0 \text{ mg}\cdot\text{L}^{-1}$), relatively higher content of manganese ($0.02 \text{ mg}\cdot\text{L}^{-1}$) and iron ($1.78 \text{ mg}\cdot\text{L}^{-1}$), lower

sulphate content ($16.60 \text{ mg}\cdot\text{L}^{-1}$) and methane at $7.2 \text{ }\mu\text{g}\cdot\text{L}^{-1}$. The same parameters in the middle zone (well MW-2) were transitional between the upper and lower redox zones. When plotted on a Durov graph, the figures from the well MW-2 were more similar to MW-3 than MW-1 (Fig. 2).

To summarise, field measurements and chemical analysis indicated mixed groundwater redox zones, where oxygen and nitrate reduction dominated in the upper zone (MW-1) and Fe and sulphate reduction prevailed in the lower zone (MW-3). There was also some indication of methanogenesis in the lower zone.

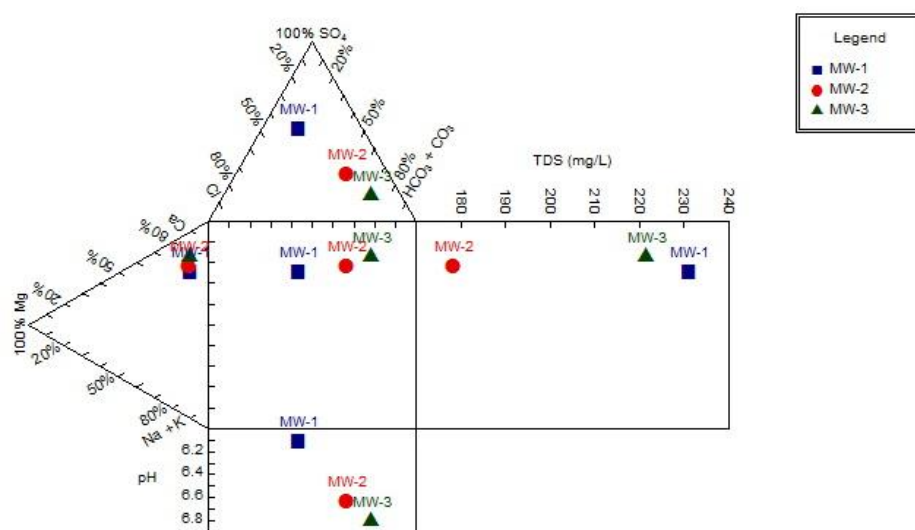


Fig. 2: Durov graph showing basic groundwater chemistry for the three wells samples (MW-1 = upper zone, MW-2 = middle zone, MW-3 = lower zone).

3.2 Concentration of CEs in groundwater

As with the inorganic parameters, CEs, ethene and ethane exhibited clear stratification with depth, with groundwater from the upper zone (MW-1) containing $1\,004 \text{ }\mu\text{g}\cdot\text{L}^{-1}$ of total CEs, whereas samples from the middle (MW-2) and lower (MW-3) zones contained $5\,883 \text{ }\mu\text{g}\cdot\text{L}^{-1}$ and $6\,187 \text{ }\mu\text{g}\cdot\text{L}^{-1}$, respectively. Changes in the concentration of individual CEs and ethene (a degradation product) indicated the varying extent to which the parent contaminant (PCE) had degraded along the aquifer profile. Reductive dechlorination, as expressed by the chlorine number, decreased with increasing depth. The higher chlorine number in the upper zone indicates PCE as dominant, with concentrations of VC and ethene below their respective detection limits. Reductive dechlorination of PCE into

CEs was also observed in the middle and lower zones. VC and ethene were detected in both zones, though at low concentrations. Decreased chlorine number values at depth coincide with Fe reducing to sulphate-reducing conditions, which are more favourable for reductive dechlorination (Bradley and Chapelle, 2010).

This finding is supported by correlation of TOC, E_h , pH and redox sensitive compounds with chlorine number, with a strong positive correlation identified between chlorine number and sulphate (correlation coefficient ≥ 0.99 , $p\text{-uncorr} \leq 0.01$), both decreasing with increasing depth. Local redox conditions, however, were sub-optimal (insufficiently reducing) for rapid reductive dechlorination of the less chlorinated ethene, *cis*-1,2-DCE. Accumulation of *cis*-1,2-DCE has often been observed in the lower zones of aquifers (together with VC) at sites where reductive dechlorination is not engineered but occurs naturally (Bradley and Chapelle, 2010).

3.3 Bacteria and functional genes at different groundwater zones

Highest levels of total bacterial biomass were observed in groundwater from the middle zone (Table 1). The middle zone also had highest levels of *Dehalococcoides mccartyi*, the sulphate-reducing gene *apsA* and the nitrite reductase gene *nirS*. Levels of chloro-respiring *Dehalobacter* sp. were relatively similar in groundwater from the upper and middle layers. The relative abundance of chloro-respiring *Desulfurospirillum* sp., on the other hand, did not differ markedly with depth. Gene *vcrA* was detected at high relative abundance in groundwater from the lower zone, while gene *bvcA* was hardly detectable at any depth.

Table 1: Relative abundance of total bacterial biomass (U16SRT), nitrite reductase gene *nirS*, sulphate-reducing gene *apsA*, chlororespiring bacteria *Dehalococcoides* sp., *Dehalobacter* sp., *Desulfurospirillum* sp. and the *vcrA* and *bvcA* genes in groundwater, based on qPCR (unitless).

	MW-1 1.0–1.5 m bgl	MW-2 2.0–2.5 m bgl	MW-3 2.6–3.1 m bgl
U16SRT	0.25	1.71	0.47
<i>nirS</i>	0.34	2.96	0.23
<i>apsA</i>	0.52	2.91	0.60
<i>Dehalococcoides</i> sp.	0.10	1.94	1.02
<i>Desulfurospirillum</i> sp.	1.68	1.14	1.17
<i>Dehalobacter</i> sp.	1.07	1.69	0.14
<i>bvcA</i>	0.53	0.53	0.73
<i>vcrA</i>	0.08	0.51	23.83

Here we note that the high number of *vcrA* in lower zone could not be compared to the low number of *Dehalococcoides mccartyi* in the same zone, due to relative and not absolute quantification performed.

3.4 Concentration of CEs in soil

CEs also showed clear zonation along the vertical profile of the Quaternary aquifer (Fig. 3), with low concentrations above the groundwater table (~ 0.7 m bgl) gradually increasing with depth to a maximum of $5.5 \mu\text{g}\cdot\text{g}^{-1}$ at 2.50 to 2.75 m bgl, whereupon concentrations dropped to $1.8 \mu\text{g g}^{-1}$ (3.25 m bgl). As in the groundwater analysis, CEs exhibited a degree of reductive dechlorination in soil, with slow degradation of the parent contaminant (PCE) above 2 m bgl (chlorine number approx. 3.5) increasing at greater depths. A chlorine number of 2.9 was detected in the lowest aquifer zone.

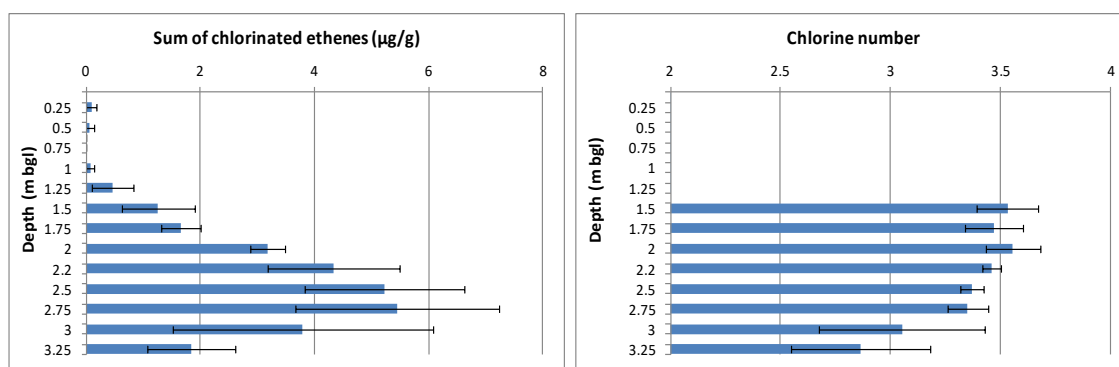


Fig. 3: Changes in total concentration of chlorinated ethenes in soil (left) and chlorine number (right) at depth. The values are arithmetic means of four measurements.

3.5 Bacteria and functional genes in soil

Highest relative bacterial biomass (roughly estimated based on quantity of 16S rRNA) was observed in the uppermost (≤ 50 cm bgl) and lowermost layers of the Quaternary sediments (Fig. 4). Nitrate-reducing bacteria (*nirK*) were detected at highest densities between 0.75 and 2.00 m bgl. Density of sulphate-reducing bacteria (*apsA*, *dsrA*) increased with depth from the surface to 2 m bgl, then decreased temporarily, and increased again from 2.5 m bgl to the lowest level sampled. Density of *Desulfitobacterium* spp. (Dsb) followed a U-shaped profile, with highest values at the top and bottom of the vertical profile, while density of *Dehalococcoides mccartyi* (DHC) and *Dehalobacter* sp. (Dre) increased with increasing depth.

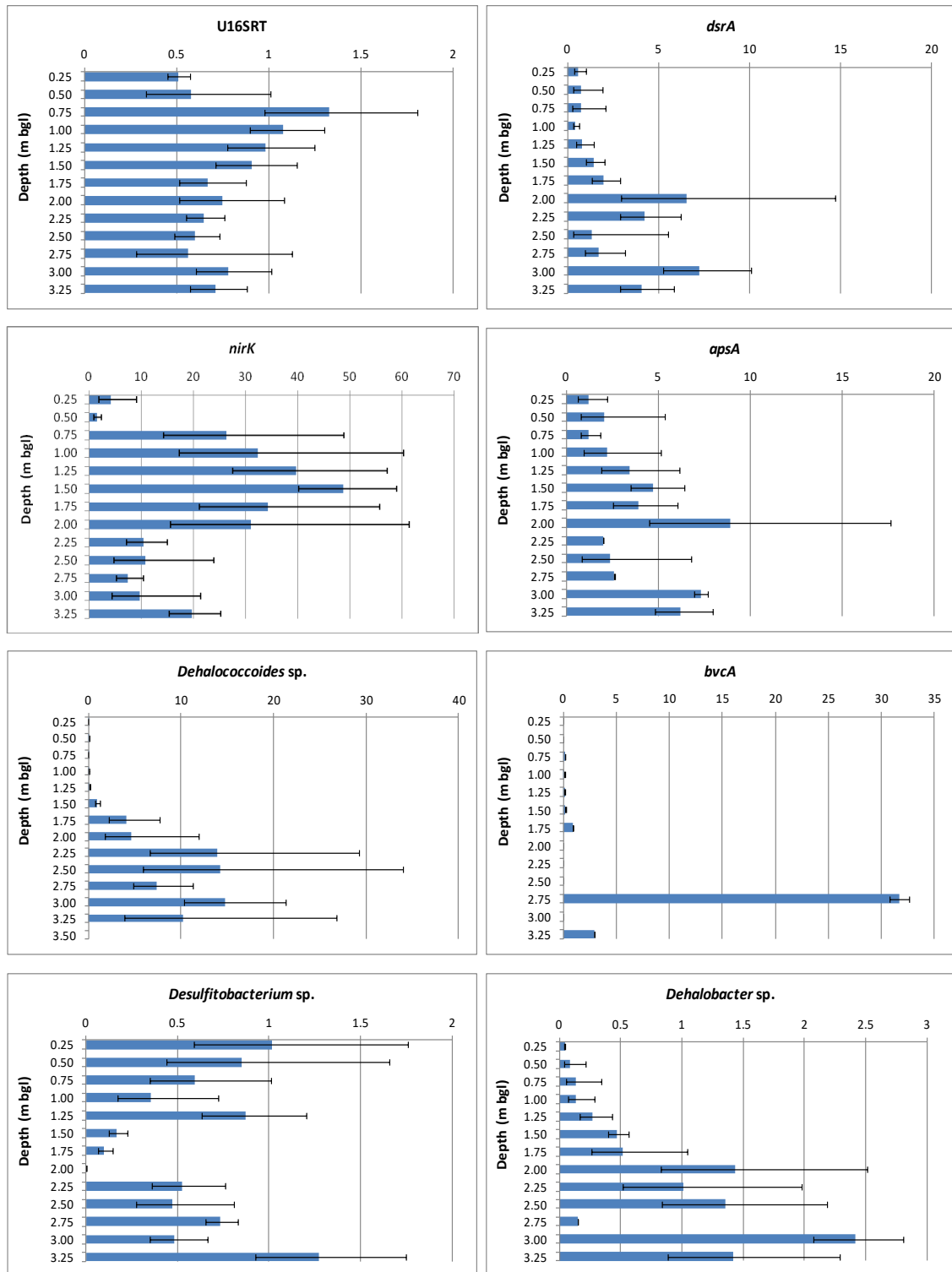


Fig. 4: Changes in total bacterial (prokaryotic) biomass, bacterial genera and functional genes in soil (in relative units) at depth. The values are arithmetic means of four measurements.

Relative vertical distribution of the gene *bvcA* did not correspond with the relative vertical distribution of *Dehalococcoides mccartyi*, *bvcA* relative abundance being very irregular with a maximum at 2.50 to 2.75 m bgl. The gene *vcrA* was not detected in most samples and thus was not displayed graphically.

Correlation analysis showed a high degree of correlation (correlation coefficient ≥ 0.91 , p -uncorr ≥ 0.01) between *Dehalobacter* sp. and *Dehalococcoides mccartyi*, and between total concentration of CEs and *Dehalococcoides mccartyi* (Table 2).

Table 2: Correlation matrix with values for soil parameters given in the lower triangle of the matrix and the two/tailed probabilities that pairs (p -uncorr) are uncorrelated in the upper triangle. Pearson parametric coefficients were calculated using PAST software (Hammer et al., 2001). Results in bold indicate significant correlations at p -uncorr ≥ 0.01 . (For abbreviations, see Subsection 3.5).

	<i>nirK</i>	<i>dsrA</i>	U16SRT	DHC	Dsb	<i>apsA</i>	Dre	Chlor. ethenes
<i>nirK</i>		0.18	0.09	0.27	0.12	0.05	0.22	0.35
<i>dsrA</i>	-0.63		0.32	0.23	0.36	0.11	0.45	0.33
U16SRT	0.74	0.49		0.31	0.45	0.15	0.25	0.54
DHC	0.53	0.57	-0.50		0.24	0.06	0.01	0.01
Dsb	-0.71	-0.46	0.39	0.57		0.17	0.24	0.21
<i>apsA</i>	0.81	0.72	-0.67	-0.78	0.64		0.04	0.16
Dre	-0.59	-0.38	0.55	0.91	-0.57	0.83		0.07
Chlor. ethenes	-0.47	-0.48	0.32	0.92	-0.60	0.65	-0.77	

3.6 Next generation sequencing (NGS)

NGS was used to characterise bacterial communities in groundwater at different depths (upper, middle, lower) in relation to physico-chemical conditions and the potential for reductive dechlorination of CEs.

Sequencing produced 81 624 sequence reads with an average length of 182 bases. Each of the samples contained between 20 856 and 35 263 reads. Sequence data were normalised to the group with least sequences by randomly selecting the number of sequences from each sample. Highest number of OTUs (bacterial diversity) was identified in the upper zone, with numbers subsequently dropping with increasing depth.

Correspondingly, estimates of species richness (Chao, 1984) were markedly lower in the middle and lower zones. Non-shared species, i.e. species uncommon in two or all three zones, were most frequent in the upper zone (737) and least frequent in the lower zone (145). Phylogenetic composition of the upper and middle zone bacterial communities was more similar to each other than to that in the lower zone (Fig. 5).

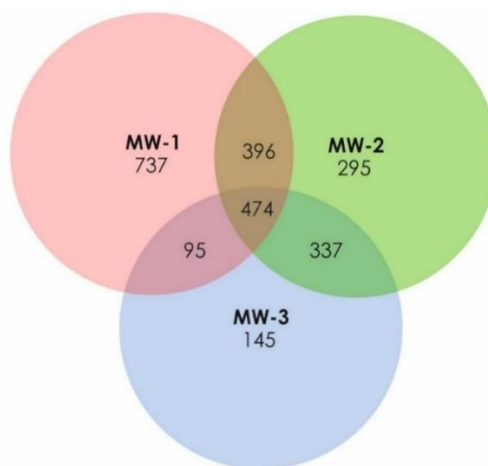


Fig. 5: Venn diagram of bacterial communities (OTUs) present at different depths in the aquifer (distance 0.03/OTUs at 97% similarity) (Němeček et al., 2017).

Bacteria of the phylum *Proteobacteria*, i.e. *Betaproteobacteria*, prevailed in groundwater samples from all three zones (Fig. 6). A similar dominance by *Betaproteobacteria* has also been identified at other sites contaminated with chlorinated hydrocarbons (Kotik et al., 2013). The most abundant of the *Betaproteobacteria* were the families *Gallionelaceae*, *Comamonadaceae*, *Oxalobacteraceae* and *Hydrogenophylaceae*, though the abundance of individual *Betaproteobacteria* families differed at each depth (Fig. 7).

The most abundant representatives of the *Gallionelaceae* family (related to Fe^{2+} oxidation; Pedersen, 2011) were found in the lower zone. Shani et al. (2013), recorded a high correlation between occurrence of *Gallionelaceae* and presence of Fe^{2+} , both of which were commonly detected in groundwater samples from sites contaminated by CEs (Guan et al., 2013). *Gallionella* grow best under conditions of low oxygen ($0.1\text{--}1\text{ mg of O}_2\cdot\text{L}^{-1}$), with an E_h range of between +200 and +320 mV and a pH of between 6 and 7.6 (Hanert, 1981; Kucera and Wolfe, 1957); conditions similar to those observed at our study site.

Aerobic oxidation of Fe^{2+} was clearly not the dominant metabolism pathway in the lower zone of the aquifer (see section 3.1), though ‘rusty’ precipitates of oxidised Fe^{3+} were detected visually, indicating microaerophilic conditions. The genus *Gallionella* has previously been described as capable of dechlorinating TCE under the sulphate-reducing conditions (Tsai et al., 2014) prevailing in the lower zone of the aquifer.

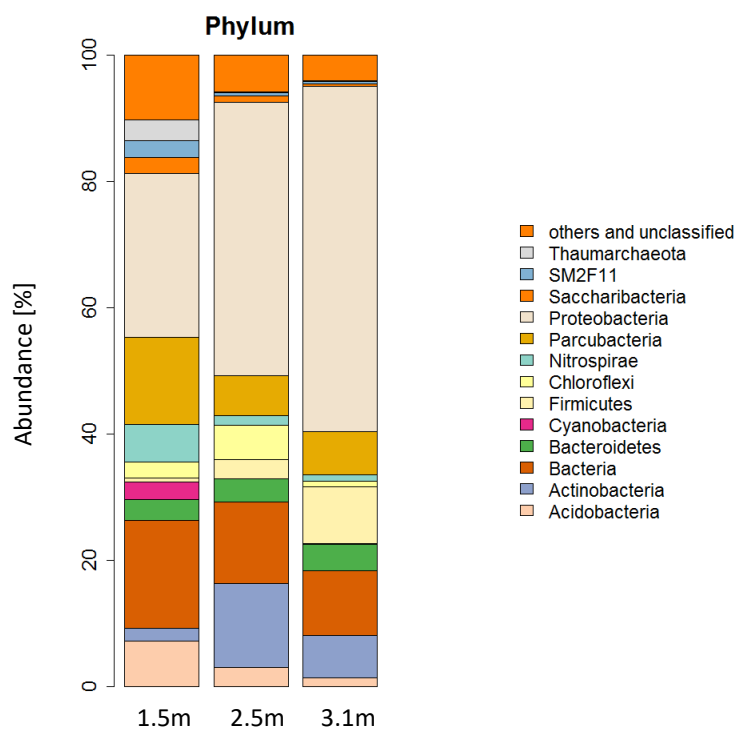


Fig. 6: Abundance of microbial taxa (phylum level) present in 1.5, 2.5 and 3.1 m bgl.

The *Burkholderiales*, *Oxalobacteraceae* and *Comamonadaceae*, have both been recorded as abundant in environments contaminated with CEs (Behrens et al., 2008), while *Rhodoferax* (family *Comamonadaceae*) is connected with aerobic assimilation of VC (Paes et al., 2015).

As expected, microorganisms known to have aerobic metabolisms (*Acidobacteria*, *Nitrospirae*) were mainly recorded in the upper and middle zones, along with some cyanobacteria (*Cyanobacteria*). *Acidobacteria*, which have flexible metabolisms, are often detected at sites contaminated with CEs (Milton et al., 2010). We also identified bacteria of the genera *Mycobacterium*, *Rhodoferax* and *Nocardiodes*, whose members are related to the microbial oxidation of lower CEs. Several members of the families *Mycobacteraceae* (phylum *Acidobacteria*) and *Nocardiodes* were documented

in the aquifer. These bacteria can utilise VC as their sole source of carbon and energy (Coleman et al., 2002a; Hartmans and De Bont, 1992).

Similarly, the genus *Rhodoferax* has also been shown to use VC as a primary growth substrate (Paes et al., 2015). This implies that microbial oxidation of VC, a degradation product of reductive dechlorination of CEs, cannot be excluded from oxic and sub-oxic zones of the aquifer.

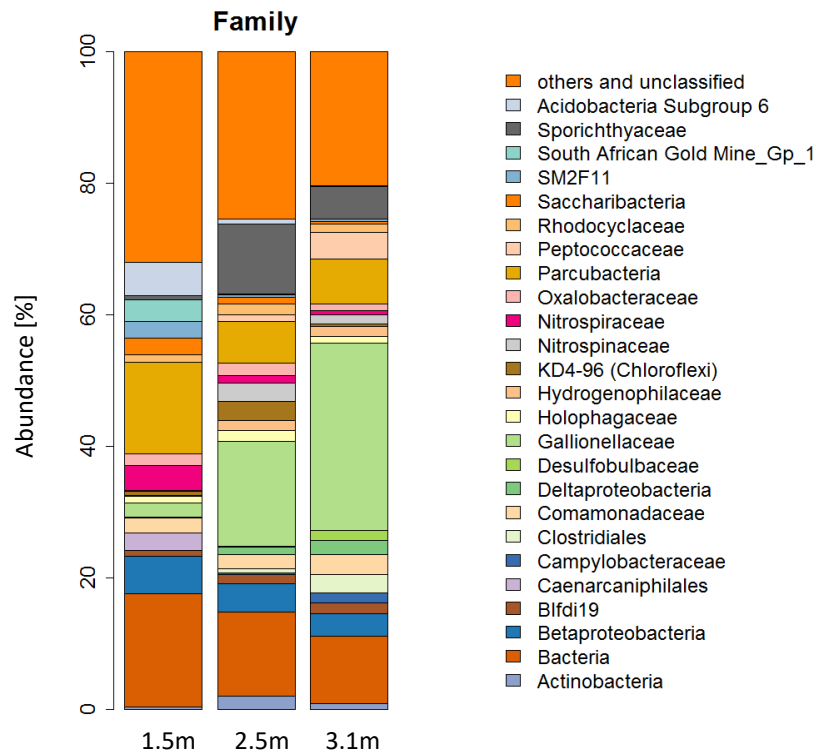


Fig. 7: Abundance of microbial taxa (family level) present in 1.5, 2.5 and 3.1 m bgl.

Surprisingly, *Parcubacteria* (Candidate phylum OD1) were very abundant in the upper zone, despite normally being found in anoxic environments (Nelson and Stegen, 2015). The same authors sequenced eight bacterial genomes of *Parcubacteria* and identified genes related to potential aerobic metabolism (oxygen as a terminal electron acceptor) in three of them. Other genes related to electron transport have yet to be identified, however; hence, the metabolic mechanisms involved remain unclear. Currently, more than 400 species have been identified in the phylum *Parcubacteria* (Solden et al., 2016), supporting our findings that *Parcubacteria* are one of the most abundant phyla at the study site, and at other sites contaminated with CEs (Dolinová et al., unpublished data).

The abundance of anaerobic microbes (*Firmicutes*, *Chloroflexi*, *Actinobacteria* and *Bacteroidetes*) was higher in the middle and/or lower zones (Fig. 8). All phyla detected were related to reductive dechlorination and were detected at other sites contaminated with CEs (Das and Kazy, 2014; Guan et al., 2013).

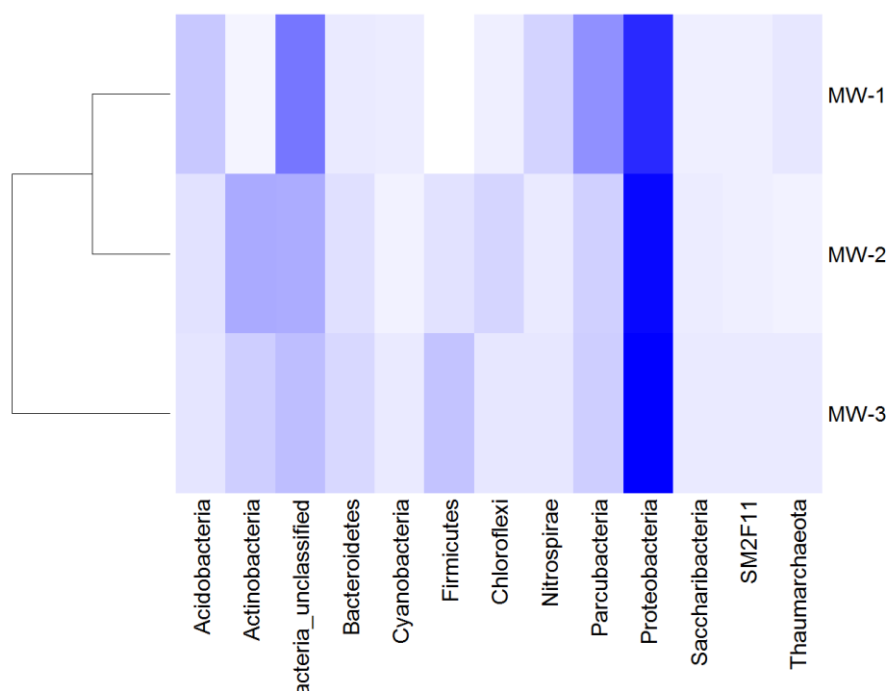


Fig. 8: Phylum level community analysis. Data obtained by NGS (Němeček et al., 2017).

Both main families of *Firmicutes*, i.e. *Clostridiaceae* and *Peptococcaceae*, were detected in groundwater from the lower zone (Fig. 9), the members of which have anaerobic metabolisms, e.g. anaerobic fermenting *Clostridiaceae* (Das and Kazy, 2014). Members of the family *Peptococcaceae* are related to anaerobic metabolism and are active under Fe- or nitrate-reducing conditions (Das and Kazy, 2014). *Bacteroidetes*, on the other hand, are active under sulphate-reducing conditions (Milton et al., 2010).

The phylum *Chloroflexi* is associated with reductive dechlorination. A member of this phylum, *Dehalococcoides mccartyi*, is known for its complete anaerobic dechlorination of PCE into ethene/ethane. *Dehalococcoides mccartyi* and other biomarkers of reductive dechlorination were identified by qPCR relatively abundant in middle and lower aquifer zones. Sulphate-reducing *Desulfobulbaceae* (*Deltaproteobacteria*) were also detected in the lower zone.

The bacterial communities identified were, in general, similar to those already described at other sites contaminated with CEs (Kotik et al., 2013). Some specific features typical for the SAP Mimoň site were identified including presence of the family *Gallionellaceae* in groundwater from the middle and lower aquifer zones and the abundance of the family *Parcubacteria* in the upper zone.

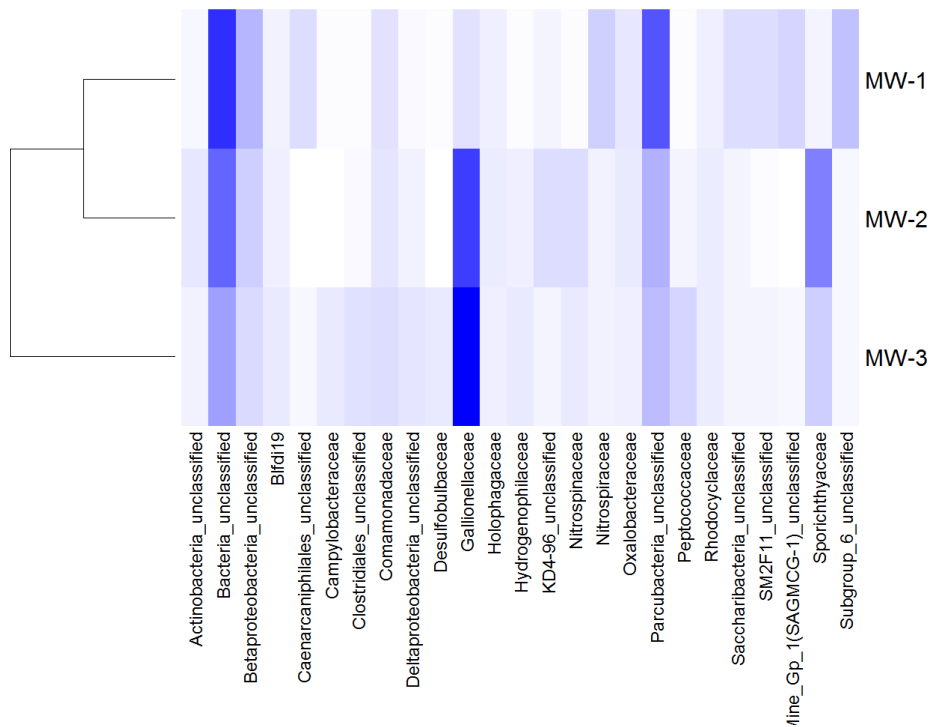


Fig. 9: Family level community analysis. Data obtained by NGS (Němeček et al., 2017).

4 Summary

The goal of this study was to characterise conditions for natural attenuation of CEs along the vertical profile of an alluvial aquifer. Despite the small thickness of the target aquifer (2.8 m), distinct stratification of redox zones was observed, from oxygen- and nitrate-reducing conditions in the upper zone to mixed Fe-reducing to sulphate reducing conditions in the lower zone of the aquifer, along with indications of methanogenesis.

Heterogeneity in redox conditions was most probably the reason for differences in the extent of CEs degradation along the aquifer's vertical profile. A higher degree of PCE degradation coincided with Fe-reducing to sulphate-reducing conditions in the lower part of the aquifer, conditions favourable for biological reductive dechlorination. This finding is supported by a high positive correlation between chlorine number and sulphate concentration in groundwater.

Despite the presence of ethene in groundwater as a non-chlorinated product of reductive dechlorination, the local environment was insufficiently reducing for rapid complete natural reductive dechlorination of the parent PCE.

NGS analysis revealed highest microbial community diversity in the aerobic upper zone, and higher similarity between the upper and middle zone communities. Vertical heterogeneity in the microbial community reflected redox zoning, i.e. while aerobic bacteria (*Acidobacteria*, *Nitrospirae*) were abundant in the upper zone, anaerobic microbes (phyla *Firmicutes*, *Chloroflexi*, *Actinobacteria* and *Bacteroidetes*) or sulphate-reducing *Desulfobulbaceae* (phylum *Proteobacteria*), common at sites contaminated by CEs, were higher in the middle and/or lower zones. An important finding was the high abundance of the family *Gallionellaceae*, related to oxidation of Fe^{2+} , in the middle and lower zones.

qPCR analysis also revealed microbial vertical zonation. The nitrite reductase gene *nirK* was most abundant in the upper soil zone, while maximum density of the sulphate reduction genes *apsA* and *dsrA* was found at deeper levels. This corresponds generally with the prevalent redox conditions (see above). Similarly, the relative abundance of dechlorinators (*Dehalococcoides mccartyi* and *Dehalobacter* sp.) in the soil was highest at depths where sulphate-reducing conditions were prevalent.

Some genera related to microbial oxidation of CEs were also identified by NGS analysis (i.e. *Mycobacterium*, *Rhodospirillum rubrum*, *Nocardioides*), indicating that microbial oxidation of PCE degradation intermediates cannot be excluded.

These results imply that vertical stratification of key biological and hydrochemical markers must be considered when a) assessing natural chlorinated ethene attenuation, even in shallow aquifers; b) designing monitoring networks or when evaluating data collected from wells with long screens; and c) during the design phase of engineered stimulation for biological dechlorination of chlorinated contaminants. For example, treatment of CEs in the oxic zone of an aquifer using enhanced *in situ* anaerobic bioremediation may take longer. In the case of high groundwater and/or native oxygen (and/or nitrate) flux, such treatment may well prove impractical.

III. Development of nanofibre carriers for sampling microbial communities

1 Background

A crucial step in the molecular genetic analysis of microbial communities present at contaminated sites is appropriate sampling. Groundwater sampling may be complicated by a) the initial pumping of polluted waters including soil microorganisms present in the vicinity of the well and b) the influence of filtration in the laboratory. Regular soil sampling is impossible due to the high costs of drilling up to 5 m deep profiles.

In the recent past, there were almost no possibilities for monitoring autochthonous microflora from contaminated groundwater using trapping systems. We found only two systems based on activated carbon, the first developed and applied at the University of Leipzig (Bombach et al., 2009; Schurig et al., 2014) and the second used by the commercial company Envirogen Technologies (USA). To the best of our knowledge, no system has been developed based on nanofibres.

The aim of this study was to develop nanofibre carriers for microbial biomass designed for repeated usage and for short-term and long-term monitoring of contaminated localities. We intended to develop a small nanofibre carrier without preferential growth of microorganisms that was easily transportable and suitable for DNA isolation. We also evaluated the effect of nanofibre carrier material and preservation during transport to the laboratory on DNA yield. Long-term applicability was tested using qPCR. Finally, the NGS results from different arrangements and densities of nanofibres and from different matrices (nanofibres, groundwater, soil) were compared.

2 Materials and methods

2.1 Study sites

Five contaminated localities were chosen across the Czech Republic for testing the nanofibre carriers: Ústí nad Labem, Prague (Praha), Vysoké Mýto, Náměšť and Oslavou and Jablůnkov (Fig. 1). All sites were contaminated with mixtures of chlorinated hydrocarbons with a prevalence of CEs.



Fig. 1: Location of the CE contaminated sites studied within this study.

Characteristics of the test wells for evaluating the impact of transport technique are shown in Table 1. Chemical analysis directed to chlorinated hydrocarbons is shown in Table 2.

Table 1: Characterization of the test wells in the experiment evaluating transport techniques.

Locality	well designation	well type	cheese whey application
Horní Počernice	HP-92	monitoring	–
Vysoké Mýto – Tomášková Cihelna	HV-37	application	05/2013
Vysoké Mýto – Karosa, sklad plynů	HV-12	application	05/2013
Jablunkov	A-1	monitoring*	06/2013
Náměšť nad Oslavou – Velamos	NA-14	application	09/2013

*. influenced by cheese whey application.

Table 2: Chemical analysis of test wells in the experiment evaluating transport techniques.

Locality	Date	Chemical analysis
Horní Počernice	03/2013	\sum CES 170 $\mu\text{g}\cdot\text{L}^{-1}$, 72% cisDCE +23% VC
	06/2013	\sum CES 83 $\mu\text{g}\cdot\text{L}^{-1}$, 87% cisDCE +22% VC
	09/2013	\sum CES 380 $\mu\text{g}\cdot\text{L}^{-1}$, 31% PCE + 16% TCE + 43% cisDCE +9% VC
Vysoké Mýto – Tomášková Cihelna	04/2013	\sum CES 1200 $\mu\text{g}\cdot\text{L}^{-1}$, 27% cisDCE +73% VC
	07/2013	\sum CES 330 $\mu\text{g}\cdot\text{L}^{-1}$, 66% cisDCE +30% VC
	10/2013	\sum CES 1200 $\mu\text{g}\cdot\text{L}^{-1}$, 75% cisDCE +25% VC
Vysoké Mýto – Karosa, gass storage	04/2013	\sum CES 1300 $\mu\text{g}\cdot\text{L}^{-1}$, 93% PCE + 6% cisDCE
	07/2013	\sum CES 155 $\mu\text{g}\cdot\text{L}^{-1}$, 79% cisDCE +20% VC
	10/2013	\sum CES 50 $\mu\text{g}\cdot\text{L}^{-1}$, 66% cisDCE +22% trans DCE + 7% VC
Jablunkov	04/2013	\sum CES 4900 $\mu\text{g}\cdot\text{L}^{-1}$, 14% PCE + 65% cisDCE +19% VC
	09/2013	\sum CES 5900 $\mu\text{g}\cdot\text{L}^{-1}$, 98% cisDCE +1.5% VC
Náměšť nad Oslavou – Velamos	04/2013	\sum CES 1550 $\mu\text{g}\cdot\text{L}^{-1}$, 54% cisDCE +45% VC
	07/2013	\sum CES 700 $\mu\text{g}\cdot\text{L}^{-1}$, 79% cisDCE +19% VC

Tests of nanofibre carriers with and without coaxial protective fibre (CPF), as well as a comparison of individual sample matrices, took place at Spolechemie a.s. in Ústí nad Labem (Fig. 1). Only wells with a high microbial abundance (RW6A-7, RW6A-42, RW6A-45) and without active remediation were selected for nanofibre carrier submersion. An example of the chemical analysis of chlorinated hydrocarbons is shown in Table 3. During the last year of the experiment (7.6. 2017), 3m³ of a Fenton like reagent (H₂O₂) was applied to wells RW6A-41, 42, 43.

Table 3: Chemical analysis of wells in an experiment with nanofibre carrier arrangement. Concentrations of pollutants are in $\mu\text{g}\cdot\text{L}^{-1}$.

Well	Sampling	VC	1.1-DCE	1.2-c-DCE	1.2-t-DCE	TCE	PCE	Sum of CEs
RW6A-7	13.10.2011	27.7	1,3	558	3	94.7	85.1	802.6
RW6A-42	9.4.2014	21.1	1.9	497	5.3	109	15.4	649.7
RW6A-45	14.5.2012	27,8	1.9	97.7	4.3	23.3	17.6	184.2

2.2 Electrospinning and designing of nanofibre carriers

Each nanofibre carrier was prepared using polyurethane nanofibres (Larithane 1083) and polyester silk support thread (SLOTERA, 167f 25x1x1). The polyurethane nanofibres were prepared using needleless electrospinning from a free liquid surface and a high voltage source. The surface density of the nanofibres was adjusted by production rate, resulting in a surface density of 5 dtex ($0.56 \text{ g}\cdot\text{m}^{-2}$, production rate $216 \text{ m}\cdot\text{min}^{-1}$) and 10 dtex ($1.12 \text{ g}\cdot\text{m}^{-2}$, production rate $108 \text{ m}\cdot\text{min}^{-1}$). The support threads were arranged into six different arrangements: cylindrical, multi-cluster linear, planar, tassle, linear and circular. The components used for each shape are listed in Table 4.

Table 4: Composition of prepared nanofibre carriers – italic letters mark the components which have to be removed prior to DNA extraction.

Arrangement	Components
Multi-cluster linear	support thread + nanofibres + <i>hot melt adhesive</i> + <i>fishing line</i>
Linear	support thread + nanofibres
Tassle	support thread + nanofibres + <i>plastic cable tie</i>
Cylindrical	support thread + nanofibres + <i>polyamide support construction</i> + <i>hot melt adhesive</i>
Planar	support thread + nanofibres + <i>hot melt adhesive</i> + <i>fishing line</i>
Circular	support thread + nanofibres

The final nanofibre carriers consisted of 3 m of support thread with nanofibres. The threads being prepared as two variants, i.e. with and without CPF. With CPF, the surface of the nanofibres was protected by a tangential cross coil of polyamide 6 monofilament (11 dtex fineness). The nanofibre carriers were then fixed onto black high-density polyethylene tubes (Fig. 2) for submersion into the groundwater.



Fig. 2: Black high-density polyethylene tubes with nanofibre carriers inside.

Individual nanofibre carriers were constructed with six different arrangements comprising different nanofibre densities, both without CPF (Table 5) and with CPF (Table 6), and these were submerged at the Spolchemie site.

Table 5: Summary carrier arrangements used in experiment with threads without CPF.

Arrangement and nanofibre density				
5/10 dtex	5/10 dtex	5/10 dtex	5/10 dtex	5/10 dtex
multi-cluster linear	linear	tassle	cylindrical	planar

Table 6: Summary of carrier arrangements used in experiment with threads with CPF.

Arrangement and nanofibre density							
thread	density	thread	density	thread	density	thread	density
w/wo CPF*	dtex	w/wo CPF	dtex	w/wo CPF	dtex	w/wo CPF	dtex
-	3/5/10	-	3/5/10	-	3/5/10	-	3/5/10
linear		tassle		planar		circular	

* w/wo – with/without

2.2.1 Multi-cluster linear arrangement

The multi-cluster linear arrangement has previously been used (CZ patent No. 305698); however, we modified the arrangement by increasing the number of nanofibres in individual bundles and removal of the nylon fibres. This arrangement was chosen due to its solid and compact structure, allowing modifications during the manufacturing process. A technical drawing of the multi-cluster linear arrangement is displayed in Fig. 3

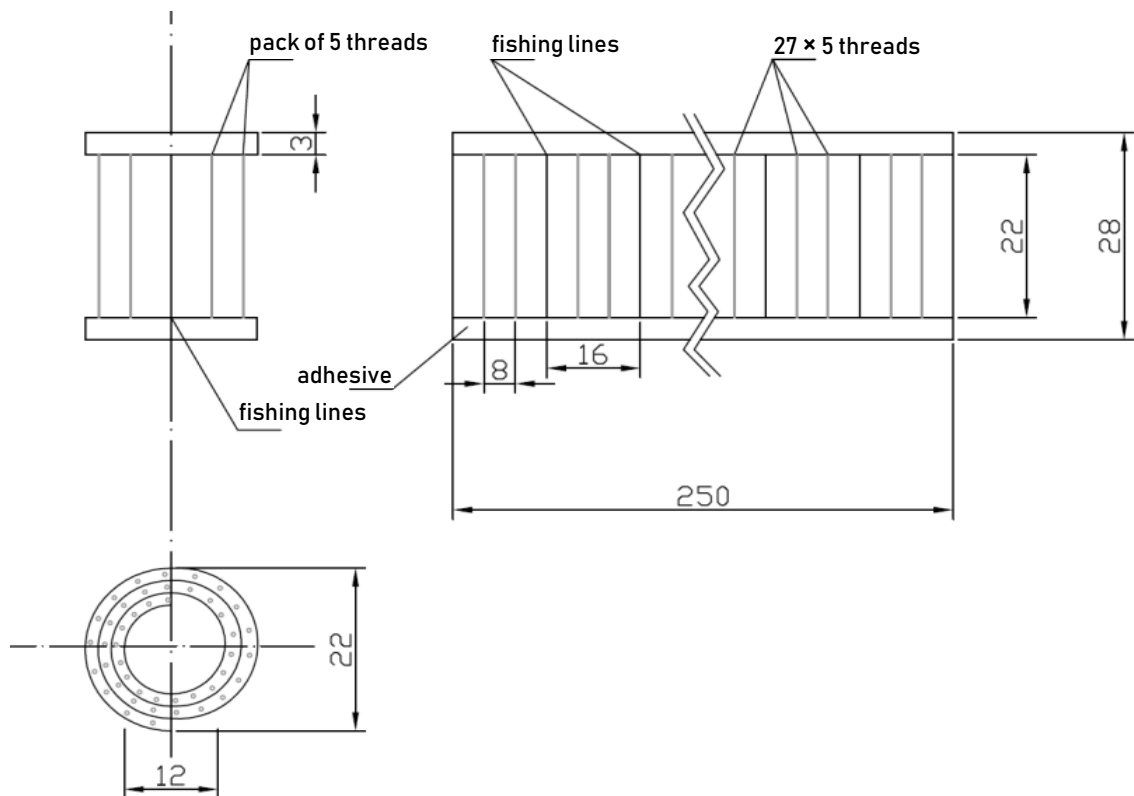


Fig. 3: Technical drawing of multi-cluster linear arrangement. Dimensions in mm.

2.2.2 Linear arrangement

The fibres were arranged in a linear bundle and then divided using a small gas burner with a mild flame. The resultant rigid connection meant there was no tendency for the end fibres to fray. The distance between connections was 3 cm, the total length of fibres for each nanofibre carrier arrangement being the same (3 m). A technical drawing of the linear arrangement is displayed in Fig. 4.

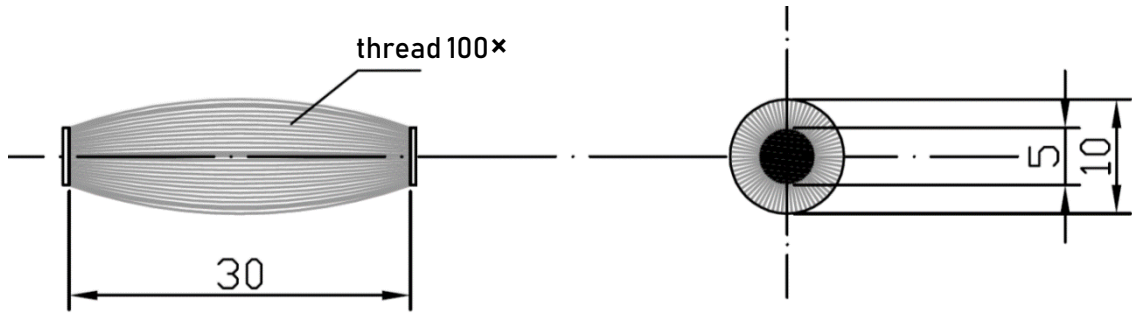


Fig. 4: Technical drawing of the linear arrangement of support thread. Dimensions in mm.

2.2.3 Tassel arrangement

The design of the tassel arrangement followed a similar principle to the linear arrangement, but with the threads and nanofibres connected with a plastic cable tie. The main bundle of fibres was divided into two parts in order to open the structure. The spacing between the centres of each nanofibre carrier was 2–2.5 cm in order to further open the structure and increase the contact area. The individual nanofibre carriers may be fixed during production by the main carrying thread that connects the fibres and defines their mutual distance, as well as allowing the distance to vary). A technical drawing of the tassel arrangement is displayed in Fig. 5.

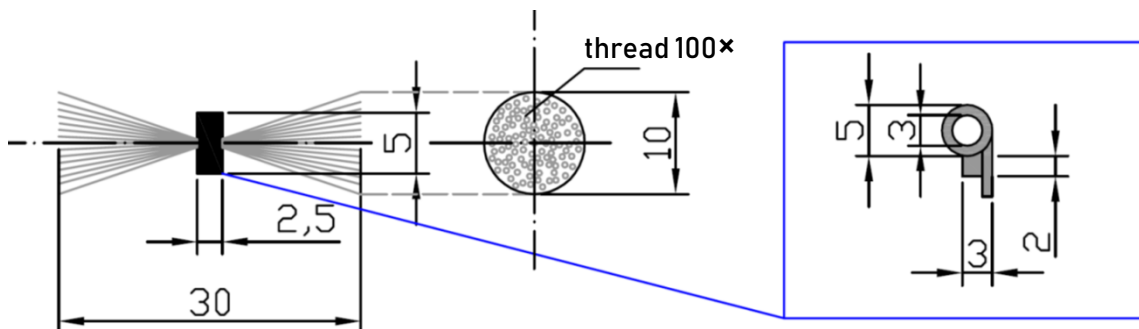


Fig. 5: Technical drawing of tassel arrangement. Dimensions in mm.

2.2.4 Cylindrical arrangement

The fibres were evenly deposited on the support structure, with the filaments tangentially connected by hot melt adhesive. The individual nanofibre carriers were prepared in order that they could be cut off at a point where no supporting fibres were present. A technical drawing of the cylindrical arrangement is displayed in Fig. 6.

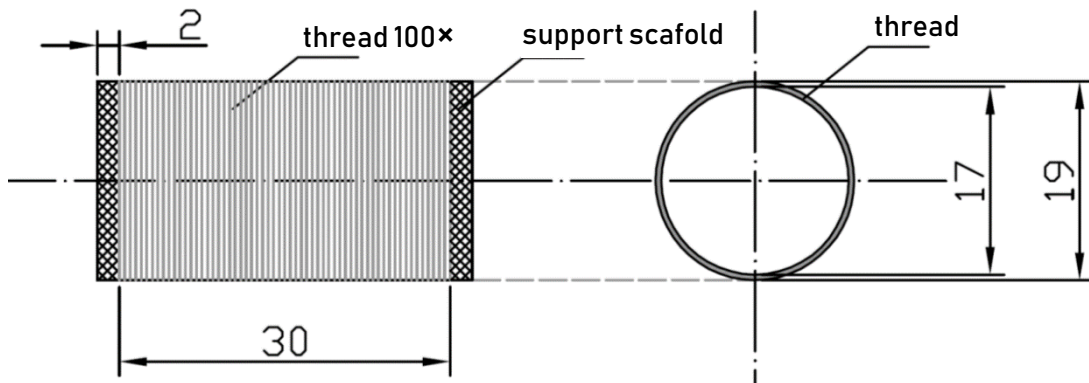


Fig. 6: Technical drawing of the cylindrical arrangement. Dimensions in mm.

2.2.5 Planar arrangement

The planar arrangement is the simplest form for collection of a microbial biomass. On each nanofibre carrier, 3 m fibres were arranged close to each other and parallel, with two supporting nylon fibers (fishing line) at the sides (see technical drawing, Fig. 7). The final shape and size of the nanofibre carrier is defined by transverse connections from melt adhesive at the exact distance on the inner and outer sides.

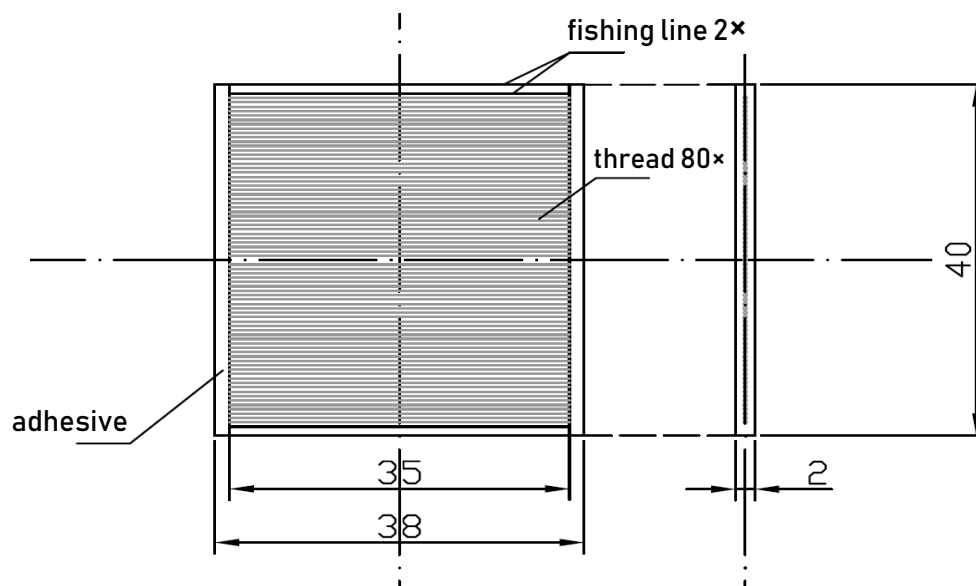


Fig. 7: Technical drawing of the planar arrangement. Dimensions in mm.

2.2.6 Circular arrangement

The nanofibre carrier consisted of a single support thread with a nanofibre layer and a coaxial protective fibre. Nanofibre coating threads with CPF (3 m in length) were wound in several layers (2–3 mm roll width) onto a 10–11 mm diameter roller. Subsequently, the fibre coil was transversally connected at a single point via a fixing filament, which at the same time allowed the connection of the nanofibre carrier to a larger unit. The final nanofibre thread was arranged into a circular arrangement. A technical drawing of the circular arrangement is displayed in Fig. 8.

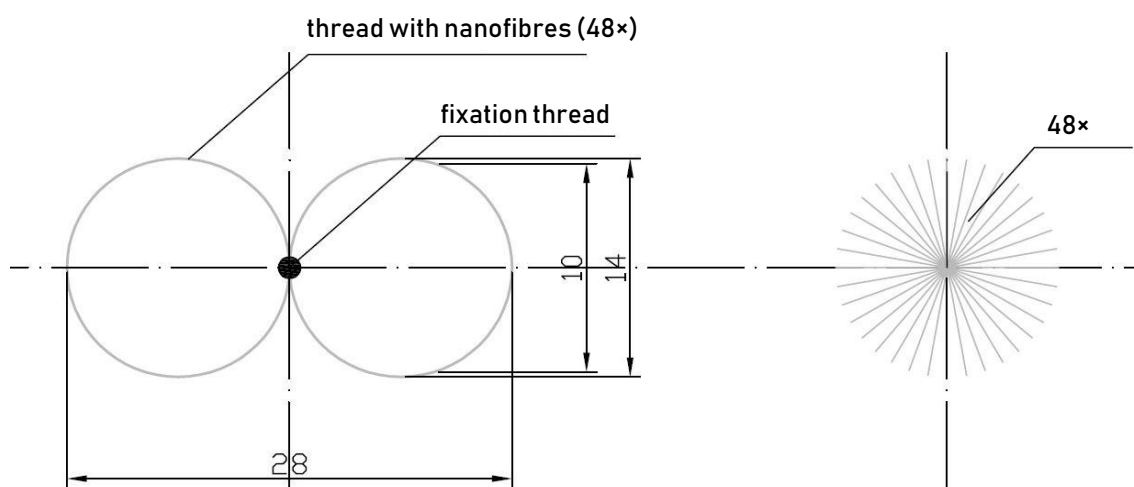


Fig. 8: Technical drawing of the circular arrangement. Dimensions in mm.

2.3 Sample preservation during transport

Four transport variants from actual contaminated sites were compared:

- cooled box (CB)
- dry ice (CO₂)
- liquid nitrogen (N₂)
- RNA later

Three variants were used to examine temperature stability, a cooled box, dry ice and liquid nitrogen, the last variant representing chemical stabilization with RNA later and transportation in a cooled box. Two large sampling campaigns (Table 7) took place during the experiment, the interval between the first and last sampling within each campaign being more than 24 hours due to the distance between localities (Fig. 1, Table 7).

Table 7: Contaminated locality with test wells, dates when individual nanofibre carriers were submerged and data when the transport experiments were performed.

Locality	Well	Carriers installation	First sampling	Second sampling
Horní Počernice	HP-92	20. 6. 2013	22. 8. 2013	24. 10. 2013
Tomášková cihelna	HV-37	16. 4. 2013	21. 8. 2013	23. 10. 2013
Karosa – sklad plynů	HV-12	16. 4. 2013	21. 8. 2013	23. 10. 2013
Jablůnkov	A-1	24. 4. 2013	22. 8. 2013	24. 10. 2013
Velamos	NA-14	15. 4. 2013	22. 8. 2013	24. 10. 2013

2.4 Selection of the best nanofibre carrier

2.4.1 Test of nanofibre carrier material

The six different nanofibre carrier arrangements with different nanofibre densities with CPF and without CPF were submerged at the Spolchemie site (designated wells RW6A-7, RW6A-42 and RW6A-45). The scheme of experiments for selected nanofibre carriers is displayed in Fig. 9. Subsequently, the nanofibre carriers were immediately transported to the laboratory in cooled box. DNA was isolated from 0.5 g of thread and the stability of the microbial biofilm tested using real-time PCR with the universal 16S rRNA primer. Composition of biofilms was tested using NGS to compare the bacterial diversity of different arrangements.

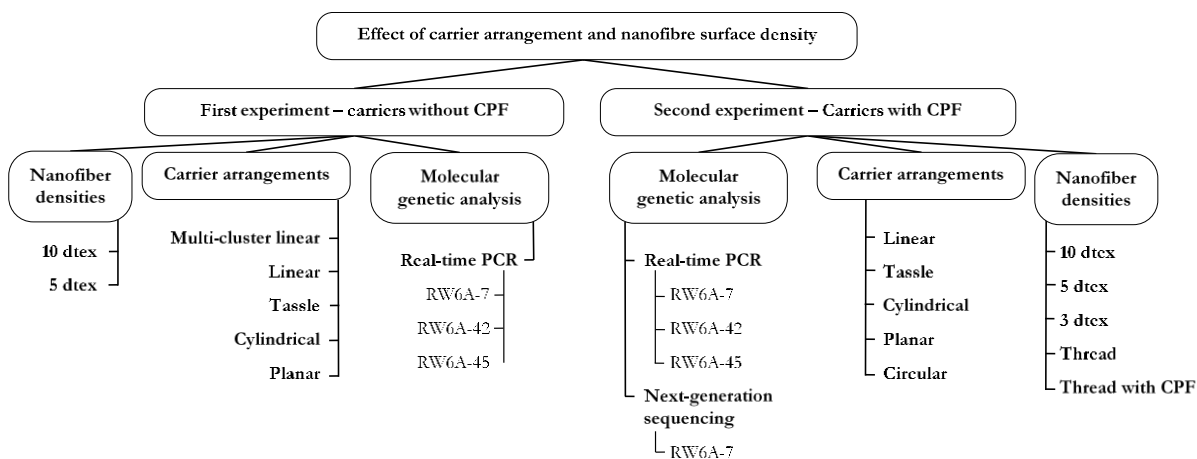


Fig. 9: Scheme of nanofibre carriers experiment at Spolchemie site.

Thread without coaxial protective fibre

Extensive three-year testing of the nanofibre carriers took place over five sampling campaigns at the Spolchemie site (Table 8), during which 131 nanofibre carriers of all shape variants and nanofibre densities were analyzed. Biofilm stability, DNA yield and inhibition were evaluated using molecular genetic analysis.

Table 8: Schedule of long-term testing of nanofibre carriers without CPF at the Spolchemie site.

Locality	Well	Carriers installation	First sampling	Second sampling	Third sampling	Fourth sampling	Fifth sampling
Spolchemie	RW6A-7	10. 11. 2014	18. 12. 2014	19. 4. 2015	29. 7. 2015	18. 7. 2016	26. 6. 2017
Spolchemie	RW6A-42	10. 11. 2014	18. 12. 2014	19. 4. 2015	29. 7. 2015	18. 7. 2016	26. 6. 2017
Spolchemie	RW6A-45	10. 11. 2014	18. 12. 2014	19. 4. 2015	29. 7. 2015	18. 7. 2016	26. 6. 2017

Thread with coaxial protective fibre

Five sampling campaigns took place over a two-year experiment, during which 300 nanofibre carriers were tested (Table 9). Biofilm stability, DNA yields and inhibition within molecular genetic analysis were evaluated.

Table 9: Schedule of long-term testing of nanofibre carriers with CPF at the Spolchemie site.

Locality	Well	Carriers installation	First sampling	Second sampling	Third sampling	Fourth sampling	Fifth sampling
Spolchemie	RW6A-7	9. 4. 2015	29. 7. 2015	20. 10. 2015	2. 12. 2015	18. 7. 2016	26. 6. 2017
Spolchemie	RW6A-42	9. 4. 2015	29. 7. 2015	20. 10. 2015	2. 12. 2015	18. 7. 2016	26. 6. 2017
Spolchemie	RW6A-45	9. 4. 2015	29. 7. 2015	20. 10. 2015	2. 12. 2015	18. 7. 2016	26. 6. 2017

2.4.2 Effect of matrix

The experiment assessing matrix effect was performed over a single sampling campaign at Spolchemie (Table 10), during which groundwater, nanofibre carriers and soil were collected. Microbial communities from the three different matrices were then compared using molecular genetics methods. On 19. July 2016, soil samples were collected near monitoring well RW6A-42 by drilling at 7.2 m and 8.4 m. The depths from which soil samples were collected corresponded to the levels at which the nanofibre carriers were submerged. Groundwater samples and four different nanofibre carrier arrangements (surface density 10 dtex) were collected from well RW6A-42.

Table 10: Sampling campagne for different matrix (soil, groundwater, nanofibre carrier) comparison.

Locality	Well	Matrix	Carriers installation	Sampling
Spolchemie	near RW6A-42	soil	-	19. 7. 2016
Spolchemie	RW6A-42	groundwater	-	18. 7. 2016
Spolchemie	RW6A-42	carrier	9. 4. 2015	18. 7. 2016

2.4.3 Effect of selected arrangements and nanofibre density on bacterial diversity

The aim of this test was to verify whether microbial colonization occurs with similar or different taxonomic composition, thus comparing whether the bacterial diversity of different arrangements differed. All prepared nanofibre arrangements with CFP (density 10 dtex) were used. A second aim was to monitor the influence of nanofibre density on the microbial biofilm forming on the planar arrangement (thread; thread with CPF; 3, 5 and 10 dtex nanofibre density). The overall goal of the experiment was to monitor changes between each variant when compared to water. The RW6A-7 well was selected for this part of the experiment.

2.5 DNA isolation

Owing to the similarity of the biofilms formed on the nanofibre carriers and the biofilm in soil, DNA was extracted from the nanofibre carriers using the FastDNA SPIN Kit for Soil, as described in Chapter 1 of the Experimental section, subchapter 2.4, Molecular genetic analysis. Thereafter, the DNA concentration in the samples was measured using a Qubit® 2.0 fluorometer.

2.6 Molecular genetic analysis

Real-time PCR analysis was performed as described in Chapter 1 of the Experimental section, subchapter 2.4. Two types of test were used in this study. First, Primer U16SRT, which characterizes total bacterial biomass, was used to assess the rate of biofilm growth. Secondly, a primer characterizing presence of specific bacterial degraders was also tested to evaluate nanofibre carrier use during the remediation process. NGS analysis was performed as described in Chapter 2 of the Experimental section, subchapter 2.7.

3 Results and discussion

We developed a compact nanofibre carrier for reliable long-term sampling of microbial biomass in polluted localities. The nanofibre carrier is of sufficient mechanical stability and is protected by a polyethylene tube during its submersion into the monitoring well. We succeeded in designing a nanofibre carrier that can be easily handled in the molecular genetic laboratory with DNA isolation of high quality.

3.1 Development of the nanofibre carrier

Polyurethane (Larithane 1083) was chosen as a suitable material for electrospinning nanofibres as it allows strong microbial colonization, mainly due to its hydrophobic nature and high surface to volume ratio (Kriklavova and Lederer, 2010). Protection of the nanofibre layer on the support thread was developed mainly in order to overcome poor abrasion resistance, which limits manipulation of the sample. The coaxial protective thread was developed in collaboration with the Faculty of Textile Engineering, Department of Nonwoven Nanofibrous Materials (KNT) at TUL. The mechanical stability of the nanofibre layer was improved with coaxial protective fibre (polyamide 6, 11 dtex) wrapped around the thread with the nanofibre layer. Subsequently, new nanofibre carrier shapes were created with this protection included. Scanning electron microscopy (SEM) images of support threads and nanofibres without coaxial protective fibres are shown in Fig. 10A. The original thread with coaxial protective fibre but without nanofibre deposition is shown in Fig. 10B. Figures 10C and D show modified threads with coaxial protective fibre at different nanofibre surface densities.

The nanofibres on all the modified surfaces exhibited a typical interconnected sub-micron structure on the support thread. Clear evidence of increased nanofibre surface density is obvious when comparing Fig. 10C and D. The higher surface density led to a more dense and interconnected nanofibre net that almost covered the whole support thread, producing an improved surface for bacterial attachment. Lowered surface densities led to a more open structure, with more open spaces between the nanofibres and support threads for biofilm formation.

The following subchapters (3.1.1–3.1.6) summarize the positives and negatives of the nanofibre carrier arrangements tested.

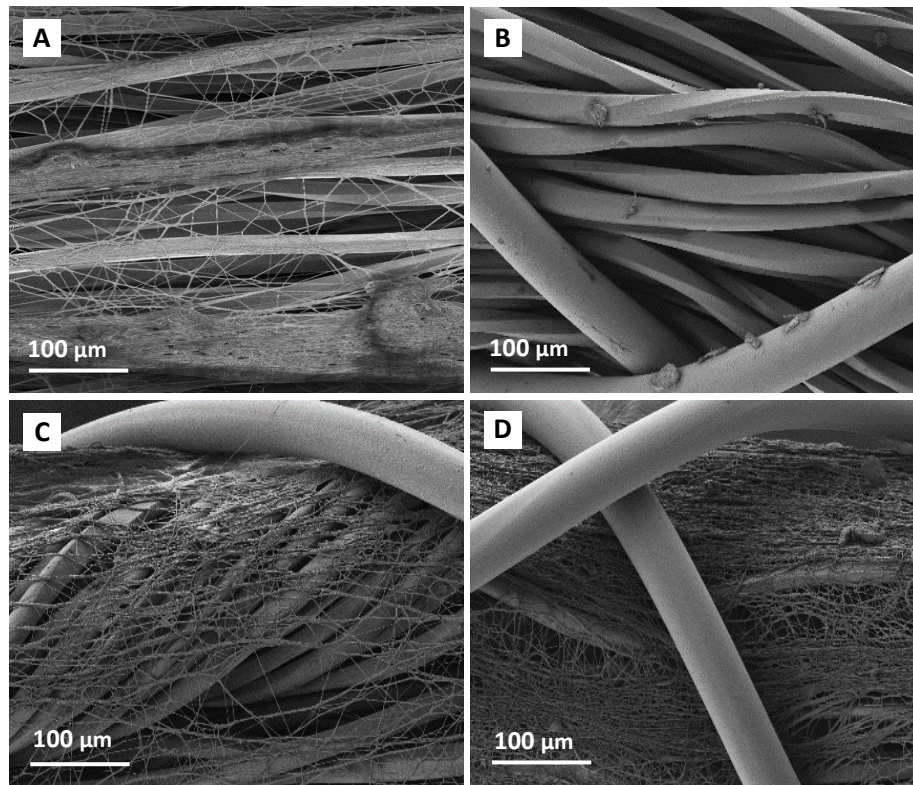


Fig. 10: SEM micrographs of modified threads with coaxial protective fibres without a nanofibre layer (A), with nanofibres without the coaxial protective fibre (surface density 5 dtex), and (B) with nanofibre surface densities of 3 dtex (C) and 10 dtex (D); Scale bar 100 μm . Image by P. Kejzlar, TUL.

3.1.1 Multi-cluster linear arrangement

The main disadvantage of the multi-cluster linear arrangement (Fig. 11) was multi-level time-consuming production, the large amount of hot melt adhesive needed and the associated support material, which interferes with DNA isolation. Based on this results, multi-cluster linear arrangement cannot be recommended for *in situ* monitoring.



Fig. 11: Nanofibre carriers: Multi-cluster linear arrangement.

3.1.2 Linear arrangement

The linear nanofibre carrier arrangement was developed especially for molecular genetic analysis. This nanofibre carrier is without ballast material (adhesive or support construction) and can be easily manipulated (Fig. 12). The relatively high compactness of the nanofibre carrier, however, represents a disadvantage as it can hamper contact between the nanofibre carrier surface and autochthonous bacteria, such that the resulting biofilm is not compacted. The relatively high density of the threads can additionally create local anaerobic conditions that influence growing biofilm composition, which differs from the biomass composition around the nanofibre carrier.



Fig. 12: Nanofibre carriers: Linear arrangement.

3.1.3 Tassle arrangement

The tassle arrangement (Fig. 13) was specifically developed for molecular genetic analysis and, in its current form, appears to be suitable for use in field applications. The open structure enabled sufficient contact between the surface of the fibres and the surrounding environment. On the other hand, the greater distance between the centres led to aggregation of individual fibres, reducing fibre contact with groundwater.



Fig. 13: Nanofibre carriers: Tassle arrangement.

3.1.4 Cylindrical arrangement

The cylindrical arrangement (Fig. 14) showed a high degree of flexibility and ease of preparation and automation. This arrangement was chosen primarily because of its ‘open’ structure, which allows greater fibre contact with groundwater. In addition, it allows easy and simple modification, e.g. by changing the diameter or material used for the supporting structure or number of fibre layers. Disadvantages include the sharp ending of individual elements, which have a tendency to fray, and the high amount of ballast material needed.



Fig. 14: Nanofibre carriers: Cylindrical arrangement.

3.1.5 Planar arrangement

The planar arrangement (Fig. 15) was chosen because of its high flexibility and the high level of surface contact with the aquatic environment. A further advantage is the ease of technological processing the nanofibre carriers into their final form. On the other hand, the planar arrangement was not suitable for molecular genetic analysis due to the nanofibre carrier’s size and the presence of the supporting fishing line and other ballast material. These parts of the planar arrangement have to be removed before DNA extraction and this manipulation may lead to a loss of microbial biofilm and contamination.



Fig. 15: Nanofibre carriers: Planar arrangement.

3.1.6 Circular arrangement

The circular arrangement (Fig. 16), a modification of the linear arrangement, was specifically tested for molecular genetic analysis; hence, it has no support structures or fixation elements (e.g. adhesive, plastic cable ties, fishing line). This minimizes manipulation before DNA extraction, eliminates potential errors in pre-treatment of the sample and maximizes DNA yield. The circular arrangements also differs from the other nanofibre carriers through its open structure, which ensures very high contact with the autochthonous microflora. This is especially important for long-term monitoring as it allows the sampling of one nanofibre carrier in a series by easy cut off.



Fig. 16: Nanofibre carriers: Circular arrangement.

Table 11 summarizes the advantages and disadvantages of the different nanofibre carrier arrangements described in section above.

Table 11: Advantages and disadvantages of nanofibre carriers tested *in situ*.

Carrier arrangement	Strengths	Weaknesses
Multi-cluster linear	high fibre contact surface high porosity	large amount of adhesive multi-step preparation
Tassle	high fibre contact surface wide application possibilities	more demanding production problematic automatic production
Linear	absence of support material suitable for the molecular genetic analysis	more demanding production smaller contact surface of fibres
Cylindrical	high fibre contact surface easy and fast production	large amount of support material "sharp" ends of carriers
Planar	easy production high fibre contact surface	mechanical durability not suitable for molecular genetic testing
Circular	absence of support material easy production high fibre contact surface suitable for the molecular genetic analysis	low fibre density for certain applications (solution – modification with applied load)

3.2 Effect of transport method on DNA yield

Preservation of nanofibre carrier biomass during transport to the laboratory is crucial for obtaining reproducible results; hence, the effect of transport method on DNA yield from cylindrical arrangement was assessed prior to the detailed testing of each nanofibre carrier arrangement at the five field sites. Further, as transportation can last from hours to a few days, it was necessary to test the effect of time on both sample stability and DNA yield.

During the test, it was necessary to consider both the sampling procedure *in situ* and transport time. The most important step to prevent contamination of the biofilm during sampling is the use of appropriate aseptic manipulation techniques, i.e. protective gloves should be worn and all equipment should be sterilized with ethanol before sampling the next nanofibre carrier. As the nanofibre carriers are relatively small, sterile vials or small falcons can be used for transport.

Changes in DNA yield between sampling rounds in August and October 2013 are shown in Fig. 17. The differences observed at each site were probably caused by differences in the abundance of autochthonous bacteria, and thus the rate of biofilm formation on the nanofibre carriers. The results suggest that preservation method during transportation had no influence on either DNA yield or on the quality of DNA extracted. The DNA was stable and the yield was sufficient, even after transportation using the simplest technique, i.e. in a cooled box with ice packs.

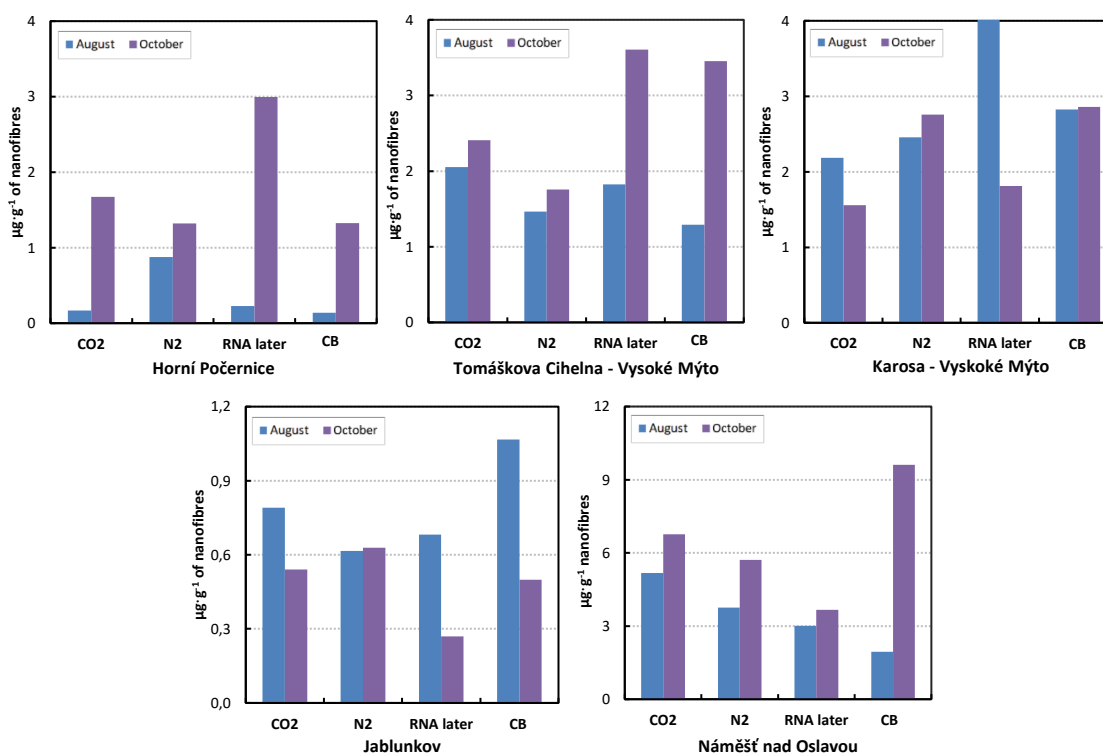


Fig. 17: Comparison of DNA yield between two sampling rounds in August and October 2013.

It is worth noting that the amount of biofilm input is an important factor, together with the DNA isolation method used. Owing to the weight limit required during the isolation procedure, just a part of the nanofibre carrier can be used; hence, it is not possible to select that part of the nanofibre carrier with the highest microbial biofilm load as this is not clearly visible. Although we presumed a homogeneous colonization on the nanofibre carrier, the reality may be different and DNA yield may differ on the nanofibre carrier.

Trends in biomass growth on the nanofibre carriers differed at each field site. At three of the five sites, for example, yield of isolated DNA increased over a two-month period. DNA yield was dependent on the period between nanofibre carrier submersion and sampling, as well as on the bacterial abundance *in situ*. Nanofibre carriers at the

Horní Počernice site had almost no DNA after two months exposure, though there was a significant increase in DNA yield after four months. This trend was also observed at the other sites, suggesting that the nanofibre carrier must be submerged for at least three months before sampling in order to obtain sufficient DNA.

To conclude, the cooled box proved to be a fully satisfactory means of transport, being neither expensive nor methodologically challenging. Further, no special preconditions or precautions were required, unlike transport with liquid nitrogen, though a fully aseptic sampling procedure was necessary in order to avoid sample contamination. Preservation of the nanofibre carriers with RNA later should be considered only if the RNA profile of the microbial community is tested.

3.3 Effect of naofibre carrier arrangement and nanofibre surface density

The study on the effects of nanofibre carrier arrangement and nanofibre surface density on DNA yield was divided into two parts. The first involved testing the five different arrangements (multi-cluster linear, tassle, cylindrical, linear and planar) without the coaxial protective fibre (CPF) and at two different nanofibre densities, 5 and 10 dtex. All nanofibre carriers were submerged into wells RW6A-7, RW6A-42 and RW6A-45 at the Spolchemie site and left for three years. Based on the results from the first year of monitoring, the second batch of modified nanofibre carriers were submerged in the same wells during the second part of the experiment. Three nanofibre carrier arrangements from the first part of the experiment (linear, tassle, planar) were selected for submersion, together with the newly developed circular arrangement, each with CPF. A comparison of nanofibre carrier morphology, with and without CPF, is displayed in Fig. 18A and B.

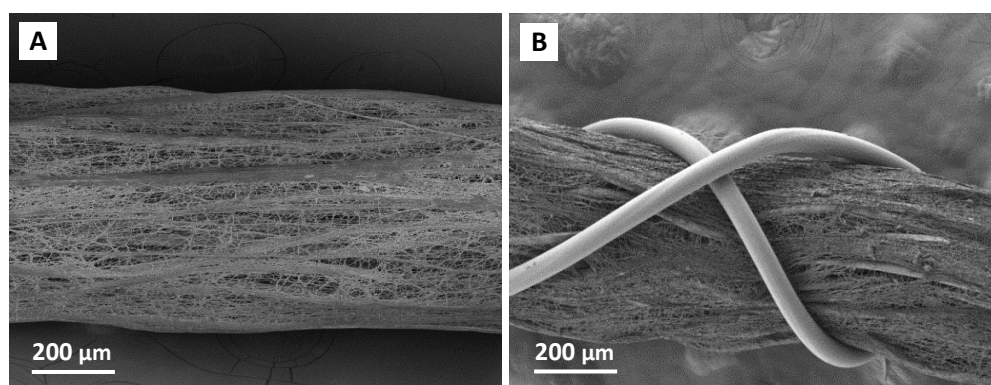


Fig. 18: SEM image of nanofibre thread (10 dtex) without coaxial protective fibre (A), and with coaxial protective fibre (B); Scale bar 200 µm. Image by P. Kejzlar, TUL.

3.3.1 Nanofibre carrier without coaxial protective fibre

Detailed tests of different nanofibre carrier arrangements without CPF were run under actual *in situ* conditions. The individual nanofibre carrier's composition and the dates of sampling rounds are listed in Table 5 and Table 8.

The nanofibre carriers in well RW6A-42 were chosen as an example summarising the long-term monitoring of this part of the experiment, with the results of the molecular genetic analysis displayed in Fig. 19. The development of Cq values in well RW6A-42 showed a gradual increase of bacterial biomass on the nanofibre carrier surface. The decrease in bacterial biomass detected over the last sampling round in June 2017 was probably caused by a remediation intervention in close proximity to the well. The same increasing trend in bacterial biofilm development was also observed at wells RW6A-7 and RW6A-45.

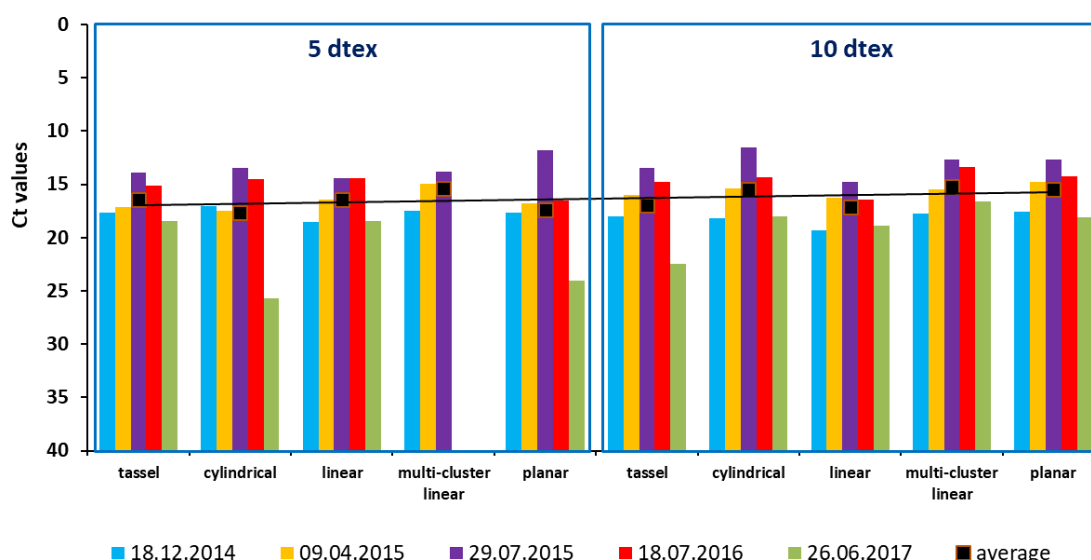


Fig. 19: Evolution of total bacterial biomass on different nanofibre carrier arrangements with nanofibre densities of 5 and 10 dtex in well RW6A-42, assessed using the U16SRT primer.

The results confirmed the long-term stability of the bacterial biofilm on each of the nanofibre carriers. Moreover, the microbial biofilm reflected actual changes ongoing at each site. Thus, nanofibre carriers without CPF can be considered as an effective tool for long-term monitoring of autochthonous microflora. One disadvantage of nanofibre carriers without CPF, however, was the low mechanical stability of the nanofibre layer during sampling and DNA isolation.

3.3.2 Nanofibre carrier with coaxial protective fibre

During the second phase, we tested the development of bacterial biofilm on improved nanofibre carriers. The addition of CPF increased the mechanical stability of the nanofibre layer, while new nanofibre carrier arrangements avoided pre-treatment prior to DNA extraction. Finally, the nanofibre carriers were prepared using support threads only, with and without CPF at a nanofibre density of 3 dtex (Table 6). The dates of sampling rounds are listed in Table 9.

As in the first phase, the nanofibre carriers submerged in well RW6A-42 were chosen as an example of long-term monitoring. The results, displayed in Fig. 20, indicated long-term stability, with no significant differences in Cq values between different sampling rounds. At the same time, Cq values for nanofibre carriers with CPF oscillated around 15 in the first sampling round, suggesting more rapid nanofibre carrier colonization with CPF and increased stability of the microbial biofilm. These trends can be explained by the more compact nanofibre structure and improved mechanical stability due to the CPF.

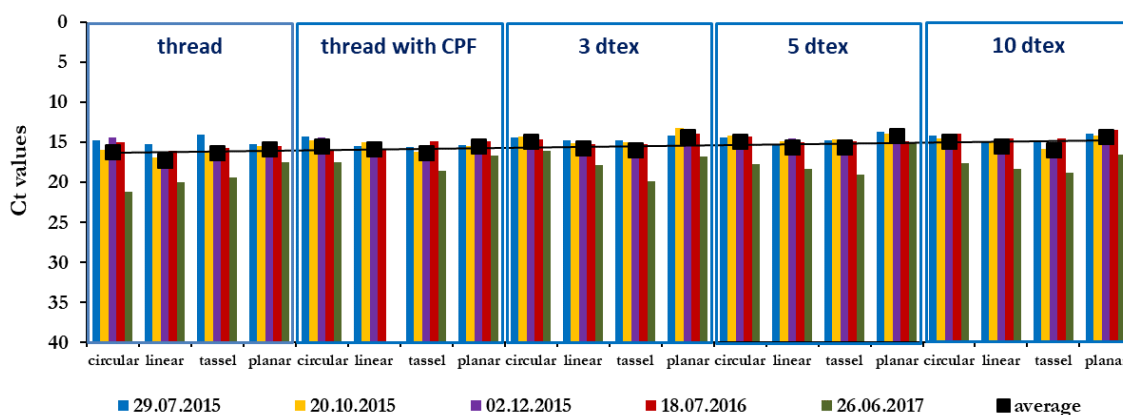


Fig. 20: Evolution of total bacterial biomass on different nanofibre carrier arrangements with different nanofibre densities in well RW6A-42, assessed using the U16SRT primer.

3.3.3 Monitoring of groundwater

The results obtained from molecular genetic analysis of the nanofibre carriers were compared with those from groundwater samples at the Spolchemie site. Changes in the abundance of total bacterial biomass in groundwater from the different wells are shown in Fig. 21. The groundwater results indicated long-term nanofibre carrier stability, complementing the results described earlier.

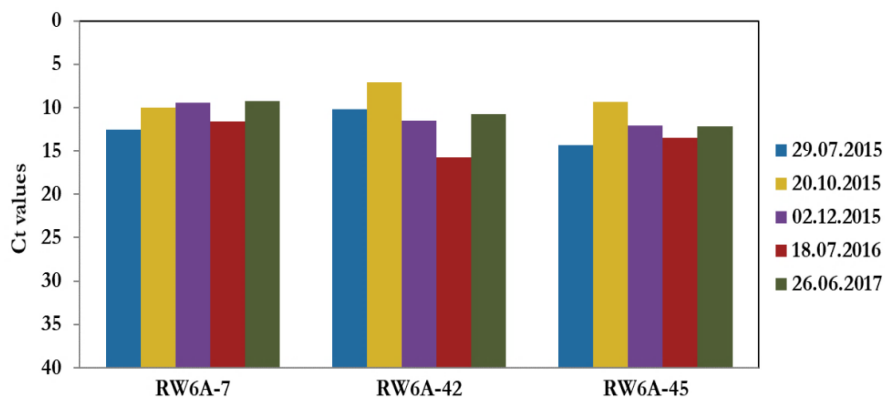


Fig. 21: Evolution of total bacterial biomass in groundwater in the monitoring wells, assessed using the U16SRT primer.

3.3.4 Nanofibre stability

Long-term testing of a series of nanofibre carriers under actual *in situ* conditions again confirmed the stability of the bacterial biofilm on the nanofibre carrier surface. SEM micrographs of nanofibre carrier threads with CPF submerged for one year are displayed in Fig. 22. The images show compact nanofibre structure with no significant damage (Fig. 22A) and extensive colonization by microorganisms (Fig. 22B). When comparing the same nanofibre carrier arrangements with and without CPF, qPCR analysis indicated a higher abundance of total bacterial biomass was observed on nanofibre carriers with CPF. The nanofibre carriers with CPF also showed more rapid growth of biofilm on their surface.

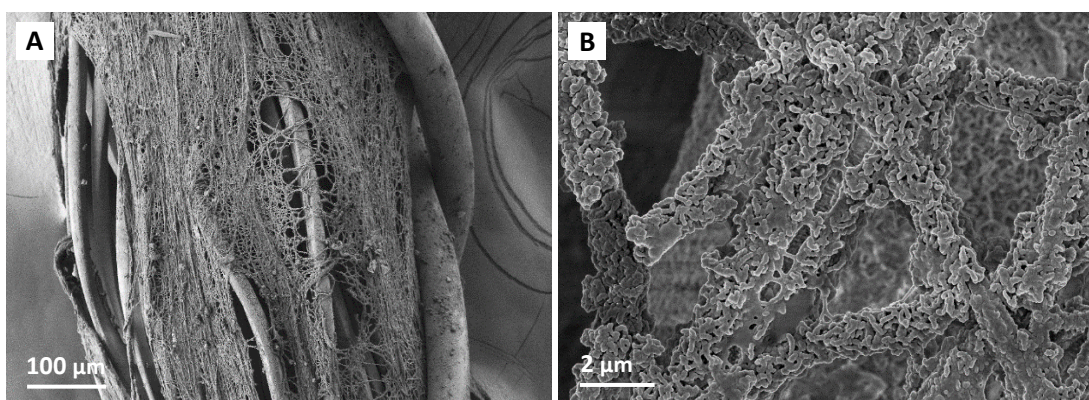


Fig. 22: SEM image of nanofibre thread at 10 dtex after one year's exposure. Scale bar 100 µm (A) and 2 µm (B). Image by P. Kejzlar, TUL.

Based on the results from the above experiments, these nanofibre carriers represent an effective tool for long-term *in situ* monitoring. The results also indicate a similar quantity of bacterial biomass on each nanofibre carrier arrangement.

3.4 Effect of nanofibre carrier arrangement on bacterial diversity

3.4.1 Influence of arrangement

The composition of bacterial communities on different nanofibre carrier arrangements was performed using NGS. Nanofibre density 10 dtex was chosen to be tested due to the best DNA yield during whole experiment. The OTU graph (Fig. 23) shows a similar bacterial diversity on all the arrangements, even during the final sampling described in subchapters 3.3.1 and 3.3.2. The differences observed tend to reflect the abundance of individual taxa rather than bacterial diversity, which was comparable in all samples. Even the total diversity in groundwater samples was relatively similar to that on the nanofibre carriers (Fig. 25, see subchapter 3.4.2). Note that groundwater samples were not obtained by slow pumping but were taken directly from the well; hence, they better characterize the aquatic environment of the well where the nanofibre carriers were submerged rather than the situation in the vicinity of the wells.

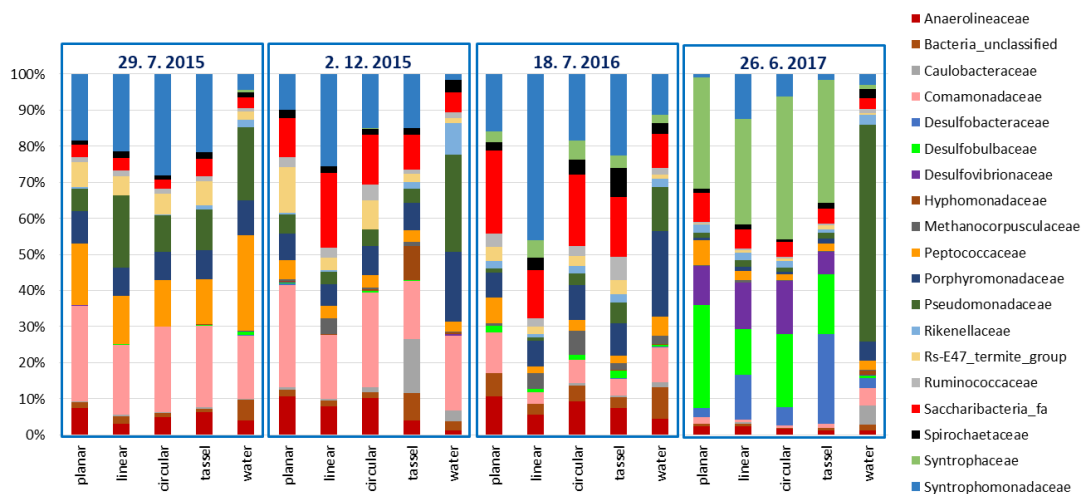


Fig. 23: Comparison of bacterial diversity between different nanofibre carrier arrangements with a nanofibre surface density of 10 dtex on the support thread and water during long-term monitoring. Bacteria with a relative abundance of over 5% are shown at family level.

The bacterial diversity during the initial test years (first and second sampling) was similar to that for the groundwater from the well, which probably represents the period when

the biofilm was forming. Sampling in 2016, however, showed a higher diversity, presumably as the surrounding environment was influencing diversity. As previously mentioned, the linear arrangement could have been subject to local anaerobic conditions.

This hypothesis was confirmed by NGS, as anaerobic *Desulfobacteraceae* and *Saccharibacteria* represented the majority of bacterial diversity, with relative abundances of over 5%.

Generally, during sampling in 2015 and 2016, the families *Anaerolineaceae*, *Comamonadaceae*, *Peptococcaceae*, *Porphyromonadaceae*, *Pseudomonadaceae* and *Syntrophomonadacea* were all detected, each predominantly associated with the CE-contaminated site.

The final sampling in 2017 showed a similar reaction for all the arrangements tested, with visible changes in bacterial community confirming that the nanofibre carriers were reacting to radical changes in local conditions (Fenton like reagent application). This would explain the massive proliferation of sulphate-reducing *Desulfobacteraceae*, *Desulfo-bulbaceae*, *Desulfovibrionaceae* and *Syntrophaceae* previously undetected in this well. In the case of groundwater, the *Pseudomonadaceae* family predominated in the final sampling.

Significant differences in bacterial dominance after two and three years of monitoring are shown as a OTU column graph in Fig. 23 and as a heat-map in Fig. 25, where the nanofibre carrier and groundwater samples are separated and clustered into their own groups.

3.4.2 Influence of nanofibre density

The influence of different nanofibre densities on microbial community structure was tested using the planar arrangement. The effect of nanofibre density was negligible during the first and second sampling; however, the third sampling showed clear differences in the frequencies of individual family. Sampling in 2017 showed proliferation of *Desulfobacteraceae* and *Desulfo-bulbaceae*, both sulphate-reducing taxa (Fig. 24), explainable as taxa competition rather than any influence of nanofibre density.

On both the nanofibre carriers and in the water, it was possible to observe an increase in the percentage of *Saccharibacteria* and a decrease in the families *Comamonadaceae* and

Peptococcaceae during sampling in 2015 and 2016. Both *Comamonadaceae* and *Peptococcaceae* are commonly found on nanofibre carriers in the early stages of biofilm formation. These taxa are capable of rapid colonization of new environments and are known for their high growth rate. In the early phases, they dominate the entire system and later stabilize at lower levels.

OTU graph (Fig. 24) shows stable bacterial communities until 2017, when remediation intervention strongly influenced the whole bacterial community.

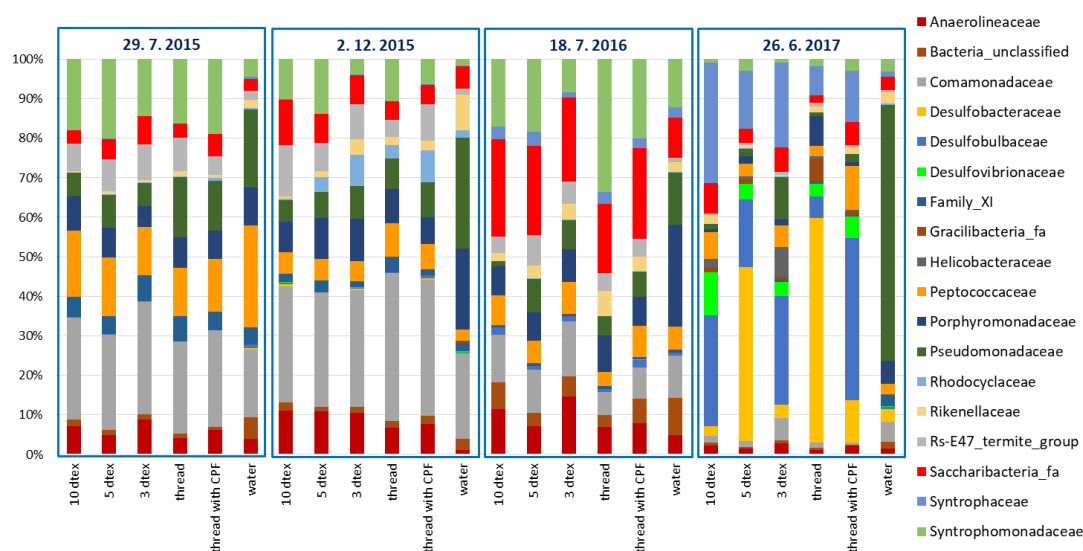


Fig. 24: Comparison of bacterial diversity between planar arrangements with different nanofibre surface densities on the support thread and water during long-term monitoring.

Bacteria with a relative abundance of over 5% are shown at family level.

The heat map (Fig. 25), which summarizes the entire experiment, confirms the partial observations outlined above. Two groups of samples were clustered separately, groundwater and the samples from 2017, which followed application of the Fenton like reagent. The similar composition of the main OTUs is evident from their matching colours, while separation of the groundwater samples was logical as it represents a different type of matrix. The largest group was made up of nanofibre carriers sampled over 2015 and 2016.

These results again confirm that nanofibre density and nanofibre carrier arrangement had no influence on the bacterial composition of newly established biofilms.

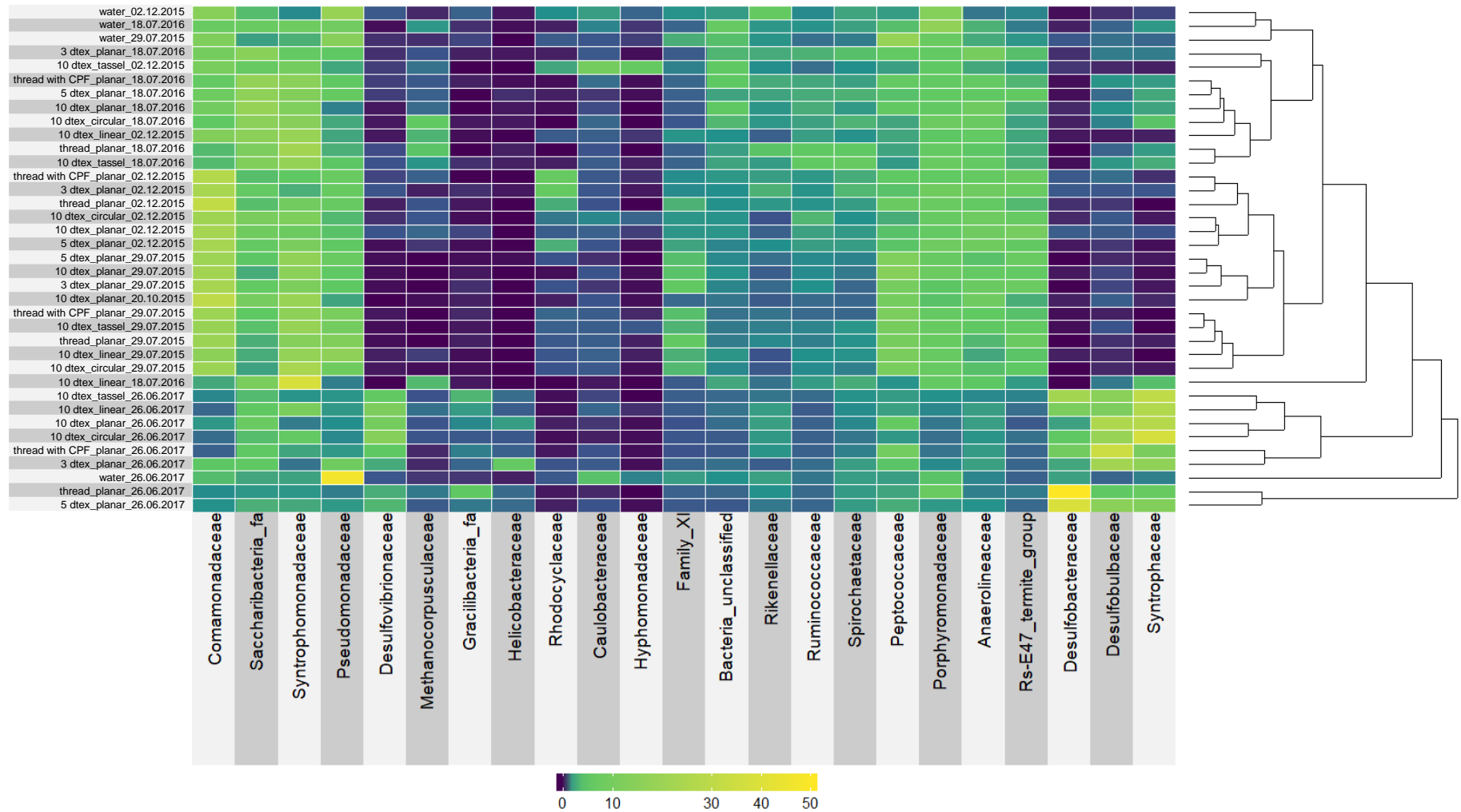


Fig. 25: Family level community analysis. Bacteria with a relative abundance of over 5% are shown at family level.

3.5 Comparison of microbial diversity in different matrices

We compared bacterial diversity at the contaminated site from soil, groundwater from well vicinity and nanofibre carrier using NGS analysis. A similar bacterial diversity was observed on each nanofibre carrier arrangement (Fig. 26). This again supports the hypothesis of similar biofilm formation on different nanofibre carrier arrangements.

Microbial community composition from both soil samples differed from that for water and the nanofibre carriers, while soil bacterial diversity from a depth of 7.2 m was completely different from that sampled at 8.4 m. Diversity at 8.4 m corresponded more closely with the bacterial consortium on the nanofibre carriers. The results obtained from the soil sample analysis point to a difficulty in interpretation of field data, i.e. even samples from the same site and the same well can often show completely different results, thus confirming the inadequacy of this matrix for systematic long-term monitoring.

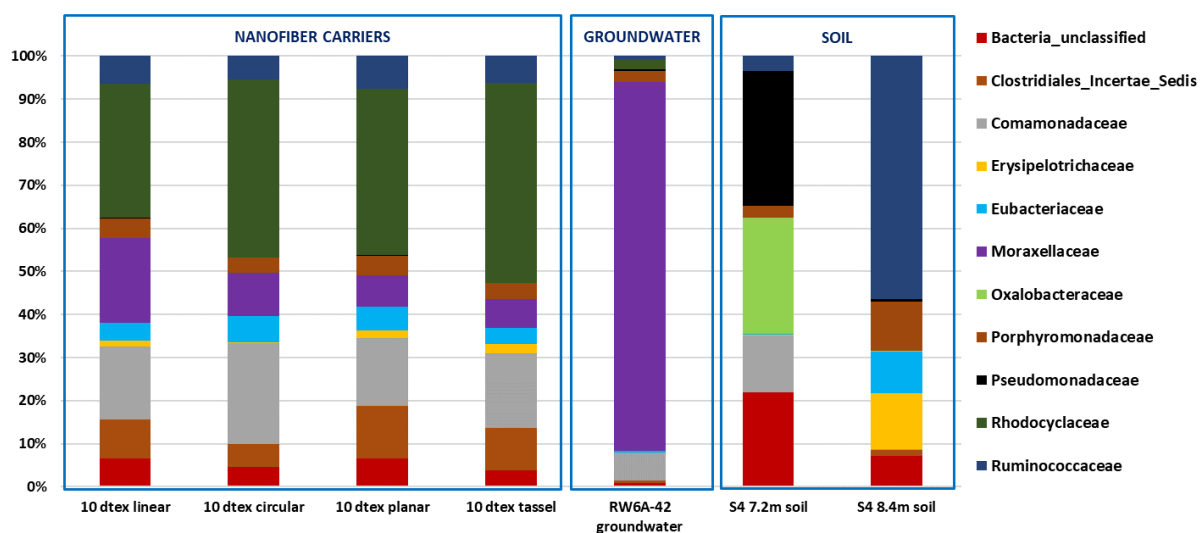


Fig. 26: Comparison of bacterial diversity between three different matrices: nanofibre carrier arrangement, groundwater obtained by slow pumping and soil from two different depths.

Bacteria with a relative abundance of over 5% are shown at family level.

The bacterial consortium in groundwater samples did not match with either the soil samples or that on the nanofibre carriers. This can be explained by the fact that groundwater was obtained by slow pumping representing a very specific environment in the well vicinity. The presumption that this way obtained groundwater should mirror bacterial community in the soil was not proved. The main difference in this case was the high frequency of the *Moraxellaceae* family in groundwater samples.

Nanofibre carriers submerged in a well, therefore, are exposed to a specific environment that differs greatly from soil and even groundwater from the vicinity but tends to mirror a bacterial community preferring growth on a matrix rather than a motile form. Moreover, not all taxa from the soil environment will be found in the aquatic environment which is also more strongly influenced by groundwater flow. This will also influence biofilm development on the nanofibre carrier, which can simulate the soil environment.

These mechanisms seem to be highly complicated and should be further explored. Nevertheless, from our study of different nanofibre carrier density and arrangement (section 3.4.1 and 3.4.2), it seems that the structure of biofilm developed on nanofibre carriers reflects well the groundwater community structure present in the well at least first months of the monitoring.

4 Summary

The experiments performed above verify the suitability of using nanofibre carriers as a tool for microbial biomass sampling from actual sites. The results confirm long-term stability of the microbial biofilms.

The most suitable nanofibre carrier arrangement was selected using large-scale tests, the results indicating that a circular arrangement with the nanofibre layer protected by CPF was the most suitable. This arrangement appears to be a very promising tool for the monitoring of contaminated sites. Although the tests did not confirm an effect of different nanofibre surface density or nanofibre carrier arrangement on DNA yield or bacterial diversity. Unlike the other nanofibre carrier arrangements, circular nanofibre carriers do not need pre-treatment before DNA extraction and preparation is not time-consuming. The circular arrangement has a higher contact area compared with the linear arrangement. Use of a support thread, with the nanofibre layer protected by CPF, appears to be the best option due to the more rapid growth of a stable microbial biofilm on its surface. Using these nanofibre carriers, there is no need for the filtration of large volumes of contaminated groundwater and it is possible to transport samples over large distances.

The results obtained showed no need of special transport techniques and the individual nanofibre carriers can be transported in a simple cooling box, potentially using a courier service.

THESIS
CONCLUSION

Molecular genetic analysis of natural microbial communities from remediated areas had only been explored marginally when I began my studies. The main benefits of my thesis therefore, are in establishing reliable methods for analysis of microbial DNA from complex environmental matrices, their employment in diagnostics and the precise tailoring of remediation strategies most suitable for a given polluted site. I also developed, and later patented, a range of nanofibre carriers applicable for long-term monitoring of polluted areas.

Determination of microbial community structure in environmental samples from contaminated sites is impossible using cultivation methods, and for this reason, I explored the use of advanced molecular genetic techniques. First, I implemented a method for isolation of quality DNA from groundwater and soil samples. The achievement of a reliable, quick and cheap method for DNA isolation was a fundamental key-step for the whole experimental section of this study. In parallel, qPCR and NGS techniques were established and adjusted to obtain comprehensive data on natural microbial communities.

Concerning evaluation of remediation strategies, I found that:

- Short-term biological monitoring is suitable for site characterization when deciding which remediation method should be used. Any final decision on supportive substrate application (e.g. whey, sodium lactate, glycerol) can then be made based on an evaluation of an adequate number of microbial markers. Physico-chemical parameters alone do not provide sufficient information on ongoing microbial dechlorination; thus, it is impossible to clearly determine which substrate is the best to apply at any given site. Ideally, objective site characterization requires a combination of chemical, physical and biological analyses.
- Vertical stratification of key biological and hydrochemical parameters must be considered when assessing CE biodegradation, even in shallow aquifers. For example, treatment of CEs in the oxic zone of an aquifer using enhanced *in situ* anaerobic bioremediation may prove impractical.
- Long-term monitoring is suitable for the evaluation of remediation activities and for ensuring that the following steps efficiently clean up polluted sites.

- Very strong chemical remediation activity (Fenton-like reaction, nZVI) caused an almost complete disappearance of autochthonous microflora; however, only affected the bioremediation processes temporarily, especially in highly permeable terrains with faster groundwater flow.
- The application of a supportive substrate usually led to improved bacterial community growth. Durability was directly dependent on the local properties of the remediation site. Low terrain permeability with slow groundwater flow resulted in a longer effect, even when applying a smaller dose of the substrate. The opposite effect might be expected at sites of high permeability or faster groundwater flow.
- The differences in biodegradation activity at different contaminated sites were mainly caused by different rates of groundwater flow, geochemical conditions and concentration of toxicants.

Concerning the microbial communities at the contaminated site, it was found that:

- Vertical stratification of different microbial communities can be expected based on prevalent redox conditions.
- Highest microbial diversity was found in the aerobic upper zones and decreased with increasing depth and anaerobic conditions. Anaerobic microbes (*Firmicutes*, *Chloroflexi*, *Actinobacteria*, *Bacteroidetes* and *Gallionellaceae*) or sulphate-reducing (e.g. *Desulfobulbaceae*, phylum *Proteobacteria*) were all common at sites contaminated by CEs.
- Organohalide-respiring bacteria responded positively to chemical remediation activity, which decreases high concentrations of CE pollutants. An influx of untreated groundwater from the surroundings led to rapid re-inoculation of bacteria, with bacterial reductive dechlorination typically increasing when compared to biodegradation before remediation.
- Organohalide-respiring, sulphate-reducing and denitrifying bacteria, along with reductive dehalogenase genes responsible for dechlorination of vinyl chloride, all responded positively to biostimulation.

- Abundance of specific bacteria involved in biodegradation typically increases hundreds or thousands of times following chemical remediation followed by stimulation using an organic substrate. These trends have been proven independently at different localities, only varying in time-scale.

In parallel, a series of nanofibre carriers were developed in order to obtain representative material for long-term monitoring of microbial communities. Sampling of groundwater is rather complicated, requiring slow pumping to obtain samples from the vicinity around the well, and soil sampling on a regular base is impossible because of the high cost of the drilling technology. Available trapping systems were not directly suitable for contaminated groundwater; hence, a range of nanofibre carriers were developed that combine the advantages of nanofibres with high specific surface area and tested *in situ*.

The resulting nanofibre carriers, protected by firm polyethylene tubes, can easily be used for long-term monitoring of bacteria at contaminated localities. Importantly, the nanofibre carriers exhibited non-preferential growth of microorganisms and were compact, small, easily transportable and suitable for DNA isolation in the laboratory. Their long-term stability was confirmed following more than 36 months installation *in situ*. NGS results from different matrices, different arrangements and different nanofibre densities indicate that the nanofibre carriers offer a great opportunity for molecular analysis of microorganisms in polluted groundwater.

The most appropriate nanofibre carrier design, allowing for the rapid formation of a stable biofilm and subsequent DNA isolation, was a circular thread arrangement with a nanofibre layer protected by CPF. Thanks to the nanofibre carriers, there is no need for the filtration of large volumes of groundwater and samples can be simply transported in a cooled box.

The individual shapes and the composition of the nanofibre carriers were patented (utility model No. 31266).

The list of published papers is as follows:

- Dolinová, I., Štrojsová, M., Černík, M., Němeček, J., Macháčková, J., & Ševců, A. (2017). Microbial degradation of chloroethenes: a review. *Environmental Science and Pollution Research*, 24(15), 13262-13283. (IF, 2.80)
- Dolinová, I., Czinnerová, M., Dvořák, L., Stejskal, V., Ševců, A., & Černík, M. (2016). Dynamics of organohalide-respiring bacteria and their genes following *in situ* chemical oxidation of chlorinated ethenes and biostimulation. *Chemosphere*, 157, 276-285. (IF, 4.43)
- Němeček, J., Dolinová, I., Macháčková, J., Špánek, R., Ševců, A., Lederer, T., & Černík, M. (2017). Stratification of chlorinated ethenes natural attenuation in an alluvial aquifer assessed by hydrochemical and biomolecular tools. *Chemosphere*, 184, 1157-1167. (IF, 4.43)
- Fraraccio, S., Strejcek, M., Dolinova, I., Macek, T., & Uhlík, O. (2017). Secondary compound hypothesis revisited: Selected plant secondary metabolites promote bacterial degradation of cis-1, 2-dichloroethylene (cDCE). *Scientific Reports*, 7(1), 8406. (IF, 4.12)
- Dolinová, I., Špánek, R., Ševců, A., & Dvořák, L. Aplikace molekulárně-genetických metod. pro studium procesů biodegradace chlorovaných uhlovodíků v podzemních vodách., *Vodní Hospodářství*, 2017
- Nechanická, M., Dolinová, I., Vlková, D., Dvořák, L., Využití nanovláknenných nosičů pro monitoring biomasy na kontaminované lokalitě, *Vodní hospodářství*, 2018
- Nechanická, M., Dolinová, I., Vlková, D., & Dvořák, L. (2017). Development of Nanofiber Carrier For Monitoring of Biomass At A Contaminated Site. In *Conference Proceeding*. Brno: Tanger Ltd.

Active participation in international conferences dealing with soil microbial diversity and bioremediation:

- Dolinová et al. Evaluation of enhanced reductive dehalogenation of chlorinated ethenes *in situ* using molecular and statistical methods. 8th International Conference on the Environmental Effects of Nanoparticles and Nanomaterials, 3. – 5. July 2013, Aix-en-Provence, France
- Dolinová et al., Metabolic pathways of *Pseudomonas fluorescens* ICT in the perspective of groundwater bioremediation. 5th Annual Argonne Soil Metagenomic Meeting, 2. – 4. October 2013, Chicago, USA
- Dolinová et al., Nanofibre biomass carriers as a valuable tool for analysis of microbial community at polluted locality. BioTech 2014 and 6th Czech-Swiss Symposium, 11. – 14. June, 2014, Prague, Czech Republic
- Dolinová et al., Nanofibre biomass carriers as a promising tool for genetic analysis of microbial community from highly polluted sites. First Global Soil Biodiversity Conference, 2. – 5. December 2014, Dijon, France
- Dolina et al., Development of nanofiber biomass carriers for effective sampling: differences in microbial community on carriers and groundwater. 3rd Thünen Symposium on Soil Metagenomics, 14. – 16. December 2016, Braunschweig, Germany
- Dolinová et al., NGS analysis of autochthonous microbial communities from groundwater contaminated with chlorinated ethenes. BAGECO 2017 (14th Symposium on Bacterial Genetics and Ecology), 04. – 08. June 2017, Aberdeen, United Kingdom

List of References

- APHA, AWWA, WEF, 2012. Standard Methods for the Examination of Water and Wastewater, 22 edition. ed. American Water Works Assn, Washington, DC.
- Arciero, D., Vannelli, T., Logan, M., Hopper, A.B., 1989. Degradation of trichloroethylene by the ammonia-oxidizing bacterium *Nitrosomonas europaea*. *Biochem Biophys Res Commun* 159, 640–643.
- Aulenta, F., Beccari, M., Majone, M., Papini, M.P., Tandoi, V., 2008. Competition for H₂ between sulfate reduction and dechlorination in butyrate-fed anaerobic cultures. *Process Biochem.* 43, 161–168. <https://doi.org/http://dx.doi.org/10.1016/j.procbio.2007.11.006>
- Azizian, M.F., Marshall, I.P., Behrens, S., Spormann, A.M., Semprini, L., 2010. Comparison of lactate, formate, and propionate as hydrogen donors for the reductive dehalogenation of trichloroethene in a continuous-flow column. *J. Contam. Hydrol.* 113, 77–92. <https://doi.org/10.1016/j.jconhyd.2010.02.004>
- Bælum, J., Chambon, J.C., Scheutz, C., Binning, P.J., Laier, T., Bjerg, P.L., Jacobsen, C.S., 2013. A conceptual model linking functional gene expression and reductive dechlorination rates of chlorinated ethenes in clay rich groundwater sediment. *Water Res* 47, 2467–2478.
- Baji, A., Mai, Y.-W., Wong, S.-C., Abtahi, M., Chen, P., 2010. Electrospinning of polymer nanofibers: Effects on oriented morphology, structures and tensile properties. *Compos. Sci. Technol.* 70, 703–718. <https://doi.org/10.1016/j.compscitech.2010.01.010>
- Behrens, S., Azizian, M.F., McMurdie, P.J., Sabalowsky, A., Dolan, M.E., Semprini, L., Spormann, A.M., 2008. Monitoring Abundance and Expression of “Dehalococoides” Species Chloroethene-Reductive Dehalogenases in a Tetrachloroethene-Dechlorinating Flow Column. *Appl. Environ. Microbiol.* 74, 5695–5703. <https://doi.org/10.1128/AEM.00926-08>
- Ben-Dov, E., Brenner, A., Kushmaro, A., 2007. Quantification of Sulfate-reducing Bacteria in Industrial Wastewater, by Real-time Polymerase Chain Reaction (PCR) Using *dsrA* and *apsA* Genes. *Microb. Ecol.* 54, 439–451. <https://doi.org/10.1007/s00248-007-9233-2>
- Bewley, R., Hick, P., Rawcliffe, A., 2015. Meeting the challenges for bioremediation of chlorinated solvents at operational sites: a comparison of case studie, in: *Proceeding of the 13th International UFZ-Deltarez Conference on Sustainable Use and Management of Soil, Sediment and Water Resources.* 9-12 June 2015. Copenhagen. Denmark.
- Bhardwaj, N., Kundu, S.C., 2010. Electrospinning: A fascinating fiber fabrication technique. *Biotechnol. Adv.* 28, 325–347. <https://doi.org/10.1016/j.biotechadv.2010.01.004>
- Bhowmik, A., Ishimura, K., Nakamura, K., Takamizawa, K., 2012. Degradation activity of *Clostridium* species DC-1 in the cis-1, 2-dichloroethylene contaminated site in the presence of indigenous microorganisms and *Escherichia coli*. *J. Mater. Cycles Waste Manag.* 14, 212–219.
- Bombach, P., Chatzinotas, A., Neu, T.R., Kästner, M., Lueders, T., Vogt, C., 2009. Enrichment and characterization of a sulfate-reducing toluene-degrading microbial consortium by combining in situ microcosms and stable isotope probing techniques. *FEMS Microbiol. Ecol.* 71, 237–246.
- Bourne, D.G., McDonald, I.R., Murrell, J.C., 2001. Comparison of *pmoA* PCR primer sets as tools for investigating methanotroph diversity in three Danish soils. *Appl. Environ. Microbiol.* 67, 3802–3809.
- Bouwer, E.J., Norris, R., Hincee, R., Brown, R., McCarty, P., Semprini, L., Wilson, J., Kampbell, D., Reinhard, M., Borden, R., 1994. Bioremediation of chlorinated solvents using alternate electron acceptors. *Handb. Bioremediation* 149–175.
- Bradley, P.M., 2003. History and Ecology of Chloroethene Biodegradation: A Review. *Bioremediation J.* 7, 81–109. <https://doi.org/10.1080/713607980>
- Bradley, P.M., Chapelle, F.H., 2010. Biodegradation of chlorinated ethenes, in: *In Situ Remediation of Chlorinated Solvent Plumes.* Springer, pp. 39–67.

- Bradley, P.M., Chapelle, F.H., 1998. Microbial mineralization of VC and DCE under different terminal electron accepting conditions. *Anaerobe* 4, 81–87.
- Chambon, J.C., Bjerg, P.L., Scheutz, C., Bælum, J., Jakobsen, R., Binning, P.J., 2013. Review of reactive kinetic models describing reductive dechlorination of chlorinated ethenes in soil and groundwater. *Biotechnol. Bioeng.* 110, 1–23.
- Chang, Y., Okeke, B., Hatsu, M., Takamizawa, K., 2001. In vitro dehalogenation of tetrachloroethylene (PCE) by cell-free extracts of *Clostridium bifermentans* DPH-1. *Bioresour. Technol.* 78, 141–147.
- Chang, Y.-C., Ikeutsu, K., Toyama, T., Choi, D., Kikuchi, S., 2011. Isolation and characterization of tetrachloroethylene- and cis-1, 2-dichloroethylene-dechlorinating propionibacteria. *J. Ind. Microbiol. Biotechnol.* 38, 1667–1677.
- Chao, A., 1984. Nonparametric estimation of the number of classes in a population. *Scand. J. Stat.* 265–270.
- Chapelle, F.H., Bradley, P.M., Casey, C.C., 2005. Behavior of a chlorinated ethene plume following source-area treatment with Fenton's reagent. *Groundw. Monit. Remediat.* 25, 131–141.
- Cheng, D., He, J., 2009. Isolation and characterization of “Dehalococcoides” sp. strain MB, which dechlorinates tetrachloroethene to trans-1, 2-dichloroethene. *Appl. Environ. Microbiol.* 75, 5910–5918.
- Chládek, L., Vojta, P., Nemeč, M., Horáková, D., Piller, B., Jelinek, J., Skopálek, B., Kosar, K., Sruma, T., 2000. Carrier of biomass, method of fermentation therewith and devices therefor. WO2000049140 A2.
- Claesson, M.J., Wang, Q., O'Sullivan, O., Greene-Diniz, R., Cole, J.R., Ross, R.P., O'Toole, P.W., 2010. Comparison of two next-generation sequencing technologies for resolving highly complex microbiota composition using tandem variable 16S rRNA gene regions. *Nucleic Acids Res.* gkq873.
- Clifford, R.J., Milillo, M., Prestwood, J., Quintero, R., Zurawski, D.V., Kwak, Y.I., Waterman, P.E., Lesho, E.P., Mc Gann, P., 2012. Detection of Bacterial 16S rRNA and Identification of Four Clinically Important Bacteria by Real-Time PCR. *PLoS ONE* 7. <https://doi.org/10.1371/journal.pone.0048558>
- Coleman, N.V., 2015. Primers: functional genes for aerobic chlorinated hydrocarbon-degrading microbes, in: *Hydrocarbon and Lipid Microbiology Protocols*. Springer, pp. 141–175.
- Coleman, N.V., Bui, N.B., Holmes, A.J., 2006. Soluble di-iron monooxygenase gene diversity in soils, sediments and ethene enrichments. *Environ. Microbiol.* 8, 1228–1239.
- Coleman, N.V., Mattes, T.E., Gossett, J.M., Spain, J.C., 2002a. Phylogenetic and kinetic diversity of aerobic vinyl chloride-assimilating bacteria from contaminated sites. *Appl. Environ. Microbiol.* 68, 6162–6171.
- Coleman, N.V., Mattes, T.E., Gossett, J.M., Spain, J.C., 2002b. Biodegradation of cis-dichloroethene as the sole carbon source by a β -proteobacterium. *Appl. Environ. Microbiol.* 68, 2726–2730.
- Coleman, N.V., Spain, J.C., 2003. Epoxyalkane: coenzyme M transferase in the ethene and vinyl chloride biodegradation pathways of mycobacterium strain JS60. *J. Bacteriol.* 185, 5536–45.
- Costello, A.M., Lidstrom, M.E., 1999. Molecular characterization of functional and phylogenetic genes from natural populations of methanotrophs in lake sediments. *Appl. Environ. Microbiol.* 65, 5066–5074.
- Cupples, A.M., Spormann, A.M., McCarty, P.L., 2003. Growth of a Dehalococcoides-like microorganism on vinyl chloride and cis-dichloroethene as electron acceptors as determined by competitive PCR. *Appl. Environ. Microbiol.* 69, 953–959.
- CZ patent No. 305698 B6; <http://isdv.upv.cz/doc/FullFiles/Patents/FullDocuments/305/305698.pdf>
- ČSN EN 1484. 1998. Water analysis - Guidelines for the determination of total organic carbon (TOC) and dissolved organic carbon (DOC).
- ČSN EN ISO 7150-1. 1994. Water quality. Determination of ammonium. Part 1: Manual spectrometric method.

- ČSN EN ISO 10304–1. 2007. Water quality – determination of dissolved anions by liquid chromatography of ions – part 1: determination of bromide, chloride, fluoride, nitrate, nitrite, phosphate and sulfate.
- ČSN EN ISO 11885. 2007. Water quality — determination of selected elements by inductively coupled plasma optical emission spectrometry (ICP-OES).
- ČSN EN ISO 9963-1. 1994. Water quality -- Determination of alkalinity - part 1: Determination of total and composite alkalinity.
- Dabrock, B., Riedel, J., Bertram, J., Gottschalk, G., 1992. Isopropylbenzene (cumene)—a new substrate for the isolation of trichloroethene-degrading bacteria. *Arch Microbiol* 158, 9–13.
- Damgaard, I., Bjerg, P.L., Bælum, J., Scheutz, C., Hunkeler, D., Jacobsen, C.S., Tuxen, N., Broholm, M.M., 2013a. Identification of chlorinated solvents degradation zones in clay till by high resolution chemical, microbial and compound specific isotope analysis. *J. Contam. Hydrol.* 146, 37–50.
- Damgaard, I., Bjerg, P.L., Jacobsen, C.S., Tsitonaki, A., Kern-Jespersen, H., Broholm, M.M., 2013b. Performance of Full-Scale Enhanced Reductive Dechlorination in Clay Till. *Groundw. Monit. Remediat.* 33, 48–61.
- Danko, A.S., Luo, M., Bagwell, C.E., Brigmon, R.L., Freedman, D.L., 2004. Involvement of linear plasmids in aerobic biodegradation of vinyl chloride. *Appl. Environ. Microbiol.* 70, 6092–6097.
- Das, R., Kazy, S.K., 2014. Microbial diversity, community composition and metabolic potential in hydrocarbon contaminated oily sludge: prospects for in situ bioremediation. *Environ. Sci. Pollut. Res.* 21, 7369–7389.
- DeWeerd, K.A., Mandelco, L., Tanner, R.S., Woese, C.R., Suflita, J.M., 1990. *Desulfomonile tiedjei* gen. nov. and sp. nov., a novel anaerobic, dehalogenating, sulfate-reducing bacterium. *Arch. Microbiol.* 154, 23–30.
- Dey, K., Roy, P., 2009. Degradation of trichloroethylene by *Bacillus* sp.: isolation strategy, strain characteristics, and cell immobilization. *Curr. Microbiol.* 59, 256–260.
- Dolinová, I., Czinnerová, M., Dvořák, L., Stejskal, V., Ševců, A., Černík, M., 2016a. Dynamics of organohalide-respiring bacteria and their genes following in-situ chemical oxidation of chlorinated ethenes and biostimulation. *Chemosphere* 157, 276–285.
- Dolinová, I., Špánek, R., Ševců, A., Dvořák, L., 2016b. Aplikace molekulárně-genetických metod. pro studium procesů biodegradace chlorovaných uhlovodíků v podzemních vodách. *Vodní hospodářství*, 1. vyd. 5–10.
- Dolinová, I., Štrojsová, M., Černík, M., Němeček, J., Macháčková, J., Ševců, A., 2017. Microbial degradation of chloroethenes: a review. *Environ. Sci. Pollut. Res.* 24, 13262–13283.
- Doughty, D.M., Sayavedra-Soto, L.A., Arp, D.J., Bottomley, P.J., 2005. Effects of Dichloroethene Isomers on the Induction and Activity of Butane Monooxygenase in the Alkane-Oxidizing Bacterium “*Pseudomonas butanovora*.” *Appl. Environ. Microbiol.* 71, 6054–6059. <https://doi.org/10.1128/aem.71.10.6054-6059.2005>
- Dowd, S.E., Callaway, T.R., Wolcott, R.D., Sun, Y., McKeenan, T., Hagevoort, R.G., Edrington, T.S., 2008. Evaluation of the bacterial diversity in the feces of cattle using 16S rDNA bacterial tag-encoded FLX amplicon pyrosequencing (bTEFAP). *BMC Microbiol.* 8, 1.
- Duhamel, M., Mo, K., Edwards, E.A., 2004. Characterization of a highly enriched Dehalococcoides-containing culture that grows on vinyl chloride and trichloroethene. *Appl. Environ. Microbiol.* 70, 5538–5545.
- Dzionek, A., Wojcieszynska, D., Guzik, U., 2016. Natural carriers in bioremediation: A review. *Electron. J. Biotechnol.* 23, 28–36. <https://doi.org/10.1016/j.ejbt.2016.07.003>
- Edgar, R.C., Haas, B.J., Clemente, J.C., Quince, C., Knight, R., 2011. UCHIME improves sensitivity and speed of chimera detection. *Bioinformatics* 27, 2194–2200.
- Egli, C., Scholtz, R., Cook, A.M., Leisinger, T., 1987. Anaerobic dechlorination of tetrachloromethane and 1,2-dichloroethane to degradable products by pure cultures of *Desulfobacterium* sp. and *Methanobacterium* sp. *FEMS Microbiol Lett* 43, 257–261. <https://doi.org/10.1111/j.1574-6968.1987.tb02154.x>

- Egli, C., Tschan, T., Scholtz, R., Cook, A.M., Leisinger, T., 1988. Transformation of tetrachloromethane to dichloromethane and carbon dioxide by *Acetobacterium woodii*. *Appl. Environ. Microbiol.* 54, 2819–2824.
- Elango, V.K., Ligginstoffer, A.S., Fathepure, B.Z., 2006. Biodegradation of vinyl chloride and cis-dichloroethene by a *Ralstonia* sp. strain TRW-1. *Appl. Microbiol. Biotechnol.* 72, 1270–1275.
- Ellis, D.E., Lutz, E.J., Odom, J.M., Buchanan, R.J., Bartlett, C.L., Lee, M.D., Harkness, M.R., DeWeerd, K.A., 2000. Bioaugmentation for accelerated in situ anaerobic bioremediation. *Environ. Sci. Technol.* 34, 2254–2260.
- Ensign, S.A., Hyman, M.R., Arp, D.J., 1992. Cometabolic degradation of chlorinated alkenes by alkene monooxygenase in a propylene-grown *Xanthobacter* strain. *Appl. Environ. Microbiol.* 58, 3038–3046.
- Envirogen Technologies; <http://www.envirogen.com/welcome/home/>
- Fathepure, B.Z., Boyd, S.A., 1988. Reductive dechlorination of perchloroethylene and the role of methanogens. *FEMS Microbiol. Lett.* 49, 149–156.
- Fathepure, B.Z., Elango, V.K., Singh, H., Bruner, M.A., 2005. Bioaugmentation potential of a vinyl chloride-assimilating *Mycobacterium* sp., isolated from a chloroethene-contaminated aquifer. *FEMS Microbiol. Lett.* 248, 227–234.
- Finneran, K.T., Forbush, H.M., VanPraagh, C.V.G., Lovley, D.R., 2002. *Desulfitobacterium metallireducens* sp. nov., an anaerobic bacterium that couples growth to the reduction of metals and humic acids as well as chlorinated compounds. *Int. J. Syst. Evol. Microbiol.* 52, 1929–1935.
- Fletcher, K.E., Ritalahti, K.M., Pennell, K.D., Takamizawa, K., Löffler, F.E., 2008. Resolution of culture *Clostridium bifermentans* DPH-1 into two populations, a *Clostridium* sp. and tetrachloroethene-dechlorinating *Desulfitobacterium hafniense* strain JH1. *Appl. Environ. Microbiol.* 74, 6141–6143.
- Fraga, D., Meulia, T., Fenster, S., 2014. Real-time PCR. *Curr. Protoc. Essent. Lab. Tech.* 8, 10–3.
- Frasconi, D., Frascario, S., Nocentini, M., Pinelli, D., 2013. Aerobic/anaerobic/aerobic sequenced biodegradation of a mixture of chlorinated ethenes, ethanes and methanes in batch bioreactors. *Bioresour Technol* 128, 479–86. <https://doi.org/10.1016/j.biortech.2012.10.026>
- Frasconi, D., Pinelli, D., Nocentini, M., Baleani, E., Cappelletti, M., Fedi, S., 2008. A kinetic study of chlorinated solvent cometabolic biodegradation by propane-grown *Rhodococcus* sp. PB1. *Biochem. Eng. J.* 42, 139–147. <https://doi.org/http://dx.doi.org/10.1016/j.bej.2008.06.011>
- Frasconi, D., Zanolli, G., Danko, A.S., 2015. In situ aerobic cometabolism of chlorinated solvents: A review. *J. Hazard. Mater.* 283, 382–399. <https://doi.org/http://dx.doi.org/10.1016/j.jhazmat.2014.09.041>
- Fung, J.M., Morris, R.M., Adrian, L., Zinder, S.H., 2007. Expression of reductive dehalogenase genes in *Dehalococcoides ethenogenes* strain 195 growing on tetrachloroethene, trichloroethene, or 2,3-dichlorophenol. *Appl. Environ. Microbiol.* 73, 4439–45. <https://doi.org/10.1128/aem.00215-07>
- Furukawa, K., 2006. Oxygenases and dehalogenases: molecular approaches to efficient degradation of chlorinated environmental pollutants. *Biosci. Biotechnol. Biochem.* 70, 2335–2348.
- Futagami, T., Goto, M., Furukawa, K., 2008. Biochemical and genetic bases of dehalorespiration. *Chem. Rec.* 8, 1–12.
- Futamata, H., Harayama, S., Watanabe, K., 2001a. Group-specific monitoring of phenol hydroxylase genes for a functional assessment of phenol-stimulated trichloroethylene bioremediation. *Appl. Environ. Microbiol.* 67, 4671–4677.
- Futamata, H., Harayama, S., Watanabe, K., 2001b. Diversity in kinetics of trichloroethylene-degrading activities exhibited by phenol-degrading bacteria. *Appl. Microbiol. Biotechnol.* 55, 248–253.
- Futamata, H., Nagano, Y., Watanabe, K., Hiraishi, A., 2005. Unique kinetic properties of phenol-degrading *Variovorax* strains responsible for efficient trichloroethylene degradation in a chemostat enrichment culture. *Appl. Environ. Microbiol.* 71, 904–911.
- Genomics, 2018; http://www.genomics.cn/en/navigation/show_navigation?nid=2640, verified 2.6. 2018

- Gerritse, J., Drzyzga, O., Kloetstra, G., Keijmel, M., Wiersum, L.P., Hutson, R., Collins, M.D., Gottschal, J.C., 1999. Influence of different electron donors and acceptors on dehalorespiration of tetrachloroethene by *Desulfitobacterium frappieri* TCE1. *Appl. Environ. Microbiol.* 65, 5212–5221.
- Gerritse, J., Renard, V., Gomes, T.P., Lawson, P.A., Collins, M.D., Gottschal, J.C., 1996. *Desulfitobacterium* sp. strain PCE1, an anaerobic bacterium that can grow by reductive dechlorination of tetrachloroethene or ortho-chlorinated phenols. *Arch. Microbiol.* 165, 132–140.
- Gibson, S.A., Sewell, G.W., 1992. Stimulation of reductive dechlorination of tetrachloroethene in anaerobic aquifer microcosms by addition of short-chain organic acids or alcohols. *Appl. Environ. Microbiol.* 58, 1392–1393.
- Grosterm, A., Edwards, E.A., 2006. Growth of *Dehalobacter* and *Dehalococcoides* spp. during degradation of chlorinated ethanes. *Appl. Environ. Microbiol.* 72, 428–436.
- Guan, X., Liu, F., Xie, Y., Zhu, L., Han, B., 2013. Microbiota associated with the migration and transformation of chlorinated aliphatic hydrocarbons in groundwater. *Environ. Geochem. Health* 35, 535–549.
- Hägglom, M.M., Fennell, D.E., Ahn, Y.-B., Ravit, B., Kerkhof, L.J., 2006. ANAEROBIC DEHALOGENATION OF HALOGENATED ORGANIC COMPOUNDS: NOVEL STRATEGIES FOR BIOREMEDIATION OF CONTAMINATED SEDIMENTS OF CONTAMINATED SEDIMENTS OF CONTAMINATED SEDIMENTS, in: *Soil and Water Pollution Monitoring, Protection and Remediation*. Springer, pp. 505–521.
- Halsey, K.H., Doughty, D.M., Sayavedra-Soto, L.A., Bottomley, P.J., Arp, D.J., 2007. Evidence for Modified Mechanisms of Chloroethene Oxidation in *Pseudomonas butanovora* Mutants Containing Single Amino Acid Substitutions in the Hydroxylase α -Subunit of Butane Monooxygenase. *J. Bacteriol.* 189, 5068–5074. <https://doi.org/10.1128/jb.00189-07>
- Hamamura, N., Page, C., Long, T., Semprini, L., Arp, D.J., 1997. Chloroform cometabolism by butane-grown CF8, *Pseudomonas butanovora*, and *Mycobacterium vaccae* JOB5 and methane-grown *Methylosinus trichosporium* OB3b. *Appl. Environ. Microbiol.* 63, 3607–3613.
- Hanada, S., Shigematsu, T., Shibuya, K., Eguchi, M., Hasegawa, T., Suda, F., Kamagata, Y., Kanagawa, T., Kurane, R., 1998. Phylogenetic analysis of trichloroethylene-degrading bacteria newly isolated from soil polluted with this contaminant. *J. Ferment. Bioeng.* 86, 539–544.
- Hanert, H.H., 1981. The genus *Gallionella*, in: *The Prokaryotes*. Springer, pp. 509–515.
- Harker, A.R., Kim, Y., 1990. Trichloroethylene degradation by two independent aromatic-degrading pathways in *Alcaligenes eutrophus* JMP134. *Appl. Environ. Microbiol.* 56, 1179–1181.
- Harkness, M., Fisher, A., Lee, M.D., Mack, E.E., Payne, J.A., Dworatzek, S., Roberts, J., Acheson, C., Herrmann, R., Possolo, A., 2012. Use of statistical tools to evaluate the reductive dechlorination of high levels of TCE in microcosm studies. *J. Contam. Hydrol.* 131, 100–18. <https://doi.org/10.1016/j.jconhyd.2012.01.011>
- Hartmans, S., De Bont, J., 1992. Aerobic vinyl chloride metabolism in *Mycobacterium aurum* L1. *Appl. Environ. Microbiol.* 58, 1220–1226.
- Hartmans, S., De Bont, J.A.M., Tramper, J., Luyben, K.C.A., 1985. Bacterial degradation of vinyl chloride. *Biotechnol Lett* 7, 383–388.
- Hata, J., Miyata, N., Kim, E.-S., Takamizawa, K., Iwahori, K., 2004. Anaerobic degradation of cis-1, 2-dichloroethylene and vinyl chloride by *Clostridium* sp. strain DC1 isolated from landfill leachate sediment. *J. Biosci. Bioeng.* 97, 196–201.
- He, J., Ritalahti, K.M., Yang, K.-L., Koenigsberg, S.S., Löffler, F.E., 2003. Detoxification of vinyl chloride to ethene coupled to growth of an anaerobic bacterium. *Nature* 424, 62.
- He, J., Sung, Y., Krajmalnik-Brown, R., Ritalahti, K.M., Löffler, F.E., 2005. Isolation and characterization of *Dehalococcoides* sp. strain FL2, a trichloroethene (TCE)- and 1,2-dichloroethene-respiring anaerobe. *Env. Microbiol* 7, 1442–50. <https://doi.org/10.1111/j.1462-2920.2005.00830.x>

- Heald, S., Jenkins, R.O., 1994. Trichloroethylene removal and oxidation toxicity mediated by toluene dioxygenase of *Pseudomonas putida*. *Appl. Environ. Microbiol.* 60, 4634–4637.
- Henry, S., Baudoin, E., López-Gutiérrez, J.C., Martin-Laurent, F., Brauman, A., Philippot, L., 2004. Quantification of denitrifying bacteria in soils by nirK gene targeted real-time PCR. *J. Microbiol. Methods* 59, 327–335. <https://doi.org/10.1016/j.mimet.2004.07.002>
- Holliger, C., Hahn, D., Harmsen, H., Ludwig, W., Schumacher, W., Tindall, B., Vazquez, F., Weiss, N., Zehnder, A.J., 1998. *Dehalobacter restrictus* gen. nov. and sp. nov., a strictly anaerobic bacterium that reductively dechlorinates tetra- and trichloroethene in an anaerobic respiration. *Arch. Microbiol.* 169, 313–321.
- Holmes, A.J., Costello, A., Lidstrom, M.E., Murrell, J.C., 1995. Evidence that participate methane monooxygenase and ammonia monooxygenase may be evolutionarily related. *FEMS Microbiol. Lett.* 132, 203–208.
- Holmes, V.F., He, J., Lee, P.K., Alvarez-Cohen, L., 2006. Discrimination of multiple *Dehalococcoides* strains in a trichloroethene enrichment by quantification of their reductive dehalogenase genes. *Appl. Environ. Microbiol.* 72, 5877–5883.
- Hug, L.A., Maphosa, F., Leys, D., Löffler, F.E., Smidt, H., Edwards, E.A., Adrian, L., 2013. Overview of organohalide-respiring bacteria and a proposal for a classification system for reductive dehalogenases. *Phil Trans R Soc B* 368, 20120322.
- Hutchens, E., Radajewski, S., Dumont, M.G., McDonald, I.R., Murrell, J.C., 2004. Analysis of methanotrophic bacteria in Movile Cave by stable isotope probing. *Environ. Microbiol.* 6, 111–120.
- Islam, M.A., Waller, A.S., Hug, L.A., Provart, N.J., Edwards, E.A., Mahadevan, R., 2014. New insights into *Dehalococcoides mccartyi* metabolism from a reconstructed metabolic network-based systems-level analysis of *D. mccartyi* transcriptomes. *PLoS One* 9, e94808. <https://doi.org/10.1371/journal.pone.0094808>
- Jablonski, P.E., Ferry, J.G., 1992. Reductive dechlorination of trichloroethylene by the CO-reduced CO dehydrogenase enzyme complex from *Methanosarcina thermophila*. *FEMS Microbiol Lett* 96, 55–59.
- Jin, Y.O., Mattes, T.E., 2011. Assessment and modification of degenerate qPCR primers that amplify functional genes from etheneotrophs and vinyl chloride-assimilators. *Lett. Appl. Microbiol.* 53, 576–580. <https://doi.org/10.1111/j.1472-765X.2011.03144.x>
- Jin, Y.O., Mattes, T.E., 2010. A quantitative PCR assay for aerobic, vinyl chloride- and ethene-assimilating microorganisms in groundwater. *Environ. Sci. Technol.* 44, 9036–41. <https://doi.org/10.1021/es102232m>
- Jirsák, O., Sanetrník, F., Lukáš, D., Kotek, V., Maritnová, Chaloupek, Ji., 2009. Method of nanofibres production from a polymer solution using electrostatic spinning and a device for carrying out the method. WO2005024101 A1.
- Johnson, D.R., Lee, P.K.H., Holmes, V.F., Fortin, A.C., Alvarez-Cohen, L., 2005. Transcriptional Expression of the *tceA* Gene in a *Dehalococcoides*-Containing Microbial Enrichment. *Appl. Environ. Microbiol.* 71, 7145–7151. <https://doi.org/10.1128/AEM.71.11.7145-7151.2005>
- Jugder, B.-E., Ertan, H., Lee, M., Manefield, M., Marquis, C.P., 2015. Reductive dehalogenases come of age in biological destruction of organohalides. *Trends Biotechnol.* 33, 595–610.
- Kang, J.W., 2014. Removing environmental organic pollutants with bioremediation and phytoremediation. *Biotechnol Lett* 36, 1129–39. <https://doi.org/10.1007/s10529-014-1466-9>
- Kim, E.-S., Nomura, I., Hasegawa, Y., Takamizawa, K., 2006. Characterization of a newly isolated *cis*-1, 2-dichloroethylene and aliphatic compound-degrading bacterium, *Clostridium* sp. strain KYT-1. *Biotechnol. Bioprocess Eng.* 11, 553–556.
- Kim, S., Bae, W., Hwang, J., Park, J., 2010. Aerobic TCE degradation by encapsulated toluene-oxidizing bacteria, *Pseudomonas putida* and *Bacillus* spp. *Water Sci Technol* 62, 1991–7. <https://doi.org/10.2166/wst.2010.471>

- Kim, S.-H., Harzman, C., Davis, J., Hutcheson, R., Broderick, J., Marsh, T., Tiedje, J., 2012. Genome sequence of *Desulfitobacterium hafniense* DCB-2, a Gram-positive anaerobe capable of dehalogenation and metal reduction. *BMC Microbiol.* 12, 21.
- Koh, S.-C., Bowman, J.P., Saylor, G.S., 1993. Soluble methane monooxygenase production and trichloroethylene degradation by a type I methanotroph, *Methylomonas methanica* 68-1. *Appl. Environ. Microbiol.* 59, 960–967.
- Kotik, M., Davidová, A., Voříšková, J., Baldrian, P., 2013. Bacterial communities in tetrachloroethene-polluted groundwaters: A case study. *Sci. Total Environ.* 454, 517–527.
- Krajmalnik-Brown, R., Hölscher, T., Thomson, I.N., Saunders, F.M., Ritalahti, K.M., Löffler, F.E., 2004. Genetic identification of a putative vinyl chloride reductase in *Dehalococcoides* sp. strain BAV1. *Appl. Environ. Microbiol.* 70, 6347–6351.
- Kranzioch, I., Ganz, S., Tiehm, A., 2015. Chloroethene degradation and expression of *Dehalococcoides* dehalogenase genes in cultures originating from Yangtze sediments. *Environ. Sci. Pollut. Res.* 22, 3138–3148.
- Kranzioch, I., Stoll, C., Holbach, A., Chen, H., Wang, L., Zheng, B., Norra, S., Bi, Y., Schramm, K.W., Tiehm, A., 2013. Dechlorination and organohalide-respiring bacteria dynamics in sediment samples of the Yangtze Three Gorges Reservoir. *Env. Sci Pollut Res Int* 20, 7046–56. <https://doi.org/10.1007/s11356-013-1545-9>
- Kriklavova, L., Lederer, T., 2010. The use of nanofiber carriers in biofilm reactor for the treatment of industrial wastewaters. *Nanocon Olomouc Ceska Repub.* 1–6.
- Krumholz, L.R., 1997. *Desulfuromonas chloroethenica* sp. nov. uses tetrachloroethylene and trichloroethylene as electron acceptors. *Int. J. Syst. Evol. Microbiol.* 47, 1262–1263.
- Kucera, S., Wolfe, R., 1957. A selective enrichment method for *Gallionella ferruginea*. *J. Bacteriol.* 74, 344.
- Lacinová, L., 2013. In-situ combination of bio and abio remediation of chlorinated ethenes. *Ecol. Chem. Eng. S* 20, 463–473.
- Leahy, J.G., Batchelor, P.J., Morcomb, S.M., 2003. Evolution of the soluble diiron monooxygenases. *FEMS Microbiol. Rev.* 27, 449–479.
- Lederer, T., Křiklavová, L., 2014. Operational experiences with a nanofibre biomass carrier used for the treatment of toxic industrial wastewater. *Nanocon Brno Ceska Repub.* 1–6.
- Lee, P.K., Cheng, D., Hu, P., West, K.A., Dick, G.J., Brodie, E.L., Andersen, G.L., Zinder, S.H., He, J., Alvarez-Cohen, L., 2011. Comparative genomics of two newly isolated *Dehalococcoides* strains and an enrichment using a genus microarray. *ISME J.* 5, 1014.
- Lee, P.K., Cheng, D., West, K.A., Alvarez-Cohen, L., He, J., 2013. Isolation of two new *Dehalococcoides* mccartyi strains with dissimilar dechlorination functions and their characterization by comparative genomics via microarray analysis. *Env. Microbiol* 15, 2293–305. <https://doi.org/10.1111/1462-2920.12099>
- Lee, P.K., Johnson, D.R., Holmes, V.F., He, J., Alvarez-Cohen, L., 2006. Reductive dehalogenase gene expression as a biomarker for physiological activity of *Dehalococcoides* spp. *Appl. Environ. Microbiol.* 72, 6161–6168.
- Lee, P.K., Macbeth, T.W., Sorenson, K.S., Deeb, R.A., Alvarez-Cohen, L., 2008. Quantifying genes and transcripts to assess the in situ physiology of “*Dehalococcoides*” spp. in a trichloroethene-contaminated groundwater site. *Appl. Environ. Microbiol.* 74, 2728–39. <https://doi.org/10.1128/aem.02199-07>
- Lee, T., Tokunaga, T., Suyama, A., Furukawa, K., 2001. Efficient dechlorination of tetrachloroethylene in soil slurry by combined use of an anaerobic *Desulfitobacterium* sp. strain Y-51 and zero-valent iron. *J. Biosci. Bioeng.* 92, 453–458.
- Leeson, A., Beevar, E., Henry, B., Fortenberry, J., Coyle, C., 2004. Principles and practices of enhanced anaerobic bioremediation of chlorinated solvents. Naval Facilities Engineering Service Center Port Hueneme CA.

- Lefterova, M.I., Suarez, C.J., Banaei, N., Pinsky, B.A., 2015. Next-generation sequencing for infectious disease diagnosis and management: a report of the Association for Molecular Pathology. *J. Mol. Diagn.* 17, 623–634.
- Lewin, K., Blakey, N., Cooke, D., Health and Safety Executive, L. (United K., 1993. The Validation of Methodology in the Determination of Methane in Water-Final Report. HSE CONTRACT Res. Rep.
- Li, J., de Toledo, R.A., Chung, J., Shim, H., 2014. Removal of mixture of cis-1, 2-dichloroethylene/trichloroethylene/benzene, toluene, ethylbenzene, and xylenes from contaminated soil by *Pseudomonas plecoglossicida*. *J. Chem. Technol. Biotechnol.* 89, 1934–1940.
- Li, Y., Li, B., Wang, C.-P., Fan, J.-Z., Sun, H.-W., 2014. Aerobic degradation of trichloroethylene by co-metabolism using phenol and gasoline as growth substrates. *Int. J. Mol. Sci.* 15, 9134–9148.
- Liang, B., Jiang, J., Zhang, J., Zhao, Y., Li, S., 2012. Horizontal transfer of dehalogenase genes involved in the catalysis of chlorinated compounds: evidence and ecological role. *Crit Rev Microbiol* 38, 95–110. <https://doi.org/10.3109/1040841x.2011.618114>
- Löffler, F.E., Sun, Q., Li, J., Tiedje, J.M., 2000. 16S rRNA Gene-Based Detection of Tetrachloroethene-Dechlorinating *Desulfuromonas* and *Dehalococcoides* Species. *Appl. Environ. Microbiol.* 66, 1369–1374.
- Lohner, S.T., Spormann, A.M., 2013. Identification of a reductive tetrachloroethene dehalogenase in *Shewanella sediminis*. *Philos. Trans. R. Soc. B Biol. Sci.* 368, 20120326.
- Luijten, M.L., de Weert, J., Smidt, H., Boschker, H.T., de Vos, W.M., Schraa, G., Stams, A.J., 2003. Description of *Sulfurospirillum halorespirans* sp. nov., an anaerobic, tetrachloroethene-respiring bacterium, and transfer of *Dehalospirillum multivorans* to the genus *Sulfurospirillum* as *Sulfurospirillum multivorans* comb. nov. *Int. J. Syst. Evol. Microbiol.* 53, 787–793.
- Lupa, B., Wiegel, J., 2015. *Desulfitobacterium*. *Bergeys Man. Syst. Archaea Bact.* 1–13.
- Mac Nelly, A., Kai, M., Svatoš, A., Diekert, G., Schubert, T., 2014. Functional heterologous production of reductive dehalogenases from *Desulfitobacterium hafniense* strains. *Appl. Environ. Microbiol.* 80, 4313–4322.
- Magnuson, J.K., Romine, M.F., Burris, D.R., Kingsley, M.T., 2000. Trichloroethene reductive dehalogenase from *Dehalococcoides ethenogenes*: sequence of *tceA* and substrate range characterization. *Appl. Environ. Microbiol.* 66, 5141–5147.
- Maillard, J., Charnay, M.P., Regard, C., Rohrbach-Brandt, E., Rouzeau-Szynalski, K., Rossi, P., Holliger, C., 2011. Reductive dechlorination of tetrachloroethene by a stepwise catalysis of different organohalide respiring bacteria and reductive dehalogenases. *Biodegradation* 22, 949–60. <https://doi.org/10.1007/s10532-011-9454-4>
- Maillard, J., Schumacher, W., Vazquez, F., Regard, C., Hagen, W.R., Holliger, C., 2003. Characterization of the corrinoid iron-sulfur protein tetrachloroethene reductive dehalogenase of *Dehalobacter restrictus*. *Appl. Environ. Microbiol.* 69, 4628–4638.
- Majone, M., Verdini, R., Aulenta, F., Rossetti, S., Tandoi, V., Kalogerakis, N., Agathos, S., Puig, S., Zanolli, G., Fava, F., 2015. In situ groundwater and sediment bioremediation: barriers and perspectives at European contaminated sites. *N Biotechnol* 32, 133–46. <https://doi.org/10.1016/j.nbt.2014.02.011>
- Maphosa, F., de Vos, W.M., Smidt, H., 2010. Exploiting the ecogenomics toolbox for environmental diagnostics of organohalide-respiring bacteria. *Trends Biotechnol.* 28, 308–316.
- Maphosa, F., de Vos, W.M., Smidt, H., 2010. Exploiting the ecogenomics toolbox for environmental diagnostics of organohalide-respiring bacteria. *Trends Biotechnol* 28, 308–16. <https://doi.org/10.1016/j.tibtech.2010.03.005>
- Maphosa, F., van Passel, M.W., de Vos, W.M., Smidt, H., 2012. Metagenome analysis reveals yet unexplored reductive dechlorinating potential of *Dehalobacter* sp. E1 growing in co-culture with *Sedimentibacter* sp. *Env. Microbiol Rep* 4, 604–16. <https://doi.org/10.1111/j.1758-2229.2012.00376.x>

- Marco-Urrea, E., Nijenhuis, I., Adrian, L., 2011. Transformation and carbon isotope fractionation of tetra- and trichloroethene to trans-dichloroethene by *Dehalococcoides* sp. strain CBDB1. *Environ. Sci. Technol.* 45, 1555–1562.
- Mattes, T.E., Alexander, A.K., Coleman, N.V., 2010. Aerobic biodegradation of the chloroethenes: pathways, enzymes, ecology, and evolution. *FEMS Microbiol. Rev.* 34, 445–475.
- Mattes, T.E., Coleman, N.V., Spain, J.C., Gossett, J.M., 2005. Physiological and molecular genetic analyses of vinyl chloride and ethene biodegradation in *Nocardioides* sp. strain JS614. *Arch Microbiol* 183, 95–106. <https://doi.org/10.1007/s00203-004-0749-2>
- Maymó-Gatell, X., Anguish, T., Zinder, S.H., 1999. Reductive dechlorination of chlorinated ethenes and 1, 2-dichloroethane by “*Dehalococcoides ethenogenes*” 195. *Appl. Environ. Microbiol.* 65, 3108–3113.
- McCarty, P.L., 1996. Biotic and abiotic transformations of chlorinated solvents in ground water. Presented at the Symposium on Natural Attenuation of Chlorinated Organics in Ground Water, Dallas/TX, pp. 5–9.
- McClay, K., Streger, S.H., Steffan, R.J., 1995. Induction of toluene oxidation activity in *Pseudomonas mendocina* KR1 and *Pseudomonas* sp. strain ENVPC5 by chlorinated solvents and alkanes. *Appl. Environ. Microbiol.* 61, 3479–81.
- McMurdie, P.J., Behrens, S.F., Müller, J.A., Göke, J., Ritalahti, K.M., Wagner, R., Goltsman, E., Lapidus, A., Holmes, S., Löffler, F.E., 2009. Localized plasticity in the streamlined genomes of vinyl chloride respiring *Dehalococcoides*. *PLoS Genet* 5, e1000714.
- Michotey, V., Méjean, V., Bonin, P., 2000. Comparison of Methods for Quantification of Cytochrome cd1-Denitrifying Bacteria in Environmental Marine Samples. *Appl. Environ. Microbiol.* 66, 1564–1571.
- Militon, C., Boucher, D., Vachelard, C., Perchet, G., Barra, V., Troquet, J., Peyretailade, E., Peyret, P., 2010. Bacterial community changes during bioremediation of aliphatic hydrocarbon-contaminated soil. *FEMS Microbiol. Ecol.* 74, 669–681.
- Miller, E., Wohlfarth, G., Diekert, G., 1997. Comparative studies on tetrachloroethene reductive dechlorination mediated by *Desulfitobacterium* sp. strain PCE-S. *Arch. Microbiol.* 168, 513–519.
- Miura, T., Yamazoe, A., Ito, M., Ohji, S., Hosoyama, A., Takahata, Y., Fujita, N., 2015. The Impact of Injections of Different Nutrients on the Bacterial Community and Its Dechlorination Activity in Chloroethene-Contaminated Groundwater. *Microbes Env.* 30, 164–71. <https://doi.org/10.1264/jsme2.ME14127>
- Moran, M.J., Zogorski, J.S., Squillace, P.J., 2007. Chlorinated solvents in groundwater of the United States. *Environ. Sci. Technol.* 41, 74–81.
- Mukherjee, P., Roy, P., 2012. Identification and characterisation of a bacterial isolate capable of growth on trichloroethylene as the sole carbon source. *Adv. Microbiol.* 2, 284.
- Müller, J.A., Rosner, B.M., Von Abendroth, G., Meshulam-Simon, G., McCarty, P.L., Spormann, A.M., 2004. Molecular identification of the catabolic vinyl chloride reductase from *Dehalococcoides* sp. strain VS and its environmental distribution. *Appl. Environ. Microbiol.* 70, 4880–4888.
- Nechanická, M., Dolinová, I., Vlková, D., Dvořák, L., 2017. Development of Nanofiber Carrier For Monitoring of Biomass At A Contaminated Site, in: Conference Proceeding. Tanger Ltd., Brno.
- Nelson, M.J., Montgomery, S., O’neill, E., Pritchard, P., 1986. Aerobic metabolism of trichloroethylene by a bacterial isolate. *Appl. Environ. Microbiol.* 52, 383–384.
- Nelson, M.J., Montgomery, S.O., Mahaffey, W., Pritchard, P., 1987. Biodegradation of trichloroethylene and involvement of an aromatic biodegradative pathway. *Appl. Environ. Microbiol.* 53, 949–954.
- Nelson, M.J., Montgomery, S.O., Pritchard, P.H., 1988. Trichloroethylene metabolism by microorganisms that degrade aromatic compounds. *Appl. Environ. Microbiol.* 54, 604–606.
- Nelson, W.C., Stegen, J.C., 2015. The reduced genomes of *Parcubacteria* (OD1) contain signatures of a symbiotic lifestyle. *Front. Microbiol.* 6.

- Němeček, J., Dolinová, I., Macháčková, J., Špánek, R., Ševců, A., Lederer, T., Černík, M., 2017. Stratification of chlorinated ethenes natural attenuation in an alluvial aquifer assessed by hydrochemical and biomolecular tools. *Chemosphere* 184, 1157–1167.
- Neumann, A., Wohlfarth, G., Diekert, G., 1998. Tetrachloroethene dehalogenase from *Dehalospiroillum multivorans*: cloning, sequencing of the encoding genes, and expression of the *pceA* gene in *Escherichia coli*. *J Bacteriol* 180, 4140–4145.
- Nijenhuis, I., Kuntze, K., 2016. Anaerobic microbial dehalogenation of organohalides—state of the art and remediation strategies. *Curr Opin Biotechnol* 38, 33–38.
- Nishino, S.F., Shin, K.A., Gossett, J.M., Spain, J.C., 2013. Cytochrome P450 initiates degradation of cis-dichloroethene by *Polaromonas* sp. strain JS666. *Appl. Environ. Microbiol.* 79, 2263–2272.
- Niu, H., Wang, X., Li, T., 2011. Needleless Electrospinning: Developments and Performances, in: Lin, T. (Ed.), *Nanofibers - Production, Properties and Functional Applications*. InTech.
- Odom, J., Singleton, R.J., 2013. *The Sulfate-Reducing Bacteria: Contemporary Perspectives*. Springer Science & Business Media.
- Okeke, B.C., Chang, Y.C., Hatsu, M., Suzuki, T., Takamizawa, K., 2001. Purification, cloning, and sequencing of an enzyme mediating the reductive dechlorination of tetrachloroethylene (PCE) from *Clostridium bifermentans* DPH-1. *Can. J. Microbiol.* 47, 448–456.
- Oksanen, J., Blanchet, F., Kindt, R., Legendre, P., Minchin, P., O'Hara, R., Simpson, G., Solymos, P., Stevens, M., Wagner, H., 2012. *vegan: community ecology package*. R package. 'ver. 2.0–2. 2011.
- Oldenhuis, R., Vink, R.L., Janssen, D.B., Witholt, B., 1989. Degradation of chlorinated aliphatic hydrocarbons by *Methylosinus trichosporium* OB3b expressing soluble methane monooxygenase. *Appl. Environ. Microbiol.* 55, 2819–2826.
- Paes, F., Liu, X., Mattes, T.E., Cupples, A.M., 2015. Elucidating carbon uptake from vinyl chloride using stable isotope probing and Illumina sequencing. *Appl. Microbiol. Biotechnol.* 99, 7735–7743.
- Paul, L., Jakobsen, R., Smolders, E., Albrechtsen, H.-J., Bjerg, P.L., 2016. Reductive Dechlorination of Trichloroethylene (TCE) in Competition with Fe and Mn Oxides—Observed Dynamics in H₂-dependent Terminal Electron Accepting Processes. *Geomicrobiol. J.* 33, 357–366.
- Paul, L., Smolders, E., 2014. Inhibition of iron (III) minerals and acidification on the reductive dechlorination of trichloroethylene. *Chemosphere* 111, 471–477.
- Payne, K.A., Quezada, C.P., Fisher, K., Dunstan, M.S., Collins, F.A., Sjuts, H., Levy, C., Hay, S., Rigby, S.E., Leys, D., 2015. Reductive dehalogenase structure suggests a mechanism for B12-dependent dehalogenation. *Nature* 517, 513–516.
- Pedersen, K., 2011. *Gallionella*, in: *Encyclopedia of Geobiology*. Springer, pp. 411–412.
- Petrik, S., Maly, M., 2009. Production Nozzle-Less Electrospinning Nanofiber Technology. *MRS Proc.* 1240. <https://doi.org/10.1557/PROC-1240-WW03-07>
- Pfaffl, M.W., 2001. A new mathematical model for relative quantification in real-time RT-PCR. *Nucleic Acids Res.* 29, e45–e45.
- Popat, S.C., Zhao, K., Deshusses, M.A., 2012. Bioaugmentation of an anaerobic biotrickling filter for enhanced conversion of trichloroethene to ethene. *Chem. Eng. J.* 183, 98–103.
- Poritz, M., Goris, T., Wubet, T., Tarkka, M.T., Buscot, F., Nijenhuis, I., Lechner, U., Adrian, L., 2013. Genome sequences of two dehalogenation specialists - *Dehalococcoides mccartyi* strains BTF08 and DCMB5 enriched from the highly polluted Bitterfeld region. *FEMS Microbiol Lett* 343, 101–4. <https://doi.org/10.1111/1574-6968.12160>
- Regeard, C., Maillard, J., Holliger, C., 2004. Development of degenerate and specific PCR primers for the detection and isolation of known and putative chloroethene reductive dehalogenase genes. *J. Microbiol. Methods* 56, 107–118.
- Reij, M.W., Kieboom, J., de Bont, J.A., Hartmans, S., 1995. Continuous degradation of trichloroethylene by *Xanthobacter* sp. strain Py2 during growth on propene. *Appl. Environ. Microbiol.* 61, 2936–2942.

- Ritalahti, K.M., Amos, B.K., Sung, Y., Wu, Q., Koenigsberg, S.S., Löffler, F.E., 2006. Quantitative PCR targeting 16S rRNA and reductive dehalogenase genes simultaneously monitors multiple Dehalococcoides strains. *Appl. Environ. Microbiol.* 72, 2765–2774.
- RNA Center, 2018; http://rna.ucsc.edu/rnacenter/xrna/xrna_gallery.html, verified 2.6.2018
- Ryoo, D., Shim, H., Canada, K., Barbieri, P., Wood, T.K., 2000. Aerobic degradation of tetrachloroethylene by toluene-o-xylene monooxygenase of *Pseudomonas stutzeri* OX1. *Nat Biotechnol* 18, 775–778.
- Saeki, H., Akira, M., Furuhashi, K., Averhoff, B., Gottschalk, G., 1999. Degradation of trichloroethene by a linear-plasmid-encoded alkene monooxygenase in *Rhodococcus corallinus* (*Nocardia corallina*) B-276. *Microbiology* 145 (Pt 7), 1721–30. <https://doi.org/10.1099/13500872-145-7-1721>
- Scheutz, C., Durant, N. d, Dennis, P., Hansen, M.H., Jørgensen, T., Jakobsen, R., Cox, E. e, Bjerg, P.L., 2008. Concurrent ethene generation and growth of *Dehalococcoides* containing vinyl chloride reductive dehalogenase genes during an enhanced reductive dechlorination field demonstration. *Environ. Sci. Technol.* 42, 9302–9309.
- Schloss, P.D., Westcott, S.L., Ryabin, T., Hall, J.R., Hartmann, M., Hollister, E.B., Lesniewski, R.A., Oakley, B.B., Parks, D.H., Robinson, C.J., 2009. Introducing mothur: open-source, platform-independent, community-supported software for describing and comparing microbial communities. *Appl. Environ. Microbiol.* 75, 7537–7541.
- Schmidt, K.R., Gaza, S., Voropaev, A., Ertl, S., Tiehm, A., 2014. Aerobic biodegradation of trichloroethene without auxiliary substrates. *Water Res.* 59, 112–118.
- Scholz-Muramatsu, H., Neumann, A., Meßmer, M., Moore, E., Diekert, G., 1995. Isolation and characterization of *Dehalospirillum multivorans* gen. nov., sp. nov., a tetrachloroethene-utilizing, strictly anaerobic bacterium. *Arch Microbiol* 163, 48–56.
- Schurig, C., Melo, V.A., Miltner, A., Kaestner, M., 2014. Characterisation of microbial activity in the framework of natural attenuation without groundwater monitoring wells?: a new Direct-Push probe. *Environ. Sci. Pollut. Res.* 21, 9002–9015.
- Semprini, L., 1997. Strategies for the aerobic co-metabolism of chlorinated solvents. *Curr. Opin. Biotechnol.* 8, 296–308.
- Shani, N., Rossi, P., Holliger, C., 2013. Correlations between environmental variables and bacterial community structures suggest Fe (III) and vinyl chloride reduction as antagonistic terminal electron-accepting processes. *Environ. Sci. Technol.* 47, 6836–6845.
- Sharma, P.K., McCarty, P.L., 1996. Isolation and characterization of a facultatively aerobic bacterium that reductively dehalogenates tetrachloroethene to cis-1, 2-dichloroethene. *Appl. Environ. Microbiol.* 62, 761–765.
- Sharma, V., Sharma, A., 2013. Nanotechnology: an emerging future trend in wastewater treatment with its innovative products and processes. *Nanotechnology* 1.
- Shigematsu, T., Hanada, S., Eguchi, M., Kamagata, Y., Kanagawa, T., Kurane, R., 1999. Soluble methane monooxygenase gene clusters from trichloroethylene-degrading *Methylobacter* sp. strains and detection of methanotrophs during in situ bioremediation. *Appl. Environ. Microbiol.* 65, 5198–5206.
- Shin, K., 2010. Biodegradation of diphenylamine and cis-dichloroethene. PhD Thesis Georgia Institute of Technology.
- Silva, M.D., Daprato, R.C., Gomez, D.E., Hughes, J.B., Ward, C.H., Alvarez, P.J.J., 2006. Comparison of bioaugmentation and biostimulation for the enhancement of dense nonaqueous phase liquid source zone bioremediation. *Water Environ. Res.* 2456–2465.
- Smidt, H., de Vos, W.M., 2004. Anaerobic microbial dehalogenation. *Annu Rev Microbiol* 58, 43–73. <https://doi.org/10.1146/annurev.micro.58.030603.123600>
- Smith, K.S., Costello, A.M., Lidstrom, M.E., 1997. Methane and trichloroethylene oxidation by an estuarine methanotroph, *Methylobacter* sp. strain BB5. 1. *Appl. Environ. Microbiol.* 63, 4617–4620.
- Smits, T.H.M., Devenoges, C., Szynalski, K., Maillard, J., Holliger, C., 2004. Development of a real-time PCR method for quantification of the three genera *Dehalobacter*, *Dehalococcoides*, and

- Desulfotobacterium in microbial communities. *J. Microbiol. Methods* 57, 369–378. <https://doi.org/10.1016/j.mimet.2004.02.003>
- Solden, L., Lloyd, K., Wrighton, K., 2016. The bright side of microbial dark matter: lessons learned from the uncultivated majority. *Curr. Opin. Microbiol.* 31, 217–226.
- Steffan, R.J., Sperry, K.L., Walsh, M.T., Vainberg, S., Condee, C.W., 1999. Field-scale evaluation of in situ bioaugmentation for remediation of chlorinated solvents in groundwater. *Environ. Sci. Technol.* 33, 2771–2781.
- Stirling, D.I., Dalton, H., 1979. The fortuitous oxidation and cometabolism of various carbon compounds by whole-cell suspensions of *Methylococcus capsulatus* (Bath). *FEMS Microbiol. Lett.* 5, 315–318.
- Sung, Y., 2005. Isolation and ecology of bacterial populations involved in reductive dechlorination of chlorinated solvents.
- Sung, Y., Fletcher, K.E., Ritalahti, K.M., Apkarian, R.P., Ramos-Hernández, N., Sanford, R.A., Mesbah, N.M., Löffler, F.E., 2006a. *Geobacter lovleyi* sp. nov. strain SZ, a novel metal-reducing and tetrachloroethene-dechlorinating bacterium. *Appl. Environ. Microbiol.* 72, 2775–2782.
- Sung, Y., Ritalahti, K.M., Apkarian, R.P., Löffler, F.E., 2006b. Quantitative PCR confirms purity of strain GT, a novel trichloroethene-to-ethene-respiring *Dehalococcoides* isolate. *Appl. Environ. Microbiol.* 72, 1980–1987.
- Sung, Y., Ritalahti, K.M., Sanford, R.A., Urbance, J.W., Flynn, S.J., Tiedje, J.M., Löffler, F.E., 2003. Characterization of two tetrachloroethene-reducing, acetate-oxidizing anaerobic bacteria and their description as *Desulfuromonas michiganensis* sp. nov. *Appl. Environ. Microbiol.* 69, 2964–2974.
- Suttinun, O., Lederman, P.B., Luepromchai, E., 2004. Application of terpene-induced cell for enhancing biodegradation of TCE contaminated soil. *Songklanakarin J Sci Technol* 26, 131–142.
- Suttinun, O., Müller, R., Luepromchai, E., 2009. Trichloroethylene cometabolic degradation by *Rhodococcus* sp. L4 induced with plant essential oils. *Biodegradation* 20, 281–291.
- Sutton, N.B., Grotenhuis, J.T.C., Langenhoff, A.A., Rijnaarts, H.H., 2011. Efforts to improve coupled in situ chemical oxidation with bioremediation: a review of optimization strategies. *J. Soils Sediments* 11, 129–140.
- Suyama, A., Iwakiri, R., Kai, K., Tokunaga, T., Sera, N., Furukawa, K., 2001. Isolation and characterization of *Desulfotobacterium* sp. strain Y51 capable of efficient dehalogenation of tetrachloroethene and polychloroethanes. *Biosci. Biotechnol. Biochem.* 65, 1474–1481.
- Suyama, A., Yamashita, M., Yoshino, S., Furukawa, K., 2002. Molecular characterization of the PceA reductive dehalogenase of *Desulfotobacterium* sp. strain Y51. *J Bacteriol* 184, 3419–3425.
- Tarnawski, S.-E., Rossi, P., Brennerova, M.V., Stavelova, M., Holliger, C., 2016. Validation of an Integrative Methodology to Assess and Monitor Reductive Dechlorination of Chlorinated Ethenes in Contaminated Aquifers. *Front. Environ. Sci.* 4. <https://doi.org/10.3389/fenvs.2016.00007>
- Teel, A.L., Watts, R.J., 2002. Degradation of carbon tetrachloride by modified Fenton's reagent. *J. Hazard. Mater.* 94, 179–189.
- Terzenbach, D.P., Blaut, M., 1994. Transformation of tetrachloroethylene to trichloroethylene by homoacetogenic bacteria. *FEMS Microbiol. Lett.* 123, 213–218.
- Throbäck, I.N., Enwall, K., Jarvis, Å., Hallin, S., 2004. Reassessing PCR primers targeting nirS, nirK and nosZ genes for community surveys of denitrifying bacteria with DGGE. *FEMS Microbiol. Ecol.* 49, 401–417. <https://doi.org/10.1016/j.femsec.2004.04.011>
- Tobiszewski, M., Namieśnik, J., 2012. Abiotic degradation of chlorinated ethanes and ethenes in water. *Environ. Sci. Pollut. Res.* 19, 1994–2006.
- Tsai, T., Liu, J., Chang, Y., Chen, K., Kao, C., 2014. Application of polycolloid-releasing substrate to remediate trichloroethylene-contaminated groundwater: A pilot-scale study. *J. Hazard. Mater.* 268, 92–101.
- Tsien, H.-C., Brusseau, G.A., Hanson, R.S., Waclett, L.P., 1989. Biodegradation of trichloroethylene by *Methylosinus trichosporium* OB3b. *Appl. Environ. Microbiol.* 55, 3155–3161.

- Tsien, H.-C., Hanson, R.S., 1992. Soluble methane monooxygenase component B gene probe for identification of methanotrophs that rapidly degrade trichloroethylene. *Appl. Environ. Microbiol.* 58, 953–960.
- Tsukagoshi, N., Ezaki, S., Uenaka, T., Suzuki, N., Kurane, R., 2006. Isolation and transcriptional analysis of novel tetrachloroethene reductive dehalogenase gene from *Desulfitobacterium* sp. strain KBC1. *Appl. Microbiol. Biotechnol.* 69, 543–553.
- Uchino, Y., Miura, T., Hosoyama, A., Ohji, S., Yamazoe, A., Ito, M., Takahata, Y., Suzuki, K., Fujita, N., 2015. Complete genome sequencing of *Dehalococcoides* sp. strain UCH007 using a differential reads picking method. *Stand. Genomic Sci.* 10, 102. <https://doi.org/10.1186/s40793-015-0095-9>
- Uchiyama, H., Nakajima, T., Yagi, O., Tabuchi, T., 1989. Aerobic degradation of trichloroethylene by a new type II methane-utilizing bacterium, strain M. *Agric. Biol. Chem.* 53, 2903–2907.
- Utility model No. 31266; <http://isdv.upv.cz/doc/FullFiles/UtilityModels/FullDocuments/FDUM0031/uv031266.pdf>
- van der Zaan, B., Hannes, F., Hoekstra, N., Rijnaarts, H., de Vos, W.M., Smidt, H., Gerritse, J., 2010. Correlation of *Dehalococcoides* 16S rRNA and Chloroethene-Reductive Dehalogenase Genes with Geochemical Conditions in Chloroethene-Contaminated Groundwater. *Appl. Environ. Microbiol.* 76, 843–850. <https://doi.org/10.1128/aem.01482-09>
- van Hylckama, V.J., De Koning, W., Janssen, D.B., 1996. Transformation kinetics of chlorinated ethenes by *Methylosinus trichosporium* OB3b and detection of unstable epoxides by on-line gas chromatography. *Appl. Environ. Microbiol.* 62, 3304–3312.
- Verce, M.F., Ulrich, R.L., Freedman, D.L., 2001. Transition from cometabolic to growth-linked biodegradation of vinyl chloride by a *Pseudomonas* sp. isolated on ethene. *Environ. Sci. Technol.* 35, 4242–4251.
- Verce, M.F., Ulrich, R.L., Freedman, D.L., 2000. Characterization of an Isolate That Uses Vinyl Chloride as a Growth Substrate under Aerobic Conditions. *Appl. Environ. Microbiol.* 66, 3535–3542.
- Wackett, L.P., Brusseau, G.A., Householder, S.R., Hanson, R.S., 1989. Survey of microbial oxygenases: trichloroethylene degradation by propane-oxidizing bacteria. *Appl. Environ. Microbiol.* 55, 2960–2964.
- Wackett, L.P., Gibson, D.T., 1988. Degradation of trichloroethylene by toluene dioxygenase in whole-cell studies with *Pseudomonas putida* F1. *Appl. Environ. Microbiol.* 54, 1703–1708.
- Wacławek, S., Nosek, J., Cádrová, L., Antoš, V., Černík, M., 2015. Use of various zero valent irons for degradation of chlorinated ethenes and ethanes. *Ecol. Chem. Eng. S* 22, 577–587.
- Wagner, D.D., Hug, L.A., Hatt, J.K., Spitzmiller, M.R., Padilla-Crespo, E., Ritalahti, K.M., Edwards, E.A., Konstantinidis, K.T., Löffler, F.E., 2012. Genomic determinants of organohalide-respiration in *Geobacter lovleyi*, an unusual member of the *Geobacteraceae*. *Bmc Genomics* 13, 200.
- Waller, A.S., Krajmalnik-Brown, R., Löffler, F.E., Edwards, E.A., 2005. Multiple Reductive-Dehalogenase-Homologous Genes Are Simultaneously Transcribed during Dechlorination by *Dehalococcoides*-Containing Cultures. *Appl. Environ. Microbiol.* 71, 8257–8264. <https://doi.org/10.1128/AEM.71.12.8257-8264.2005>
- Wang, X.P., Li, W.D., 2012. Fabrication and Applications of Nanofibers via Electrospinning, in: *Nanofibers: Synthesis, Properties, and Applications*, Nanotechnology Science and Technology. Nova Science Publishers Inc, [Hauppauge] New York].
- Wild, A., Hermann, R., Leisinger, T., 1996. Isolation of an anaerobic bacterium which reductively dechlorinates tetrachloroethene and trichloroethene. *Biodegradation* 7, 507–511.
- Winter, R.B., Yen, K.-M., Ensley, B.D., 1992. *Pseudomonas* or host containing toluene monooxygenase genes from *Pseudomonas*.
- Wittlingerova, Z., Machackova, J., Petruzalkova, A., Trapp, S., Vlk, K., Zima, J., 2013. One-year measurements of chloroethenes in tree cores and groundwater at the SAP Mimoň Site, Northern Bohemia. *Environ. Sci. Pollut. Res.* 20, 834–847.

- Wittlingerova, Z., Macháčková, J., Petruželková, A., Zimová, M., 2016. Occurrence of perchloroethylene in surface water and fish in a river ecosystem affected by groundwater contamination. *Environ. Sci. Pollut. Res.* 23, 5676–5692.
- Yeager, C.M., Bottomley, P.J., Arp, D.J., 2001. Cytotoxicity associated with trichloroethylene oxidation in *Burkholderia cepacia* G4. *Appl. Environ. Microbiol.* 67, 2107–15. <https://doi.org/10.1128/aem.67.5.2107-2115.2001>
- Yoshida, N., Takahashi, N., Hiraishi, A., 2005. Phylogenetic Characterization of a Polychlorinated-Dioxin-Dechlorinating Microbial Community by Use of Microcosm Studies. *Appl. Environ. Microbiol.* 71, 4325–4334. <https://doi.org/10.1128/AEM.71.8.4325-4334.2005>